Bioactive Materials 33 (2024) 460–482

Contents lists available at ScienceDirect

Bioactive Materials

journal homepage: www.keaipublishing.com/en/journals/bioactive-materials

Review article

Decellularized extracellular matrix materials for treatment of ischemic cardiomyopathy

Wei Liu [a], Xiangmei Zhang [b], Xiaokai Jiang [c,d], Binyao Dai [c,d], Liwen Zhang [c,d,*], Yang Zhu [e,f,g,**]

[a] Center for Medical Device Evaluation, National Medical Products Administration, Beijing, 100037, China
[b] Greater Bay Area Center for Medical Device Evaluation and Inspection, National Medical Products Administration, Shenzhen, 518045, China
[c] MOE Key Laboratory of Macromolecular Synthesis and Functionalization Department of Polymer Science and Engineering, Hangzhou, 310027, China
[d] Zhejiang University, Hangzhou, 310027, China
[e] State Key Laboratory of Transvascular Lmplantation Devices, Department of Polymer Science and Engineering, Zhejiang University, Hangzhou, 310027, China
[f] MOE Key Laboratory of Macromolecular Synthesis and Functionalization, Zhejiang University, Hangzhou, 310027, China
[g] Binjiang Institute of Zhejiang University, Hangzhou, 310053, China

ARTICLE INFO

Keywords:
Decellularized extracellular matrix
Ischemic cardiomyopathy
Injectable dECM
dECM patches
Myocardial infarction

ABSTRACT

Ischemic cardiomyopathy (ICM) affect millions of patients globally. Decellularized extracellular matrix materials (dECM) have components, microstructure and mechanical properties similar to healthy cardiac tissues, and can be manufactured into various forms of implantable biomaterials including injectable hydrogels or epicardial patches, which have been extensively reported to attenuate pathological left ventricular remodeling and maintain heart function. Recently, dECM medical devices for ICM treatment have been approved for clinical use or studied in clinical trials, exhibiting considerable translation potential. Cells, growth factors and other bioactive agents have been incorporated with different dECM materials to improve the therapeutic outcomes. In addition, more detailed aspects of the biological effects and mechanisms of dECM treatment are being revealed. This review summarized recent advances in dECM materials from variable sources for cardiac repair, including extraction of extracellular matrix, cell integration, smart manufacturing of injectable hydrogels and cardiac patch materials, and their therapeutic applications. Besides, this review provides an outlook on the cutting-edge development directions in the field.

1. Introduction

Ischemic cardiomyopathy (ICM) remain one of the leading causes of death worldwide over the past few decades [1–3], opposing heavy medical and financial burdens on patients and community. ICM risk factors including smoking, obesity, and sedentary lifestyles lead to accumulation of blood clots and fatty plaques on the inner walls of blood vessels [4,5]. When one or more coronary arteries are blocked, its downstream cardiomyocytes die of ischemia. As cardiomyocytes are terminally-differentiated mature cells with low endogenous regenerative capacity [6–9], loss of cardiomyocytes is widely considered irreversible [10,11]. Necrotic myocardium is gradually replaced with fibrotic scar tissue, which leads to reduced myocardium contractility and cardiac function, and heart failure (HF) at end stage [12–14].

Current surgical treatments for ICM focus on thrombolysis and restoration of myocardial blood supply to the ischemic area via bypass grafting and percutaneous coronary intervention (PCI) [15–17]. However, they cannot regenerate the lost population of cardiomyocytes or remedy the pathological mechanical conditions responsible for adverse ventricular remodeling including hypotrophy and aneurysm. Drugs including angiotensin receptor-neurolysin inhibitors, β-blockers, angiotensin-converting enzyme inhibitors, and mineralocorticoid-receptor antagonists reduce the influence of the mechanical drives for HF, but do not eliminate the latter [18–20]. Left ventricular assist devices (LVADs) and heart transplantation

Peer review under responsibility of KeAi Communications Co., Ltd.
* Corresponding author. MOE Key Laboratory of Macromolecular Synthesis and Functionalization Department of Polymer Science and Engineering, Hangzhou, 310027, China.
** Corresponding author. State Key Laboratory of Transvascular lmplantation Devices, Department of Polymer Science and Engineering, Zhejiang University, Hangzhou, 310027, China.
E-mail addresses: liuwei@cmde.org.cn (W. Liu), zhangxm@cmde.org.cn (X. Zhang), 3190103982@zju.edu.cn (X. Jiang), 3200104045@zju.edu.cn (B. Dai), 12129046@zju.edu.cn (L. Zhang), zhuyang@zju.edu.cn (Y. Zhu).

https://doi.org/10.1016/j.bioactmat.2023.10.015
Received 25 May 2023; Received in revised form 20 September 2023; Accepted 15 October 2023

are the last options [21], but limited by high invasiveness and donor shortage [22]. On the other hand, strategies of cardiomyocyte/stem cell transplantation and stimulating proliferation of remaining cardiomyocytes have been extensively investigated in clinical trials and animal studies, yet their efficiencies are expected to be improved [23,24].

Novel biomaterials have been developed to mediate the pathological mechanical environment and/or increase the efficiency of cell transplantation [25–38]. The majority of the materials could be categorized as injectable hydrogels and epicardial patches. Mechanically, both intramyocardially injected hydrogels and epicardially implanted patches can reduce the stress in cardiac wall by increasing wall thickness [39], hence preserve cardiac geometry and function. In addition to providing mechanical support, hydrogels and patches can also reduce adverse reactions including cell damage, inflammation and fibrosis, and promote desirable angiogenesis, cardiomyocyte proliferation with intrinsic bioactivity or delivered bioactive factors [40–43]. Together with some of these bioactivities, biomaterials that carry cells could extend cell retention, and better maintain their activity [44,45]. Two forms of dECM devices require different surgical procedures. Injectable hydrogels can be delivered to myocardium in a multi-point fashion via a minimally invasive transendocardial catheter system [46]. Such surgery reduces the probability of infection and anesthetic risks since it does not require open-chest procedures or full-body anesthesia. Injectable hydrogels including Algisyl (LoneStar Heart), IK-5001 (Bellerophon Therapeutics), XDROP (Deke Medtech) and VentriGel (Ventrix) have entered clinical trials, and encouraging therapeutic outcomes have been reported [46–48]. Compared to the injectable systems, epicardial patches are attached to patient epicardium through highly invasive open chest surgeries, which limited the patient population who can receive patches. Minimally invasive thoracoscopic surgeries are under investigation in pre-clinical studies [34,49,50]. However, dECM in patch forms does not need to undergo structurally disruptive digestion as the hydrogels do, thus could provide greater mechanical support to the target myocardium, and better maintain original bioactivity [51]. Novel dECM products approved by departments of medical device supervision for clinical use or in clinical trials are listed in Table 1.

The vast array of biomaterials for ICM treatment can be broadly classified as synthetic and natural polymers, according to their sources [55,56]. Synthetic polymers include polyglycerol sebacate (PGS) [57], polycaprolactone (PCL) [58], poly (lactic acid) (PLA) [59,60], poly D, L-lactic acid-*co*-glycolic acid (PLGA) [61,62], polyurethane (PU) [29], their copolymers and derivatives [63–65]. Commonly seen natural materials include gelatin, collagen, alginate, chitosan, fibrin, hyaluronic acid, and the decellularized ECM (dECM) derived from various organs [66,67]. Generally, synthetic materials are mechanically stronger, while natural materials are advantageous in terms of bioactivity. Among the investigated materials, dECM is the only category which has entered the clinical phases in both hydrogel and patch strategies.

dECM is derived from organs/tissues by removing the cells and desirably the immunogenic components, while maintaining the majority of the structural components and part of the bioactive components (including collagens, glycosaminoglycans (GAGs), proteoglycans, and matrix-bound nanovesicles) [68,69]. Therefore, dECM materials are capable of mimicking native myocardial tissue in terms of components, mechanics and microstructure while providing bioactive cues for cardiac cell adhesion and growth [70,71]. dECM can be transformed into powders, sheets, scaffolds and injectable hydrogels employing advanced processing technologies, as well as being composited with other materials for function enhancement [72]. To achieve better myocardial restoration, researchers have combined cells, growth factors and nuclei acids with dECM to mimic physiological ECM [73]. These properties have made dECM an attractive choice for cardiac repair, as demonstrated by PeriCord, VentriGel, and CorPatch, among numerous efforts in developing suitable biomaterials or tissue engineering solutions [74]. However, production of dECM inevitably causes partial loss of bioactive matrix, original structure and mechanical strength, lowering its performance [73]. To address such challenge, researchers employed advanced manufacturing techniques including electrospinning, 3D bioprinting, and microfluidics to precisely engineer dECM materials that maintain or mimic the characteristics of native cardiac ECM at multiple levels [75–77]. This review begins by providing a comprehensive overview of the structure and properties of the cardiac ECM in comparison with different dECM materials, followed by an examination of several important dECM processing techniques and their derivative materials in cardiovascular tissue engineering (Fig. 1). Key considerations in improving dECM biological function with cells and growth factors, and in fabrication of dECM patches and hydrogel, are discussed in detail. In addition, experience and challenges in clinical applications of dECM are introduced.

Table 1
Approved dECM medical devices and devices under clinical trials.

Products	Source	Form	Clinical trials	State	Ref.
CorPatch®	Porcine small intestinal submucosa (SIS)	Epicardial patch	NCT03798353	Approved	[52]
VentriGel	Porcine ventricle	Injectable hydrogel	NCT02305602	Phase I	[53]
PeriCord	Human pericardium	Epicardial patch	NCT03798353	Phase I	[54]

2. Development of dECM materials for myocardial repair

2.1. Structure and composition of cardiac ECM

Cardiac wall consists of three layers: the innermost endocardium, the myocardium, and the outer pericardium [78]. The cells and ECM present in these layers exhibit compositional variability according to the specific functional demands of each region of cardiac tissue [67,79]. Epicardial patches were generally fixed to the external surface of pericardium or myocardium [29], while hydrogel could be injected into myocardium [30,64]. Therefore, we focus more on the pericardium and myocardial ECM. The pericardium is the outermost layer and is composed of dense collagen bundles fused with abundant elastin fibers organized in waveforms, thus producing its expandability and a certain degree of freedom of movement [80]. The myocardial ECM forms the structural basis of the cardiac tissue, comprised by collagen fibrils (70 %) and polysaccharides including glycoproteins, proteoglycans, and glycosaminoglycans [81]. Fibrillar collagen is mainly composed of type I and type III collagen. Type I collagen is the main structural component of the cardiac interstitium, accounting for more than 85 % of the collagen matrix, type III collagen accounts for less than 11 %, and type IV, V, VI and VIII collagen accounts for about 4 % [82,83]. Glycoproteins including fibrin, fibronectin, and laminin play significant roles in providing secondary structural support and inducing intracellular signaling [84].

After MI, the sudden and massive loss of CM triggers acute inflammation and myocardial degradation revealing the disarray/disruption of muscle fibers [85]. Inflammatory factors including tumor necrosis factor-α (TNF-α) and transforming growth factor-β (TGF-β) stimulate myofibroblast activation and increase the expression of type I collagen [86]. Excessive deposition of type I collagen-based ECM in scar tissue stiffens the myocardium and disrupts the gap junctions of CM, hindering normal contraction [13]. Then, the ischemic myocardium undergoes ECM remodeling and gradually loses its original structure and contractile function [87]. Therefore, reconstructing ECM similar to the native state is crucial for repairing cardiac tissue.

2.2. Decellularization of different ECM

In 1948, Poel knock-crushed muscle tissue at a low temperature

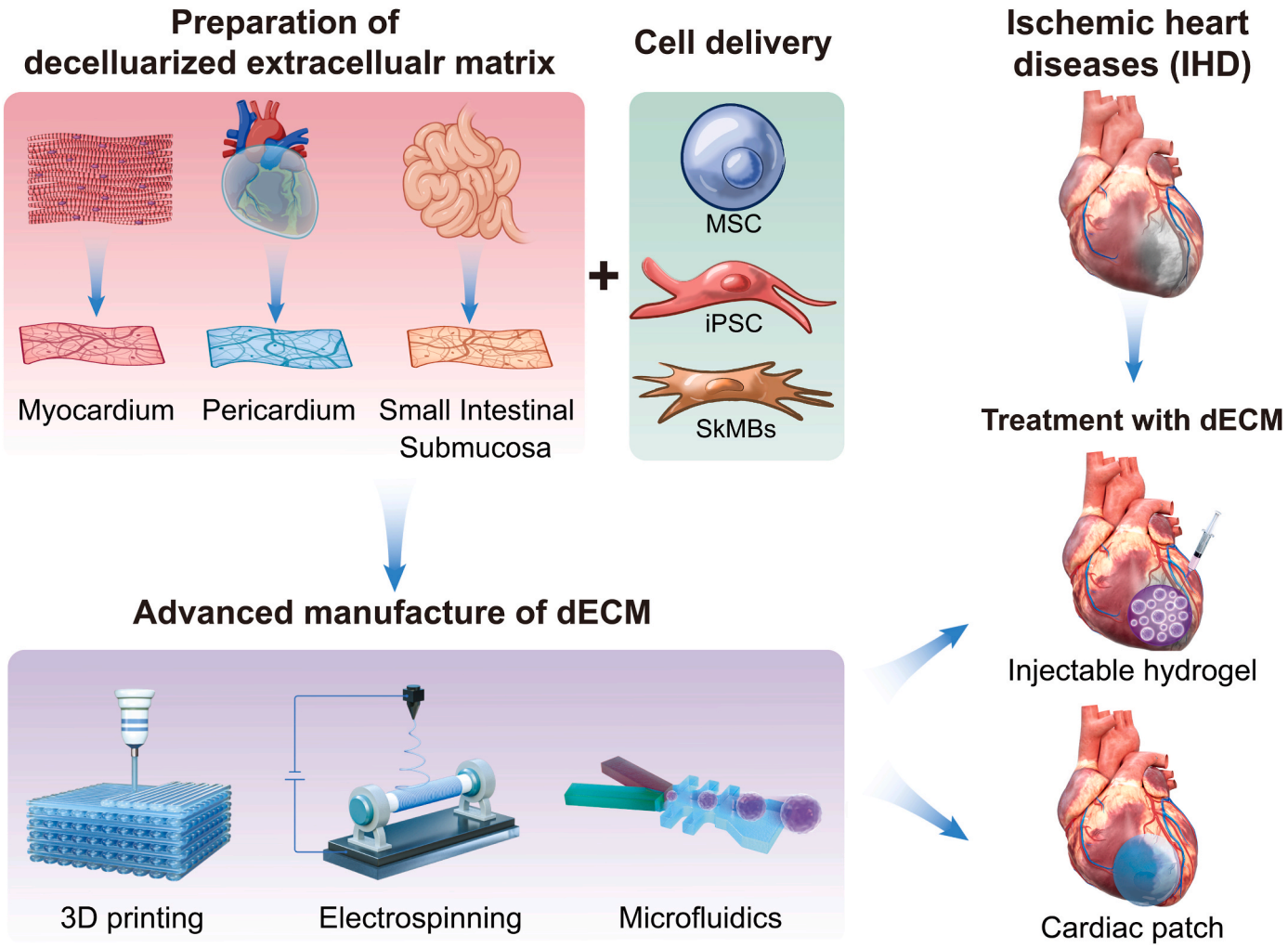

Fig. 1. Schematic representation of the application of decellularized extracellular matrix materials for cardiac repair.

(−70 °C), and homogenized the crushed tissue using a cylinder and a tight-fitting rotating plunger to obtain a decellularized homogenate, pioneered the fabrication of decellularized matrix materials [46,88]. Since then, a variety of methods have been developed to isolate tissue-specific ECM, including chemical treatments (e.g. acids and alkalis, detergents, and alcohols), biological reactions (e.g. enzymes, chelating agents) and physical degradation (e.g. pressure, mechanical, freeze-thaw, and electroporation), etc [75,89–93]. Combining two or three decellularizing methods is a general strategy to improve the efficiency of cell removal [71,94].

Since comparing decellularization of the species and sources of tissues is difficult, this review here gives representatives of dECM. In 2008, Ott et al. generated the first acellular rat whole heart (WH) through coronary perfusion on a modified Langendorff apparatus, using a chemical solution containing 1 % SDS and 1 % Triton X-100 [95]. This decellularized rat hearts retain complex ECM components throughout and retain intact chamber geometry and perfusable vascular architecture (Fig. 2A). This milestone work led the trend of whole-organ decellularized scaffolds. Afterwards, a series work of cardiac dECM (cECM) based on this protocol with varying degrees of modification have been proposed [96–101]. Momtahan et al. utilized an automation system of pressure to perfuse and decellularize tissue for reducing the detergent exposure time and achieving 98 % DNA removal [102]. DNase and RNase can be utilized to eliminate nuclei acids which cannot be cleared up by detergents [96,103]. Cutting cardiac tissues into slices can lower the requirements of decellularization due to faster permeation of chemical reagents in smaller tissues. Similarly, pericardium is a sheet-like tissue only requiring the treatment of 1 % SDS followed by DNase and RNase (Fig. 2B) [104]. The cECM and decellularized pericardium both preserved their intrinsic organization and spatial three-dimensional distribution of the native matrix fibrils, while decellularized pericardium showed larger pores (Fig. 2C) [105]. Similar to heart, liver has a high cell density. Liver dECM (liECM) are usually obtained through a combination of freeze-thawing, detergents and enzymes [106–109]. Kidney dECM (kECM) can be extracted by enzyme digestion or SDS treatment [110,111]. Decellularization of lung dECM (luECM) has been automated through vascular perfusion with detergents, despite risks of barrier damage and bleeding in the airways [112–114]. The commonly used preparation procedure of small intestinal submucosa (SIS) is to first mechanically remove serosa, bundle mucosa and lateral mucosa, leaving mainly the submucosa of the intestinal wall. The remaining DNA, RNA, and cells can then be removed from the submucosa using Triton X-100 and peracetic acid [115–122]. Recently, Palmosi et al. tested a new detergent called Tergitol 15-S-9 (15-S-9), having a lower biotoxicity, higher wettability and decellularization efficacy compared to Triton X-100 [123]. In terms of preparing soluble dECM materials, this review introduce in detail in Section 4.1.

Decellularization procedures may damage ECM structure and impair mechanical properties [100]. Enzymes and chemical reagents including alkalines and acids, may degrade matrix proteins, thus reducing the mechanical strength of dECM [124]. Alcohols can crosslink or denature collagen and other proteins, causing damage to the ultrastructure of

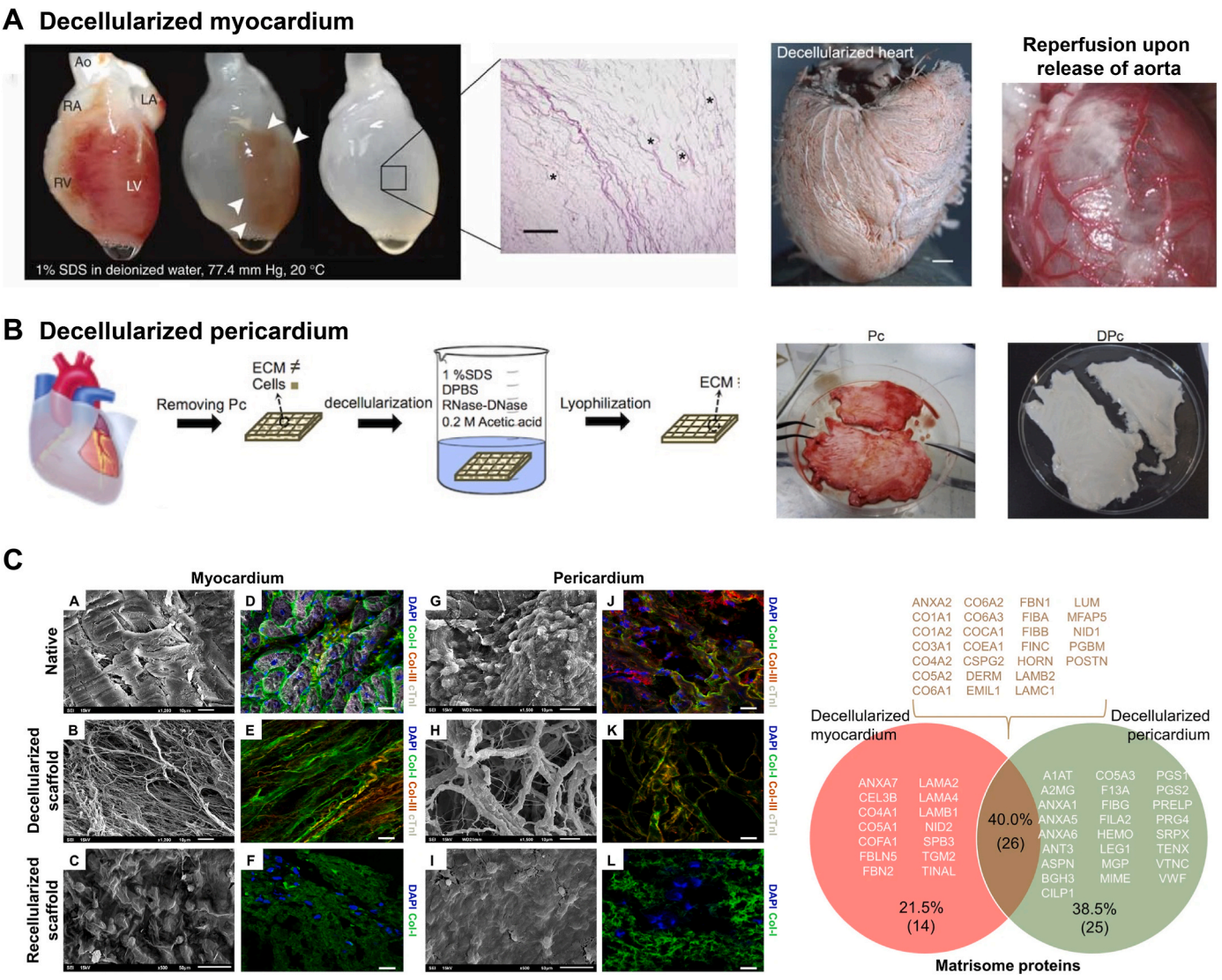

Fig. 2. dECM scaffolds from different tissues preserved variable ECM components and distinct architectures. (A) Photographs of decellularization of cadaveric rat heart using sodium dodecyl sulfate (SDS) over 12 h and H&E staining of its slice showing no intact cells or nuclei. Scale bar, 200 μm. The right row contains: macroscopic (scale bar, 1000 μm) of coronary corrosion casts of decellularized WH; reperfused decellularized WH. Modified and adapted with permission from Ref. [95]. Copyright 2008, Nature Publishing Group. (B) Schematic presentation of decellularization process of pericardium (*Pc*) and the gross images of *Pc* and decellularized *Pc* (DPc). Modified and adapted with permission from Ref. [104]. Copyright 2015, Wiley Periodicals. (C) Ultrastructure determined by SEM of the myocardium and pericardial scaffolds in terms of three states (native, decellularized and recellarized) and their immunostaining for col-I (green), col-III (red), and cTnI (white). Nuclei were counterstained with DAPI (blue). Scale bars = 50 μm. Modified and adapted with permission from Ref. [105]. Copyright 2018, Springer Nature.

dECM [122]. Ionic or non-ionic detergents (sodium dodecyl sulfate (SDS) and Triton X-100) can disrupt non-covalent bonds between proteins and cannot be removed from dECM completely [99]. The residual SDS in dECM causes cytotoxicity during recellularization in certain applications [125]. Wang et al. solved this problem by perfusing decellularized organs with 1 % Triton X-100 for 3 h in a high speed to remove SDS down to 0.01 mg/g of dry dECM [106]. Merna et al. noninvasively characterized the structural and mechanical change of whole heart during different decellularization processes via multiphoton microscopy and image correlation spectroscopy [126]. The result showed that combined treatment with enzymes and Triton X-100 significantly reduced collagen and elastin fiber densities and the compressive modulus (<20 % of native cardiac tissues), while decellularization with only Triton X-100 even increased the modulus of dECM by 150 %, higher than native tissue. However, a large amount DNA remain after Triton X-100 treatment alone [126]. Freeze-thaw treatment and pressure can disrupt the ultrastructure of ECM; direct force and pressure exerting on tissues may destroy the integrity of their basal membranes and make the final dECM difficult to hydrate [122]. All these structure and component changes of dECM caused by decellularization process affect the interaction between cells and dECM, which depend on exposure time. In this case, it is important to determine corresponding decellularization details for specific tissues/organs.

2.3. Interaction between cells and dECM

To produce off-the-shelf engineered tissues, dECM materials are sometimes recellularized *in vitro* before transplantation into patients, thereby reconstructing functions of the injured tissue with both dECM and the cells [15,74,124]. In cardiac applications, seeded cells include skeletal myoblasts (SkMBs), bone marrow-derived cells (BMSCs), mesenchymal stem cells (MSCs), embryonic stem cells (ESCs), iPSCs and cardiac stem cells (CSCs) [15,55]. In the following section, we focus on SkMBs, MSCs, ESCs and iPSCs.

SkMBs are employed for cardiac repair attributed to their autologous availability, ability to be amplified *in vitro*, and relatively good survival after implantation [127,128]. Menasché et al. injected SkMBs into and around the necrotic myocardium in patients, which improved systolic function after 5-month follow-up [129]. Carton et al. cultured C2C12 myoblasts on extracted dECM from the bovine pericardium to guide their maturation and myotubes formation [130]. However, SkMBs do not express connexin 43 (Cx43, an important gap junction protein for electrical signal conduction) or form electromechanical coupling with cardiomyocytes (CMs) *in vivo*, hence are electrically isolated from the native myocardium [131]. As reported, a higher frequency of arrhythmic events occurred in SkMB-treated patients with ventricular dysfunction compared to the placebo group [131,132].

MSCs are by far the most commonly used cell type for cardiac tissue engineering research. Due to the inherent low immunogenicity, high self-renewal ability, transdifferentiation pluripotency, and cell recruiting capability, MSCs can effectively promote cardiac repair via secretion bioactive factors, attenuating fibrosis, enhancing angiogenesis, and initiating endogenous cardiac repair [133]. MSCs could repopulate and proliferate well in porous SIS dECM sheet without changing scaffold morphology, and enhance cytokine secretion (e.g. vascular endothelial growth factor and interleukin-8) compared to residing on tissue culture plates [134–136]. Han et al. bio-printed bone-marrow MSCs (BMMSCs) with hydrogels made from cECM, liECM and skin ECM (skECM), respectively. The gene ontology (GO) functional classification of BMMSCs treated by different ECMs showed that cECM upregulated cardiomyogenesis-related genes, enriching in GO terms including regulation of actin filament bundle assembly, stress fiber assembly, and regulation of actin filament organization [103]. BMMSCs in liECM hydrogel showed more liver-relevant features, while cells in skECM hydrogel expressed more markers related to epithelial cell migration. Therefore, cECM has the greatest potential in inducing myocardial differentiation. MSCs are also able to reduce porcine xenograft adaptive immune responses [136]. However, delivering MSCs cannot build the intrinsic electrophysiological communication since they do not express Cx43 as CMs do [137].

Human pluripotent stem cells, including ESCs and iPSCs, have been used to generate various cells for cardiac repair, and dECM can prolong the lifespan of these cells after being delivered to the myocardium and upregulate the expression of cardiac transcription factors [138]. ESCs can differentiate into other types of cardiac cells, including endothelial cells and vascular smooth muscle cells. ESCs-differentiated cardiomyocytes share the same physiological characteristics of the spontaneous beating as mature cardiomyocytes. It is recognized that the microenvironment provided by cECM promoted the maturation of ESC-derived CMs, revealed by the striation patterns of cardiac troponin I and upregulation of Cx43, and improved the contractile function of these cells [139]. Hochman-Mendez et al. found that human ESC-derived CMs repopulated in cECM patches revealed electrical coupling, and recellularization restored the mechanical properties of cECM patches similar to that of fresh cadaveric cardiac tissue without decellularization [140]. iPSCs can be derived from the fibroblasts of donors, avoiding the immunogenicity and ethical issues when using ESCs [141]. iPSCs have been reported to differentiate into a variety of different cardiac cells for the treatment of cardiomyopathy on cardiac dECM slices [142]. Lu et al. perfused cardiac dECM with iPSCs to build functional engineered heart tissue, although it did not form synchronized heart tissue and may cause an arrhythmogenic substrate [97].

The anisotropic morphology of dECM patch also influences the iPSC fate and further cardiac formation. Schwan et al. laser-cut decellularized myocardium into ribbon-like shapes to form an anisotropic sheet, and cultured ESCs and iPSCs on it to build an engineered heart tissue [143]. ESCs produced detectable intracellular Ca^{2+} transients and 1.7 mN/mm^2 twitch stress, which was close to human right ventricular trabeculae. When the patch was stretched at 8 %, iPSCs on the anisotropic patch produced a higher average peak stress of 2.2 ± 0.76 mN/mm^2 with maximum peak force of 6.5 mN/mm^2 and faster twitch kinetics, benefiting cardiac tissue growth. However, the clinical use of iPSCs must be tempered due to their tumorigenic potential [144].

2.4. dECM from diverse sources for ICM therapy

dECM extracted from different tissues/organs inherits diverse biochemical components which relates to the development and formation of tissues/organs. Those dECM materials capable of rebuilding myocardial tissue and restoring cardiac function are desired to salvage ischemic myocardial injury. The advantages and disadvantages of dECM from diverse tissues for ICM treatment are overviewed and stated in Table 2.

Given the similarity in microstructure and composition to native cardiac tissue, cardiac dECM is considered by many researchers the most promising dECM material for ICM therapy. Particularly, autologous cardiac dECM (cECM) is considered by many the optimal for treating ICM, but its feasibility depends on the health condition of patients [163,164]. Alternatively, allogenic cECM is usually obtained from donors. Godier-Furnémont et al. fabricated human cECM patches at 300 μm thickness carrying MPCs to revascularize the infarcted myocardium and preserve cardiac function in the acute or chronic MI models [96]. The biochemical composition of allogenic cECM varies from donors of different ages and health conditions. As age increases, content of structural proteins including collagens and laminin increases in cECM [145,165]. In fetal and perinatal hearts, collagen I and laminin promote maturation of CMs; but gradual deposition of these components over ages increases the rigidity of myocardium and lead to fibrosis in elderly hearts [166]. In contrast, expression of elastic ECM proteins including fibronectin and elastin lowers in both the aged ECM and the MI tissues [145,166]. In addition, juvenile cECM contains a higher concentration of GAGs compared to adult counterparts, which can protect the bioactivity of soluble signaling factors and facilitate them to interact with receptors for therapeutic effects [167–170]. These active components continue to exist in dECM after decellularization, which has been demonstrated previously. Wang et al. injected neonatal mouse cECM (nmECM) into ischemic areas to prevent scar expansion, and increase angiogenesis *in vivo*, while adult cECM exhibited limited performance [145]. The nmECM promoted ErbB2 expression, which is favorable as ErbB2 level is high in embryonic and neonatal hearts, and it contributes to cardiomyocyte proliferation and preventing fibrosis [171,172].

Pericardium is a patch-like tissue supporting, which packages the heart to prevent the latter from over stretching and friction with surrounding tissues [43]. Compared to cECM scaffold, decellularized human pericardial dECM scaffolds have larger pores, benefiting cell penetration and neovascularization. In addition, pericardial dECM sheets contain more matrisome proteins (Fig. 2C), and show a typical strain-hardening behavior with higher stiffness (~2 fold) compared to the myocardium at 20 % strain [105]. Meyer et al. treated a transmural infarction sizing 4 cm with a decellularized pericardium patch, which integrated with infarcted myocardium and induced the ingrowth of capillaries and vessels [147]. Gálvez-Montón et al. observed markers (S100 and β_{III} tubulin) and structural features (amyelinated axons, a large number of transport vesicles) of newly formed nerve fibers in the decellularized pericardium applied onto the MI region [173]. Recently, Prat-Vidal et al. reported a first-in-man trial of a human pericardial dECM scaffold with stem cells (PeriCord) to treat patients with ischemic myocardial scars [54]. The PeriCord implant reduced the size of infarcted tissue, and restored patient cardiac function.

Since human cECM materials have limitations including donor shortage and batch variance [174,175], xenogeneic cECM (especially the porcine cECM) is the potential alternatives, also undergoing clinical trials [53]. Johnson et al. attempted to fabricate injectable hydrogels with human cECM and porcine cECM (pcECM), and evaluate the source/species influence [146]. They found that as adipose tissue deposition, fibrosis, ECM crosslinking increase in the donors (aged from 41 to 69),

Table 2
The advantages and disadvantages of dECM applied in ICM treatment.

dECM for ICM	Material form	Advantages	Disadvantages	Ref.
Human cECM	Epicardial patch	Allogeneic implants with lowest immunogenicity; upregulating the proliferation and cardiac-related gene expression of stem cells; high content of GAGs benefiting the preservation of growth factors	Limited source; patient-to-patient variability; high contents of matrisome matrix in aged donors; less porosity	[96,142,145]
Human cECM	Hydrogel	Allogeneic implants with lowest immunogenicity	Limited source; patient-to-patient variability; unable of self-assemble when using aged tissues; high amount of adipose tissue deposition; fibrosis and crosslinked ECM in aged donors	[146]
Human pericardium	Epicardial patch	Higher stiffness; typical stretch-hardening; encouraging vascular and nerve neoformation in scaffolds; reducing the scar size; enhancing myocardial differentiation	Calcification	[147–150]
Porcine cECM	Epicardial patch	Retaining cardiac contractility and ventricular dimensions; preventing cardiac remodeling; recruiting cardiac progenitors to differentiate into CM-like cells and form "muscle-like" fibers; upregulating the GATA binding protein (GATA4) and the myosin light chain (MYLC)	Xenogenic immunogenicity; endogenous virus	[51,151]
Porcine cECM	Hydrogel	Facilitating the infiltration of endogenous cells; promoting myocardial differentiation and contraction; enhancing neovascularization; downregulated fibrogenesis-related genes; suppressing chronic immune responses	Xenogenic immunogenicity; endogenous virus	[53,70,152,153]
Porcine pericardium	Epicardial patch	Good carrier of cells and growth factors; appropriate mechanical strength (>40 MPa) preventing left ventricle dilatation; promoting vascular formation; increasing Sca-1 cells and c-kit cells in infarcted area; restoring cardiac functions	Xenogenic immunogenicity; endogenous virus	[154,155]
Porcine SIS	Epicardial patch	Providing structure support; enhancing regenerative response to repair cardiovascular defects; lower immunogenicity compared to porcine cECM	The risk of rupture due to high pressure; no effort for myocardial differentiation; relatively-low xenogenic immunogenicity	[136,156–159]
Porcine SIS	Hydrogel	Improving cardiac function; enhancing arteriogenesis and cell infiltration	No effort for myocardial differentiation; relatively-low xenogenic immunogenicity	[160]
Rat liECM	Powders	Suppressing myocardial necrosis; promoting neovascularization and cell-induction; inducing the migration of fibroblasts	Less effects on cardiogenesis; lack comprehensive evaluation	[161,162]

human cECM gradually loses abilities to form self-assembled hydrogels. In terms of composition, about 96.1 % matrisome proteins of pcECM overlapped with those matrisome proteins detected in human heart tissues, identified by proteomics [176]. Gene ontology biological process (GOBP) analysis showed that heart-enriched proteins were both found in pcECM and human heart tissues, which play roles in muscle contraction and development. These evidences show that pcECM has human cECM-like structural and matricellular components. The differences include that pcECM contained a desirable higher sulfated GAG content for extended retention of growth factors, while human cECM has specific components including periostin and fibulin-2. pcECM also presented higher mechanical stiffness but matched energy dissipation, toughness, and ultimate stress behavior [51]. The most significant problems of pcECM are the residual endogenous virus and α-Gal epitopes, both of which induce immune responses. Sarig et al. indicated that these natural, bioactive and non-supplemented acellular pcECM patches protected cardiac function (contractility, ventricular dimensions and cardiac remodeling) from further deterioration in both acute and chronic MI models. Moreover, pcECM recruited progenitors that differentiated into CM-like cells to form self-assembled "muscle-like" fibers and constantly upregulated the GATA binding protein (GATA4) and the myosin light chain (MYLC) which improved myocardial differentiation and ventricular contractility [51]. Christman et al. developed a pcECM injectable hydrogel and confirmed its safety and efficacy in improving cardiac function in the murine and porcine MI model, and in first-in-man trial [53,153,177–179]. Recently, Diaz et al. reported that pcECM hydrogel in a murine subacute MI model upregulated several key genes involved in cardiac muscle contraction, including ATPase sarcoplasmic/endoplasmic reticulum Ca^{2+} transporting 1 (Atp2a1), downregulated fibrogenesis-related genes containing transforming growth factor-β (Tgfb3), bone morphogenetic protein-2 (Bmp 2), Bmp 4, and suppressed chronic immune responses [180]. This study provides deeper insight into the mechanism of function of pcECM injectable hydrogel in treating ICM.

Considering the cost, processing stability, and immunogenicity, researchers have also extracted dECM from other tissues for cardiac repair [70,181–183]. Among all non-cardiac dECM sources, SIS materials and porcine urinary bladder matrix (UBM) are more abundant and processible compared to cECM, with higher batch-to-batch stability for clinical application [94]. Badylak et al. applied decellularized SIS for connective tissue repair in 1995 [184]. To date, SIS has been widely studied and successfully translated into commercial products approved by FDA [185]. SIS is composed of 90 % of collagen which is higher than the cECM matrix, with type I collagen being the dominant component, and types III, IV, V and VI collagen being minor, showing low immunogenicity and inflammatory reactions in clinical use [110]. CorPatch, a SIS multilayered sheet, is so far the only FDA-approved epicardial patch for ICM treatment, which have shown to improve cardiac functions and reduce fibrosis for patients [157,159]. SIS dECM is porous with 20∼30 μm pores, making them suitable for cell delivery [137,159,186]. Furthermore, SIS powders can be enzymatically digested to obtain soluble SIS for preparation of injectable SIS hydrogels [187,188]. However, compared to cECM, SIS lacks some important functional proteins, including annexin-6 (ANXA6), agrin (AGRN), cathepsin D (CTSD) and galectin-1 (LGALS1), which facilitate growth, adhesion, spreading, and maintenance of neonatal CMs [189–191]. Yang et al. reported that cECM hydrogel better improved cardiac function, inhibited fibrosis, and maintained ventricular wall thickness in MI model compared to SIS hydrogel [189]. On the other hand, since fibroblast growth factor 2 (FGF-2) is richer in SIS dECM, SIS was effective in promoting recellularization, reparative cellular activity and angiogenesis [157].

Similar to myocardium, skeletal tissue belongs to striated muscle tissue, having fibrous structure. Skeletal dECM (sECM) has unique collagen, heparin sulfate, and decorin not found in cECM [192]. However, sECM has not been applied in ICM model to confirm its expected therapeutic effects. According to proteomics, type VI and IV collagen networks were detected in liECM, which are used to anchor interstitial blood vessels and the surrounding connective tissues [103]. Type VI

collagen can also induce mesenchymal cell growth and proliferation, making it desirable for tissue remodeling. Tabuchi et al. adhered liECM powders to the MI area, which promoted neovascularization and inhibited CMs death, leading to more residual myocardium and vessels in the liECM-treated group [162].

ECM products, in essence, are a series of proteins coded and secreted by the resident cells; the specific ECM scaffolds, in turn, build niches for the cells and send them mechanical and biochemical signals through cell membrane receptors, thereby regulating cell fate [72]. Thus, cECM materials are undoubtedly favorable choices for myocardium reconstruction. However, human cECM is limited by patient-to-patient variability, while immunogenicity is a major problem for xeno cECM. More efforts should be made to improve technologies for cECM production, to make cECM materials safer and controllable. In addition, active components in cECM for cardiac repair should be identified and extracted further through advanced analytic techniques including proteomics. Considering safety, processability, and batch-to-batch stability, CorPatch is the first dECM patch to obtain FDA clearance to enter clinical market, despite it showed less positive effects on cardiac repair compared to cECM [157]. Active components could be added into SIS to enhance cardiac repair. For example, agrin, a large extracellular heparan sulfate proteoglycan, is a promising additive to promote cardiac regeneration after MI [193]. In terms of the effectiveness of sECM and liECM for ICM, more *in vitro* and *in vivo* experiments are required to compare with cECM. There have been different strategies of dECM materials carrying cells and growth factors applied for ICM, as listed in Table 3.

3. dECM cardiac patches

3.1. Treatment effects of dECM patches for ICM

dECM patches can not only provide mechanical and structural support to the damaged myocardium, but also promote cardiac repair by intrinsic bioactivity or delivering cells or biomolecules. Sánchez et al. cultured MSCs, cardiovascular progenitor cells (CPCs), CMs (H9C2, HL-1), and human umbilical vein endothelial cells (HUVECs) on human cECM scaffolds, respectively [206]. CMs infiltrated the cECM and organize within the fibers into new muscle bundles that exhibit mature calcium dynamics and electrical coupling. Although MSCs can infiltrate

Table 3
Strategies of dECM materials in treating ICM.

dECM source	Material form	Other ingredients	Delivered cells or other biocues	Results for treating ICM	Ref.
Human myocardium	Multilayered patch	Fibrin glue	TGF-β conditioning human mesenchymal progenitor cells (MPCs)	Angiogenesis and arteriogenesis ↑; restoring heart function↑; SDF-1 expression of MPCs↑	[96]
Human pericardium	Scaffold patch	None	Wharton's jelly-derived mesenchymal stromal cells (WJ-MSCs)	Cardiac scar reduced ~9 %; left ventricular end-diastolic volume (LVEDV) and left ventricular end-systolic volume (LVESV)↓	[54]
Human pericardium	Scaffold patch	None	Adipose tissue mesenchymal stem cells (ATMSCs)	Cell retention and penetrance↑; vascularization and cardiomyogenesis↑; left ventricular ejection fraction (LVEF)↑; LVESV↓	[105]
Porcine myocardium	Scaffold patch	None	Embedded cardiac stromal cells (synCSCs) secrete factors	Scar size↓, viable myocardium↑, the proliferation of CMs↑, promoted angiogenesis and improved cardiac function	[194]
Porcine ventricular myocardium	Scaffold patch	Gelatin methacryloyl (GelMA)	Cardiac progenitor cells (CPCs)	Vascularization↑	[195]
Porcine myocardium	Scaffold patch	None	Rat myoblasts (L6, ATCC CRL-1458)	Expression of cardiac genes like Myh6 and Actn1↑	[101]
Porcine myocardium	Scaffold patch	None	CPCs, mesenchymal stem cells (MSCs), vascular endothelial growth factor (VEGF)	Cell migration↑, cardiac functions↑, remodeling and fibrosis↓, cardiomyogenesis↑, neovascularization↑	[196]
Porcine SIS	Scaffold patch	None	None	Attenuated pathological left ventricular remodeling, cardiac function↑, LVEDV↑, vascularization↑	[52, 197]
Porcine SIS	Scaffold patch	None	MSCs	T cell infiltration and adaptive immune response↓, scar tissue↓	[136]
Porcine SIS	Scaffold patch	None	Pluripotent stem cell-derived cardiovascular progenitor cells (CVPCs) and CMs	LVEF↑, left ventricular fractional shortening (LVFS)↓, cardiac function↑, ventricular dilation↓	[198]
Human lung fibroblasts	Stretchable membrane patch	Polyvinyl alcohol (PVA) hydrogel	MSCs	Cell apoptosis↓, left ventricular internal diameter (LVIDs)↓, fractional shortening (FS)↑, fibrosis in the infarcted tissue↓, myocardial differentiation↑	[199]
Porcine myocardium	Injectable hybrid hydrogel	Glucomannan	Proangiogenic peptide	Host cell infiltration↑, M2 macrophage polarization↑; angiogenesis↑; cardiomyocyte survival↑	[200]
Porcine myocardium	Hydrogel	None	None	Vascular cell migration↑; proliferative cells↑; arteriole density↑; viable myocardium↑; cardiac funcitons↑	[153, 177, 179]
Porcine myocardium	Hydrogel powders	None	None	Cardiac function↑; vessel density↑; left ventricular remodeling↓	[201]
Porcine myocardium	Hydrogel	None	CMs and stromal cell-derived factor 1 (SDF-1)	The survival and residence of transplanted CMs ↑; the coupling of transplanted CMs in the infarct area↑; angiogenesis↑	[202]
Porcine myocardium	Hydrogel	None	Human pulmonary microvascular endothelial cells (HPMVEC); adipose tissue-derived stromal cells (ASC)	Robust vascular networks with longer and thicker strcture↑; TGF-beta 1-induced differentiation↓	[203]
Porcine SIS	Hydrogel	None	None	Infarct size↓; angiogenesis↑; preservation of end-systolic left ventricular geometry; cardiac contractility↑	[187]
Porcine spleen	Hydrogel	None	iPSC, CMs and endothelial cells (ECs)	EF↑; FS↑; LVDS↓; LVDD↓; fibrosis↓; retention of delivered cells↑; neovascularization↑	[204]
Zebrafish heart	Hydrogel	None	None	LVEF↑; end-diastolic area (EDA) ↓; end-systolic area (ESA) ↓; the proliferation of CMs↑	[205]

into the three-dimensional framework of dECM and express CM marker genes, they do not adopt CM-like orientation. Compared to Matrigel and Geltrex, which commonly used as 3D cell culture materials, cECM can specifically induce iPSCs and ESCs to express cardiac-specific markers including cardiac α-myosin heavy polypeptide 6 and cardiac troponin T2 [142]. Chang et al. implanted SIS-ECM cardiac patch with MSCs into pigs, which effectively extended the retention of MSCs *in vivo* [136]. The addition of MSCs significantly reduced the immune response of adaptive T cells to SIS-ECM, but showed no other therapeutic effects, since the engineered patch was applied to a non-injury model. Tan et al. seeded bromodeoxyuridine (BrdU)-labeled MSCs on SIS-ECM material and implanted them onto the myocardial infarct area in rabbits [137]. After 28-day treatment, the authors observed that BrdU-positive MSCs migrated from the patch to the infarcted area, expressed myogenic proteins including troponin T (cTNT), differentiated into cardiomyocyte-like cells, and participated in vascular formation, increasing the capillary density in the infarct area. However, the treated infarct area did not express Cx43, indicating that MSCs did not establish electrical coupling with the host [137]. Huang et al. encapsulated CSC-secreted factors into PLGA microparticles, and embedded them into a cECM scaffold to produce a cardiac patch, avoiding using living cells. The transplanted myoECM patches reduced scaring, facilitated angiogenesis, and boosted cardiac function in rodent and porcine MI models [194].

Significant progress has been made for dECM patches in clinical translation. Prat-Vidal et al. recently reported the first-in-man results of MI patient treatment by allogeneic decellularized pericardial matrix (PeriCord) bioimplant containing human viable Wharton's jelly-derived MSCs (WJ-MSCs) [54]. This allogenic dECM/WJ-MSCs bioimplant effectively reduced the scar size in cardiac wall (~9 %) without adverse reactions like myocarditis. A SIS dECM patch product, CorPatch (CorMatrix Cardiovascular, Inc) has been approved by FDA. The four-layer CorPatch consists of structure proteins, adhesion glycoproteins, glycosaminoglycans and proteoglycans, and key growth factor (FGF-2) (Fig. 3A) [207,208]. Through releasing FGF-2, CorPatch can alter the fibroblast secretome (increasing the expression of FGF-2, VEGF and HGF), benefit angiogenesis and downregulates fibrosis pathway [197,208]. Mewhort et al. treated rats with chronic ischemia with epicardially implanted CorPatch for two weeks, and reported significant improvements in ejection fraction (EF), ESV, end-diastolic volume (EDV) and anterior wall thickness compared to non-treated groups [52]. Also, CorPatch increased the concentration of FGF-2 in myocardium and promoted post-infarct neovascularization compared to control groups. Afterwards, the porcine ischemia-reperfusion model induced by ligating the left anterior descending artery for 75 min was generated to further detect the effects of CorPatch as an epicardial patch (Fig. 3B) [209]. The results showed that CorPatch increased the thickness of epicardium, reduced fibrosis, and increased blood vessel formation. These preclinical data built a solid foundation for clinical studies. When human fibroblasts were cultured on CorPatch, their morphology and transcriptome changed to favor proangiogenic pathways and downregulated fibrotic pathways compared to SIS patches without FGF-2, which indicated that FGF-2 was a key signaling factor for post-infarct repair [197]. Fedak et al. implanted CorPatch into MI patients during bypass graft (CABG) surgeries [197]. After 6 months, CorPatch treated patients exhibited more revascularization and regional myocardial perfusion (Fig. 3C). These clinical results are inspiring and consistent with related findings from animal studies, but patch implantation still requires open-chest surgery. Minimally invasive patch implantation procedures need to be developed to lower surgical risks so that to expand the subgroup of MI patients who could benefit from ECM patch treatment.

In cardiac tissue engineering, the performance requirements for cardiac patches are quite complex. However, physicochemical decellularization processes could damage ECM bioactive composition, structure, and mechanical properties [210], and pure dECM materials lack processability and electrical conductivity [96,146]. In addition, most dECMs present challenges of weak mechanical properties and poor processability. Compositing is a viable approach to improve dECM substrate performance and supplement functions.

The incorporation of synthetic polymer materials with dECM offers a promising avenue for enhancing the mechanical properties of the latter. For instance, Pok et al. enhanced the mechanical strength of dECM patches by integrating a PCL core, elastic modulus increased from 13.2 kPa to 300 kPa [211]. Kim et al. extracted fibroblast-derived ECM (hFDM) and composited it with polyvinyl alcohol (PVA) via cyclic freeze-thaw steps, which was then punched onto a PVA/polyethylene glycol (PEG) hydrogel substrate to obtain a highly elastic and stretchable ECM membrane (Fig. 4A and B) [199]. This membrane exhibited superior performance in facilitating cell adhesion and proliferation, inducing H9C2 cell connection to form a cohesive network, which induced the formation of cardiomyocyte clusters (Fig. 4C). As a cardiac patch, the composite significantly upregulated cardiac differentiation markers of human MSCs, reduced cardiac cell death and fibrosis, and attenuated left ventricle (LV) remodeling post-MI. Da et al. first

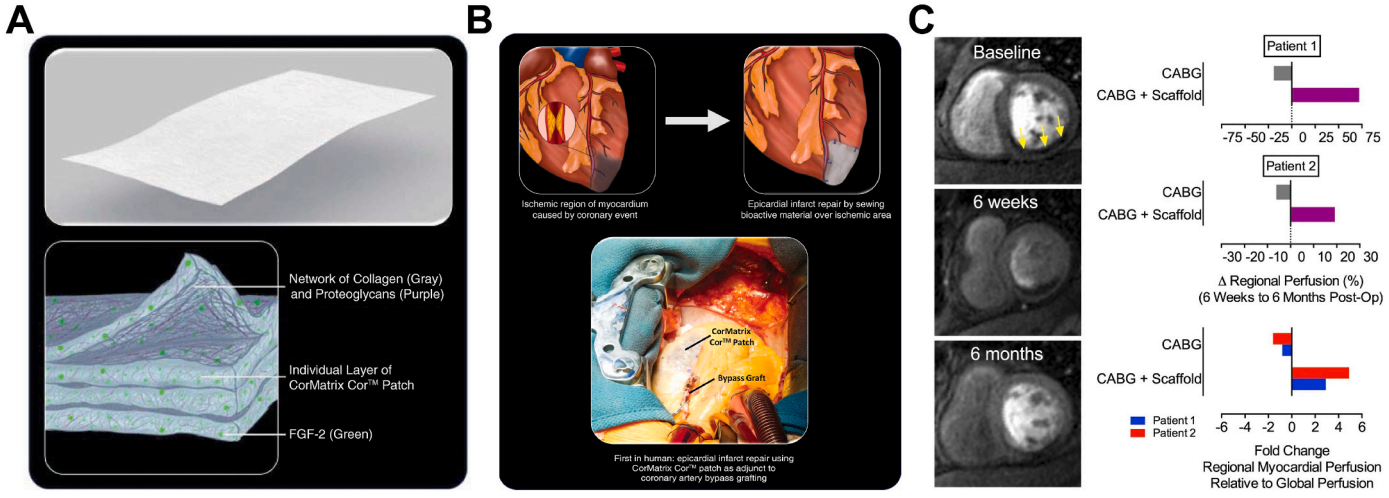

Fig. 3. A commercial epicardial patch for ICM. (A) The CorPatch sheet with 4-layer structure and its components. (B) CorPatch was used as an epicardial patch for infarct myocardial repair. Modified and adapted with permission from Ref. [208]. Copyright 2023, Future Science Group. (C) Cardiac MRI images and regional myocardial perfusion of human left ventricle treated by CorPatch at baseline, 6 week and 6 month. Modified and adapted with permission from Ref. [197]. Copyright 2023, Springer Nature.

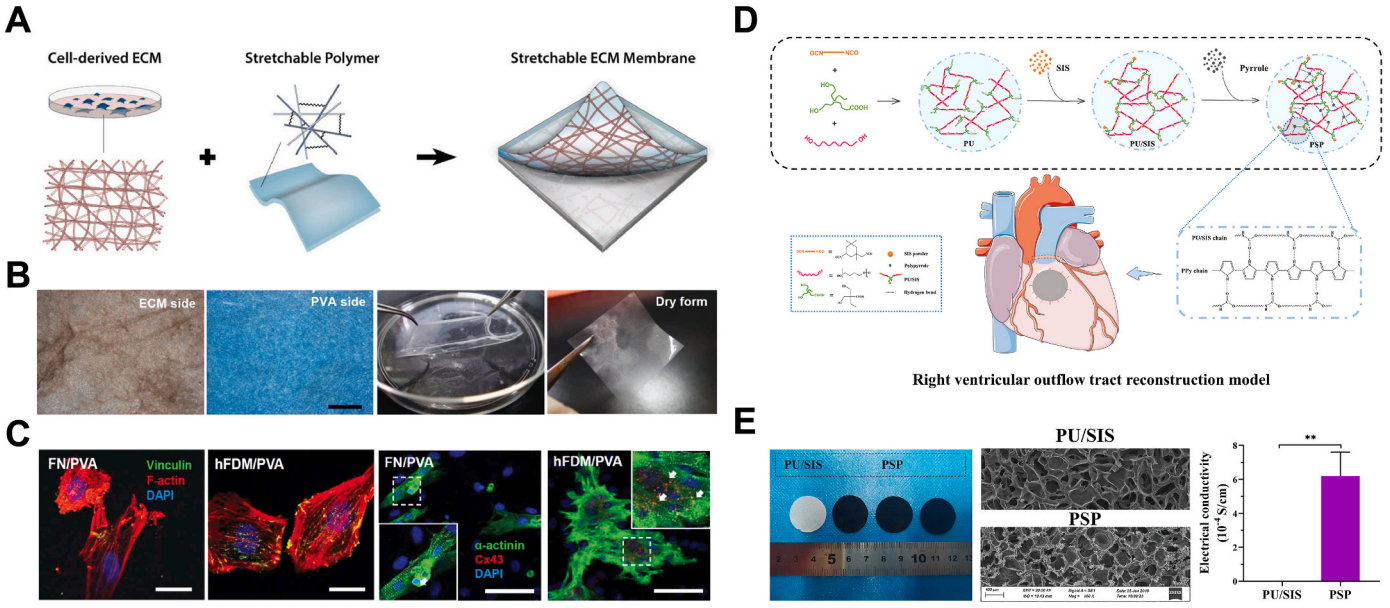

Fig. 4. Composite dECM epicardial patches for ICM. (A) Fabrication scheme and (B) photos of stretchable fibroblast-derived ECM (hFDM)/polyvinyl alcohol (PVA) membrane (hFDM/PVA) (Scale bar: 500 μm). (C) An increase in focal adhesions observed between H9C2 cells and hFDM/PVA membrane (red: f-actin; green: vinculin; blue: nuclei). Primary ventricular CM cultured on hFDM/PVA express higher levels of connexin-43 (red) and α-actinin (green) than those on fibronectin-coated membrane (FN/PVA) (scale bar: 100 μm). Modified and adapted with permission from Ref. [199]. Copyright 2019, Wiley-VCH. (D) Scheme for the fabrication process of a novel polyurethane/SIS patch (PSP) with an electrical coating for right ventricle wall replacement. (E) Gross appearance and ultrastructure of the PU/SIS and PSP composites under a SEM and their electrical conductivity properties. Modified and adapted with permission from Ref. [213]. Copyright 2022, Elsevier.

synthesized polyurethane (PU) with carboxyl side groups; and they dispersed SIS powder in PU emulsion followed by lyophilization to form PU/SIS foams which were further stabilized by amide-reactive cross-linking via N-hydroxysuccinimide (NHS) and 1-(3-dimethylaminopropyl)-3-ethylcarbodiimide hydrochloride (EDC) catalyst (Fig. 4D) [212]. The foams supported surface-polymerization of a layer of conductive material polypyrrole (PPy), yielding a PSP scaffold with electrical conductivity (0.0016 S/cm), comparable to native myocardium (Fig. 4E) [213]. As a substitute for rabbit right ventricular wall tissue, PSP promoted cell infiltration, tissue integration, and degradation, compared to bovine pericardial material, leading to a more favorable repair outcome. Kashiyama et al. developed elastic microfibrous, porous composite cardiac patches by electrospraying porcine cardiac ECM hydrogels onto electrospun polyester carbonate polyurethane urea (PECUU) membranes [214]. The patches increased retention of incorporated adipose-derived stem cells (ADSCs) on LV epicardium, improved LV contractility, and prevented remodeling 8 weeks after treatment.

Combining natural biomaterials with dECM can increase the complexity of mechanical properties and manufacture stability, but more importantly, maintain or even enhance its biological activities. Godier-Furnémont et al. decellularized human cECM slices preserving the tangential modulus of a relaxed native tissue with pores (~16.7 ± 3.5 μm) [96]. When the slices are stretched along the circumferential direction, it has large interconnected pores and smooth channels which facilitate oxygen and nutrient transport. The authors combined porous dECM slices with fibrin from patient blood and human mesenchymal progenitor cells (MPCs) to produce a three-layered patch. The porous structure of implanted patch supported cell migration into the infarcted tissue, integration with the host myocardium, and angiogenesis. Bejleri et al. bioprinted a cardiac patch composed of GelMA and cardiac dECM with encapsulated human cardiac progenitor cells (hCPC) at low temperature, which was crosslinked via white light polymerization and 37 °C bath [195]. The geometry of the patch did not change before or after the addition of cells, showing shape stability. Compared to pure GelMA patches, GelMA-cECM patches improved the differentiation and angiogenesis potential of hCPCs, as shown by higher vascularization level in a rat MI model in which the patches were epicardially implanted.

3.2. Advanced dECM patch manufacturing

Attributed to the unique biomimicry physical properties and tunable extraction methods of dECM, advanced manufacturing including electrospinning and 3D bioprinting can be employed.

Although dECM patches or hydrogel have been obtained through simplified decellularization and/or digestion, it is challenging to control or adjust them to achieve desirable properties due to their weak strength, low reproducibility and scalability [94,215–217]. Electrospinning is simple, controllable, and effective for creating ECM-mimicking microfiber and nanofiber architectures, which contain interconnected pores for faster nutrient transportation and cellular growth and proliferation [218–221]. However, it is difficult to electrospin dECM as electrospinning their synthetic polymer counterparts [222–224]. So far, there are few successful cases of electrospinning isolated dECM without the assistance of synthetic additives. There are two main methods to fabricate dECM electrospinning membranes: 1) adding dECM hydrogel to electrospun membranes of other materials, and 2) directly electrospinning dECM pre-mixed with other components [76]. The former one is essentially functionalization of electrospun membranes using dECM hydrogel, which does not influence dECM bioactivity without exposing dECM to organic reagents or high electric voltage. For example, Krishnamoorthi et al. employed wet electrospinning techniques to biofabricate a PLGA fibers which was further modified by pcECM hydrogel, preventing the denaturation of pcECM (Fig. 5A) [225]. The principal challenge of latter one is to simultaneously achieve high ECM bioactivity and fiber stability. Organic solvents and high-voltage drawing during electrospinning could denature ECM proteins and impair their bioactivity. In addition, these dECM fibers with large surface areas could be wetted and swell quickly when being exposed to water, and gradually lose fibrous morphology, leading to insufficient fiber strength and stability. Crosslinking subsequent to fiber fabrication is a convenient and effective strategy to stabilize dECM

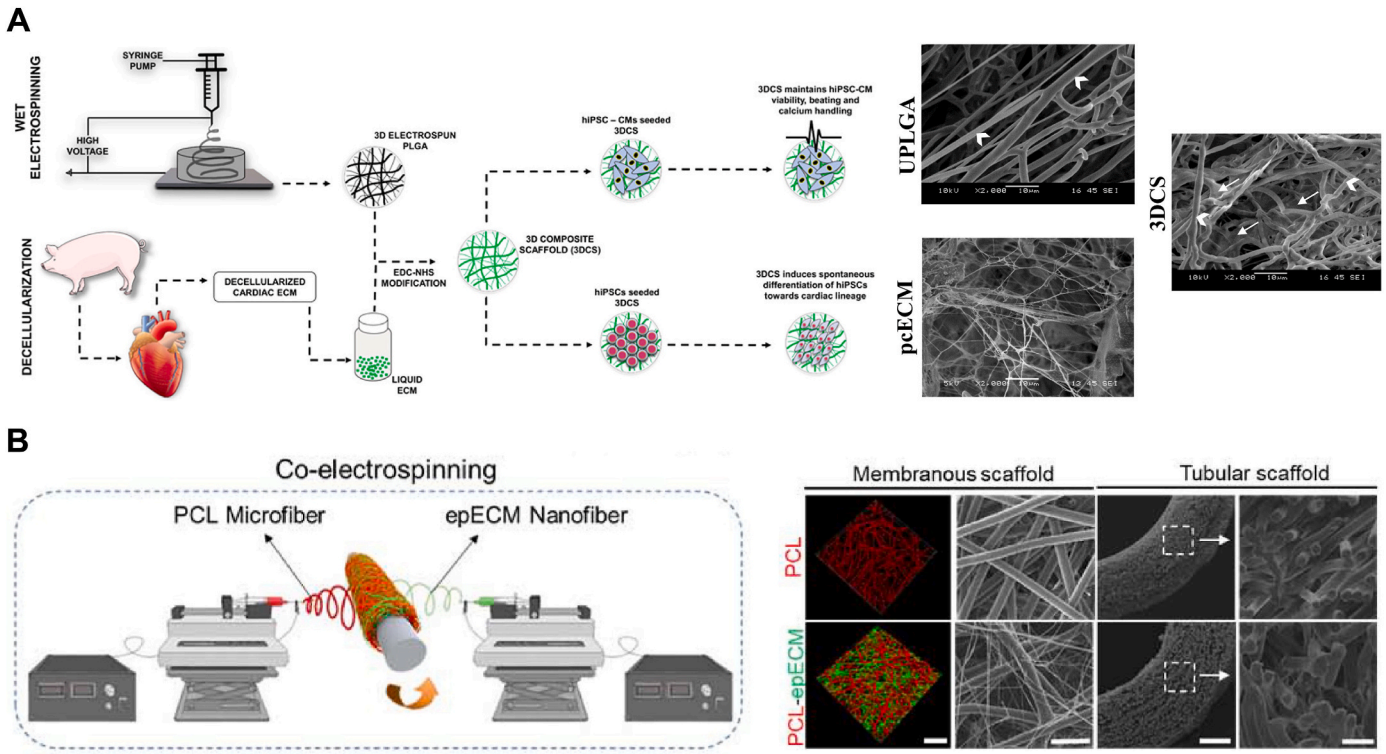

Fig. 5. Synthetic polymer-assisted electrospinning techniques. (A) A composite pcECM/PLGA membrane, 3DCS, was fabricated via wet electrospinning techniques: 1) biofabricating a PLGA fibrous scaffold, 2) modificating PLGA fibers with pcECM hydrogel, 3) seeding cells onto fibrous scaffolds; Fibrous scaffold morphologies (PLGA, pcECM and 3DCS) characterized through SEM. Modified and adapted with permission from Ref. [225]. Copyright 2020, American Chemical Society. (B) Schematic illustration of the fabrication process of hybrid fibrous scaffolds by co-electrospinning; confocal images and SEM images of PCL and PCL-epECM membranous and tubular scaffolds. Modified and adapted with permission from Ref. [228]. Copyright 2022, Elsevier B·V.

fibers. Crosslinking agents, typically glutaraldehyde (GA), are used due to their low cost but are known to leave toxic groups and decrease bioactivity, biocompatibility and fine structure of electrospun dECM [226,227].

Efforts have been made to solve the key issues in dECM electrospinning [229–233]. To avoid utilizing GA, Heydarkhan-Hagvall et al. tried adding PCL to the electrospinning precursor composing of collagen and elastin to increase fiber stability and enhance its mechanical properties [226]. Alternatively, Liu et al. co-electrospun PCL and human placental dECM from opposite sides of the collecting mandrel to build a hybrid scaffold with good mechanical property to resist blood pressure (Fig. 5B) [228]. Deng et al. otherwise coaxial electrospun aligned core-shell nanofibers composed of PCL (as the core) and dECM (as the shell) [219]. Compared to pre-blended PCL/dECM fibers, core-shell PCL/dECM fibers exhibited higher packing density and ductility. Schoen et al. attempted to improve the processability of dECM without damage to the natural properties of dECM. In this case, 1,1,1,3,3,3-hexafluoro-2-propanol (HFIP) was employed to dissolve pcECM into a homogeneous solution, which inevitably disrupted the hydrophobic domain of pcECM and denatured it. PEO was added to increase solution viscoelasticity and inhibit fiber bead formation, which led to successful fabrication of a mechanically-strong electrosinning pcECM scaffold (ES-pcECM) compared to the acellular pcECM scaffold. ES-pcECM can self-assemble at 37 °C in a humidified environment, mimicking native cardiac ECM in both structure and hydrophilicity [227]. This self-assembly process stabilized the fibers without using toxic crosslinking agents, which increased biocompatibility and alleviated immune response upon *in vivo* implantation. Despite of the denaturation of pcECM, ES-pcECM could still support the synchronized beating of natal rat CMs. However, when culturing iPSCs and MSCs, this work only analyzed the cytotoxicity of ES-pcECM without further evaluation of its effects on cardiac differentiation. In this case, it is difficult to conclude whether dECM denaturation during electrospinning lead to loss in capability of promoting regeneration. In addition, electrospinning techniques for dECM manufacture is limited by a lack of standard evaluation systems, and requires more modifications on chemistry and biofabrication in the future.

3D bioprinting is an additive fabrication process, which is highly repeatable, which is desirable in commercial production. 3D bioprinting featured with precise spatial deposition of hydrogel prepolymer solutions, cells, and bioactive factors using computer-aided design has been widely employed for fabricating biomimetic patches for ICM treatment [220,234–237]. dECM offers advantages over traditional bioinks, as it maintains the composition and micro/nano structure of natural ECM [101,238,239]. Although various 3D bioprinting technologies have been developed, only Digital Light Processing (DLP) printing and extrusion-based printing support dECM bioprinting so far. Before bioprinting dECM, it must be made into the soluble status for extrusion. Methods of solubilizing dECM is described in Section 4. Before cell encapsulation and being extruded through the deposition nozzles, the soluble dECM bioink through a process combining physical, chemical and enzymatic treatment should be adjusted to a physiological state, particularly its pH [101]. Under heating above 37 °C for a while, soluble dECM can transfer into hydrogel. These rheological properties and temperature-triggered self-assemble support its bioprinting applications.

Despite, the difficulty of dECM bioprinting is mainly attributed to the slow gelation and low mechanical strength of dECM, which hinders printability and shape fidelity of dECM constructs. For device printing, uniform heating of pre-gel constructs could theoretically achieve complete gelation, homogeneous shape fixation, and higher mechanical strength [240]. Increasing the dispensing speed and decreasing the nozzle diameter contribute to reducing the width of dECM printed columns, achieving higher patterning accuracy [241]. To increase the weak

strength and low viscosity of dECM bioinks, numerous strategies have been reported in terms of chemical modification or physical enhancement. As injectable dECM hydrogel shares this problem, the detailed methods for chemical modification is discussed in Section 5.

To improve the processability of dECM bioinks, physical strategies can be employed, including increasing the concentration of dECM solute and using support baths, sacrificial polymers, or external supporting structure to preserve dECM during gelation. Increasing the concentration of dECM solution results in denser and thinner hydrogel lines, yet highly viscous bioinks exert high shear stress to cells during extrusion, lowering cell viability [242,243]. Accordingly, 1–2% is the optimized dECM concentration balancing pros and cons [196,244]. Adding sacrificial Pluronic F-127 to dECM solution can increase the viscosity of bioink and provide mechanical support for the constructs [245,246]. During dECM gelation under 37 °C, Pluronic F-127 melts and can be removed from the scaffold. Supporting baths with reversible sol-gel transition, like a slurry of gelatin granules or a shear-thinning synthetic hydrogel, are under gel status during bioprinting, which is distinct from low-viscous dECM fluids [247–249]. For example, packed gelatin particles act like Bingham plastic during dECM bioprinting, with a high viscosity at low shear stresses but turning to a viscous fluid at higher shear stress. Extrusion of dECM fluids in such bath can be operated smoothly without mechanical resistance, while the deposited dECM is held in place [250]. The gelatin particles can then turn into solution and be removed from container. The resultant dECM scaffold is porous and longitudinally aligned. Cui et al. bioprinted a cell-laden dECM scaffold mimicking a vascularized muscle tissue in a gelatin granule-based printing reservoir with PVA to accelerate dECM crosslinking [251]. Geometrical features of printed dECM scaffold offer organized microenvironment cues which guides cell fate and improves vascularization, functional restoration, etc. Polycaprolactone (PCL) or poly (ethylene/vinyl acetate) (PEVA) scaffolds printed by traditional fusing 3D printing have sufficient structural stability and provide initial geometrical restriction to dECM pre-gel solutions [238,239,252–254]. Pati et al. developed a multi-head tissue/organ building system, which is capable of precisely positioning both PCL framework and dECM gel precursor in tissue constructs (Fig. 6A) [239]. Das et al. printed a needle-like PEVA framework to assist the fixation of pcECM bioink carrying neonatal rat CMs (Fig. 6B) [252]. Compared to collagen I 3D construct, the pcECM 3D scaffold upregulated expression of cardiac-specific proteins of CMs. Under dynamic culture condition, cardiac regulatory proteins of CMs in the pcECM scaffold presented a more aligned, uniform, rod-like structural arrangement with Z-disk integrity, and enhanced cell-cell and cell-ECM interaction. Jang et al. utilized two types of stem cell-laden dECM (hdECM containing CPCs and MSCs with VEGF factors) bioinks to construct a 3D pre-vascularized patch (Fig. 6C) [196]. hdECM recapitulated cardiac tissue specific microenvironments and significantly enhanced the maturation of cells and generation of microvascular-like tissue *in vitro*. After being adhered onto the epicardium of the rat MI model for 8 weeks, the hdECM patch significantly attenuated left ventricular remodeling and improved EF. Compared to bulk hydrogels, porous 3D bioprinted scaffolds support transportation of nutrients and metabolites, which is essential for cell viability and cellular activities. Recently, automated design and fabrication of cardiac micro-physiological devices have provided deeper insights into tissue morphogenesis, pathogenesis, and drug-induced structural and functional remodeling, which may help to reveal the repair mechanisms of dECM for ICM [255]. Yong et al. developed a tissue-sensor platform based on 3D printing of several thermoplastic inks, and embedding bioprinted cell-laden pcECM on it [256]. The pcECM bioinks containing

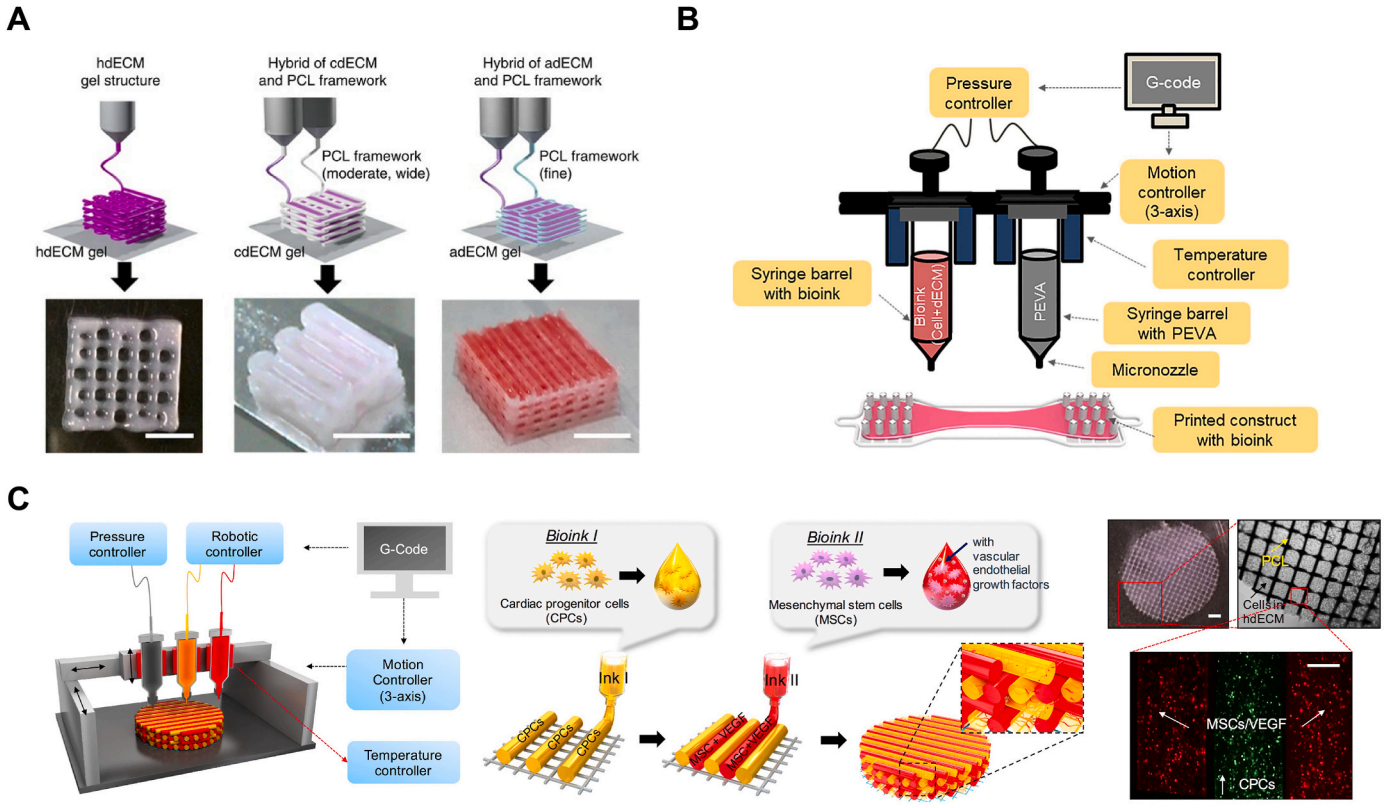

Fig. 6. dECM constructions fabricated by modified 3D bioprinting for treating ICM. (A) Tissue constructs was printed with only dECM or in combination with PCL framework (scale bar, 5 mm). Modified and adapted with permission from Ref. [101] Copyright 2014, Springer Nature. (B) Fabrication of cell-laden cECM bioink by using a 3D bioprinter. Modified and adapted with permission from Ref. [252] Copyright 2019, Elsevier. (C) Schematic illustration of the fabrication of pre-vascularized stem cell hdECM patch via a 3D printing system and the product patch including the two types of cell-laden bioink and PCL supporting layer (scale bar (left top), 1 mm; scale bar (bottom), 200 μm). Modified and adapted with permission from Ref. [196] Copyright 2020, Elsevier.

hiPSC-CMs and human cardiac fibroblasts (hCFs) were deposited in the direction parallel to the bipillar anchors onto the sensor to induce cell alignment. The aligned cells integrated into anisotropic engineered cardiac tissue, whose contractile activity and cardiac differentiation was monitored by the tissue-sensor platform. Integration of 3D bioprinting with other biofabrication techniques (including organs-on-a-chip, microfluidics-assisted extrusion bioprinting, and four-dimensional bioprinting) is expected to improve manufacture accuracy and efficiency for treating ICM by combining their corresponding advantages.

4. Injectable dECM hydrogels

4.1. Manufacture of soluble dECM

dECM can be processed into injectable materials via three main routes. The first method is to grind dECM into powders. At the time of use, the dECM powders are re-swollen in an aqueous suspension for subsequent injection. The corresponding clinical products include demineralized bone matrix (Grafton® Putty, DBX® Putty, AlloMatrix Injectable Putty), bladder matrix (MatriStem), dermis powder (AlloDerm), SIS ECM (CorMatrix Injectable ECM), etc [160,257]. Tabuchi et al. fractured dECM into powders with size below 500 μm [162]. The injectability of dECM powders depends on coupling between the particle size and the inner diameter of needles. Beachley et al. combined cryomilling and sonication techniques to treat dECM in order to obtain finer particles (<40 μm) [258]. After mixing with GAG polymers at 1:1, the dECM hydrogel reached a storage modulus of ~500 Pa compared to that of the control GAG hydrogel (~50 Pa). The second way to obtain injectable dECM is enzymatically digesting pelleted dECM into dECM solution without visible particles. The dECM solution can self-assemble into a nanofibrous hydrogel at 37 °C, allowing *in situ* gel formation upon *in vivo* injection [259]. Freytes et al. stirred dECM powders in pepsin with 0.1 M hydrochloric acid (HCl) over 48 h; the soluble dECM cross-linked into a weak hydrogel with a storage modulus between 20 and 25 Pa [259]. VentriGel was obtained by first digesting pcECM in acidified pepsin solution for 48 h under constant stirring and subsequent incubation, which presented a low storage modulus at 12.36 Pa [177,179,260]. Obviously, although pepsin is an effective method of solubilization, it can cause degradation and denaturation to dECM and damage the bioactive factors in dECM networks [261,262]. Johnson et al. found that raising the salt concentration increases the gelation time and enhances the mechanical strength of the final hydrogel [152]. The third method replaces partial digestion in the second method with extraction through high-concentration urea to retain key proteins and growth factors of dECM [263]. Poon and Uriel et al. homogenized and dispersed dECM directly at physiological pH to physically disrupt the tight structure of collagen fibrils and fibronectin, and then further treat it with a highly concentrated urea solution to break non-covalent bonds to increase the solubility of ECM proteins [264,265]. The hydrogel precursor solution obtained by this process gels not only by increasing the temperature to 37 °C, but also by lowering the pH to 4.0. Recently, Hussey et al. proposed to obtain ECM solution by resuspending pelleted ECM with subsequent ultrasonic cavitation at 20 kHz [266]. This method did not affect the triple helix structure of collagen, maintaining the integrity of collagen fibers. Compared to protease-treated dECM, the sonicated ECM self-assembled into a gel below 25 °C and kept stable and strong (~3000 Pa) between 37 °C and 4 °C. This sonicated method extended the concentration range of ECM hydrogels from 2 to 20 mg/mL (enzymatic digestion method) to 25–100 mg/mL and significantly reduced the processing time from 2 to 3 days to a few minutes.

4.2. Clinical experience of dECM hydrogel

Because dECM can gel at a physiological temperature, clinicians can inject refrigerated dECM pregels directly into damaged myocardium to rapidly form dECM hydrogels *in situ*. Christman et al. developed an injectable pcECM hydrogel (VentriGel) that self-assembled into nanofibrous and porous hydrogel scaffold in the physiological environment [179]. They tested the safety and efficacy of the injectable hydrogel in a porcine MI model [177]. During the first week after injection, cECM did not show an increased likelihood of inducing arrhythmias compared to saline, demonstrating safety for cardiac use (Fig. 7A). They verified that hydrogel injected into myocardium could maintain and increase endogenous CMs in the infarct area. Compared to saline injection, VentriGel effectively restored cardiac function, as revealed by higher EF, smaller ESV and LV (EDV) 3 months post injection. Also, this hydrogel was successfully delivered via a percutaneous and transendocardial route into myocardium, supporting minimally invasive injection. In addition, no chronic inflammatory response or thrombogenicity was observed, which laid the foundation for clinical translation of VentriGel. Christman et al. explained the mechanism of VentriGel treating heart failure via whole-transcriptome microarrays [260]. One week after VentriGel injection, myocardium exhibited reduced cardiac fibrosis/hypertrophy, recruitment of progenitor cells, induction of cardiac transcription factors, altered tissue metabolism, increased angiogenesis and vascular development, and reduced CM apoptosis. Ventrigel also altered the immune response with increased macrophage migration and activation toward the M1 phenotype which was attributed to proinflammatory and pro-remodeling responses but also necessary for tissue regeneration. First-in-man study of VentriGel treating early and late MI patients (Fig. 7B) showed that VentriGel significantly increased the maximum walk distance and quality of life scores with at 3 and 6 months post-injection without severe adverse events cause by material or mapping/injection procedure [53]. After 12-month treatment, for late MI patients, ESV showed a trend of decrease, and volume of myocardium increased [53]. VentriGel has entered phase 1 clinical trial (NCT02305602).

4.3. dECM microsphere manufacturing

dECM could be transformed into injectable microgels with micrometer-scale connected pore structure which facilitates cell migration and tissue infiltration, thus making it a promising material platform for cardiac tissue engineering. Du et al. co-cultured MSCs, and HUVECs with a mixture pregel of decellularized human lung fibroblast-derived matrix (hFDM) and collagen to form tissue-like hydrogel microspheres [267]. With extended culture time, the microgels contracted, driven by the cells and showed good pro-angiogenic ability. Microfluidic technologies have been applied to fabricate microspheres by utilizing various polymers in combination of cells and growth factors. Lin et al. utilized a microfluidic system to fabricate porcine decellularized peripheral nerve matrix (pDNM) hydrogel microspheres (Fig. 8A) [268]. The pDNM microgel provided a highly bioactive microenvironment to support cell growth and proliferation (Fig. 8B). Lee et al. utilized a flow-focusing microfluidic device to continuously produce dECM microgels composed of cECM, liECM, luECM, kECM and SIS with a controlled and uniform size (Fig. 8C). Cells were reprogrammed into induced cardiac (iCar) cells and embedded in cECM hydrogel microspheres, that latter protected cell viability when passing the microchannel. Immunofluorescence staining of iCar cells in cECM beads showed positive cardiac markers including cTNT and α-actinin (Fig. 8D). The small size of dECM microspheres theoretically support minimally-invasive injection via percutaneous coronary intervention.

5. Functional enhancement of dECM hydrogels

While dECM from natural tissues has excellent bioactivity and potential to promote tissue regeneration, their slow and incomplete gelation kinetics limit the stability of their constructs and make it difficult to match the mechanical properties of natural myocardium. dECM self-assembled hydrogels usually present poor mechanical properties, making them prone to collapse, and limit their applications in cases where

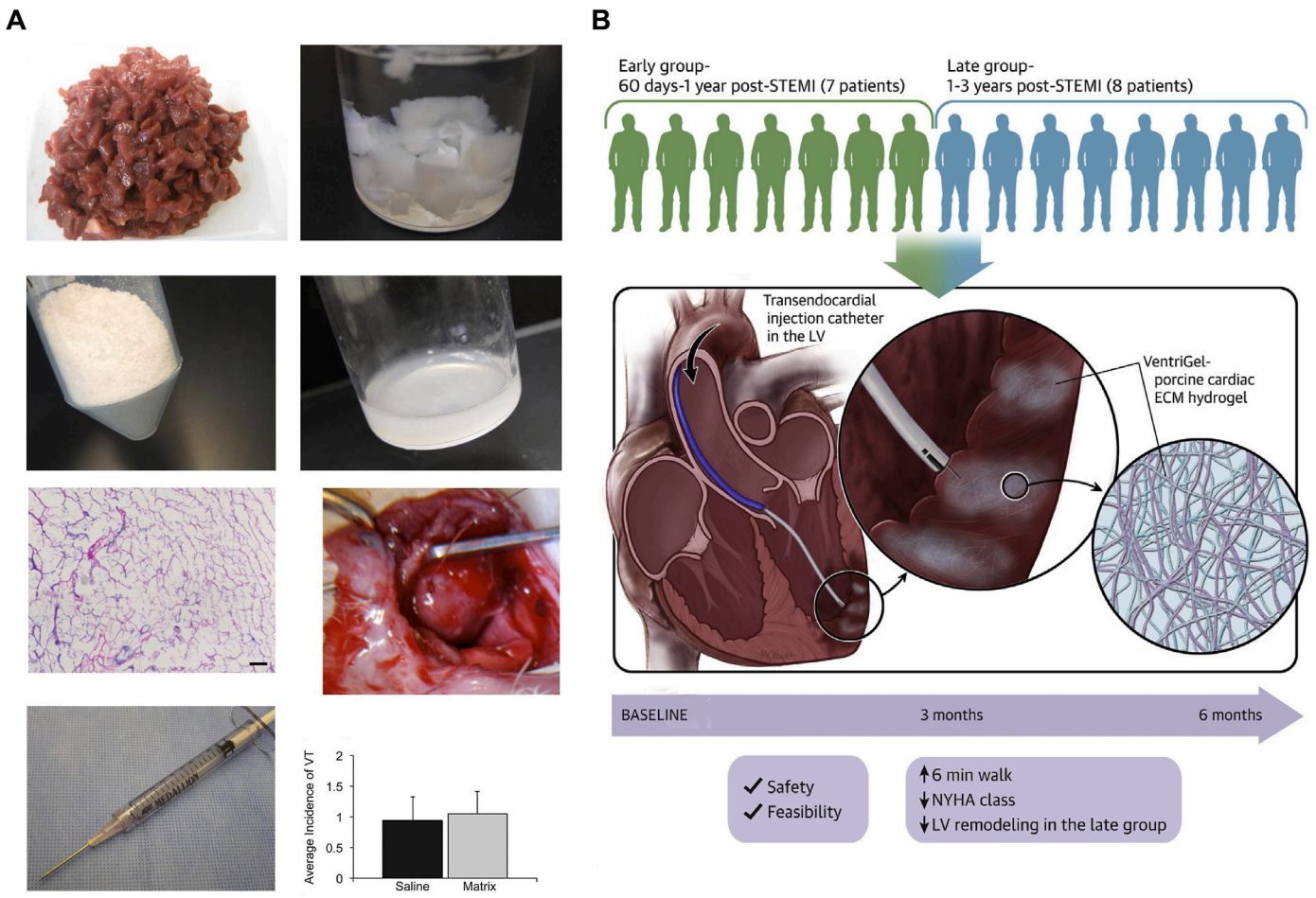

Fig. 7. A commercial and injectable dECM product (Ventrigel).(A) Porcine ventricular myocardium is sliced and then decellularized, milled into powders and solubilized through enzymatic digestion which allows for injection via syringe and a 27-gauge needle; the hematoxylin and eosin staining of a histological section reveals cellular removal; electrocardiogram was recorded in rats 1 week post-injection of Ventrigel to detect arrhythmia inducibility. Modified and adapted with permission from Ref. [177] Copyright 2012, Elsevier. (B) The first-in-man study of pcECM hydrogel treating early and late MI patients Modified and adapted with permission from Ref. [53] Copyright 2019, Elsevier.

high stiffness is desirable [270,271]. dECM gelation is influenced by digesting duration, temperature, ionic strength, pH, concentration [152,272,273]. After decellularization and digestion, most dECM hydrogels at a final concentration of 6–8 mg/mL exhibited the low storage modulus ranging from 10°-10^{2} Pa [152,167,259]. Interestingly, Yang et al. obtained a relatively-robust dECM hydrogel at only 5 mg/mL with a storage modulus of 300–400 Pa, by an optimized pretreatment which removed cells with only the non-ionic gentle detergent (Triton X −100) and shortened digestion duration in the pepsin acid solution to preserve the intrinsic strength of dECM materials [189]. Since different source tissues have different dECM compositions, their gel properties are also different and require corresponding optimization of the preparation process. However, it is inevitable to lose partial mechanical properties of the native tissues after processing. Therefore, the reasonable way to solve this problem lies in mechanical enhancement of dECM hydrogels. dECM generally can be reinforced by increasing crosslinking or compounding with other macromolecules.

Increasing the covalent crosslinking of hydrogel networks by chemical crosslinking agents is one of the common methods to strengthen dECM hydrogels. Glutaraldehyde (GA) is one of the chemical crosslinking agents and has been used in many FDA-approved ECM devices [274,275]. GA molecules mainly form hydrolysable Schiff base crosslinks between the ε-amino groups of lysine [276]. Pilipchuk et al. studied the effect of GA crosslinking on the mechanical properties and degradation of dermal dECM hydrogels [277]. The stiffness of dECM increased 9–15.33 folds with longer GA treatment time (0.5 h–24 h). Compared to uncrosslinked dECM hydrogels which were subject to enzymatic degradation, the crosslinked dECM was effectively resistant to pepsin hydrolyzation [277]. Crosslinking between thiol groups can also reinforce dECM network, which happens under the physiological conditions without any additives [278]. Barthold et al. utilized thiol functionalized hyaluronan to crosslink the dECM scaffold via disulfide crosslinking with cysteine groups on collagen fibers, thereby achieving a modulus of 26 kPa [278]. However, this method also exhibited a slow gelation dynamic, taking more than 30 min to a high-degree gelation. In addition, light-triggered crosslinking/photocrosslinking has been widely applied to stiffen ECM constructs. There are two main dECM photocrosslinking mechanisms: 1) bonding between methacrylate or acrylate groups pre-grafted on dECM, and 2) bonding between tyrosine residues on dECM proteins. Upon exposure to light, the added photo-initiator generates free radicals and initiates crosslinking between the active groups. The commonly-used photo-initiators and photosensitizers include 1-[4-(2-hydroxyethoxy) phenyl]-2-hydroxy-2-methyl-1-propan-1-one (I2959), lithium phenyl-2,4,6-trimethylbenzoylphosphinate (LAP), and ruthenium/sodium persulfate (dERS) [253]. Bejleri et al. formulated a new bioprinting ink consisting of GelMA, dECM, and CPC cells [195]. At low temperature, the viscosity of GelMA increased rapidly, stabilizing the printed structures, followed by photo-crosslinking to form a GelMA hydrogel framework, and incubation at 37 °C to induce ECM self-assembling into hydrogel. Lee et al. modified dECM with methacrylic anhydride to obtain MA-dECM

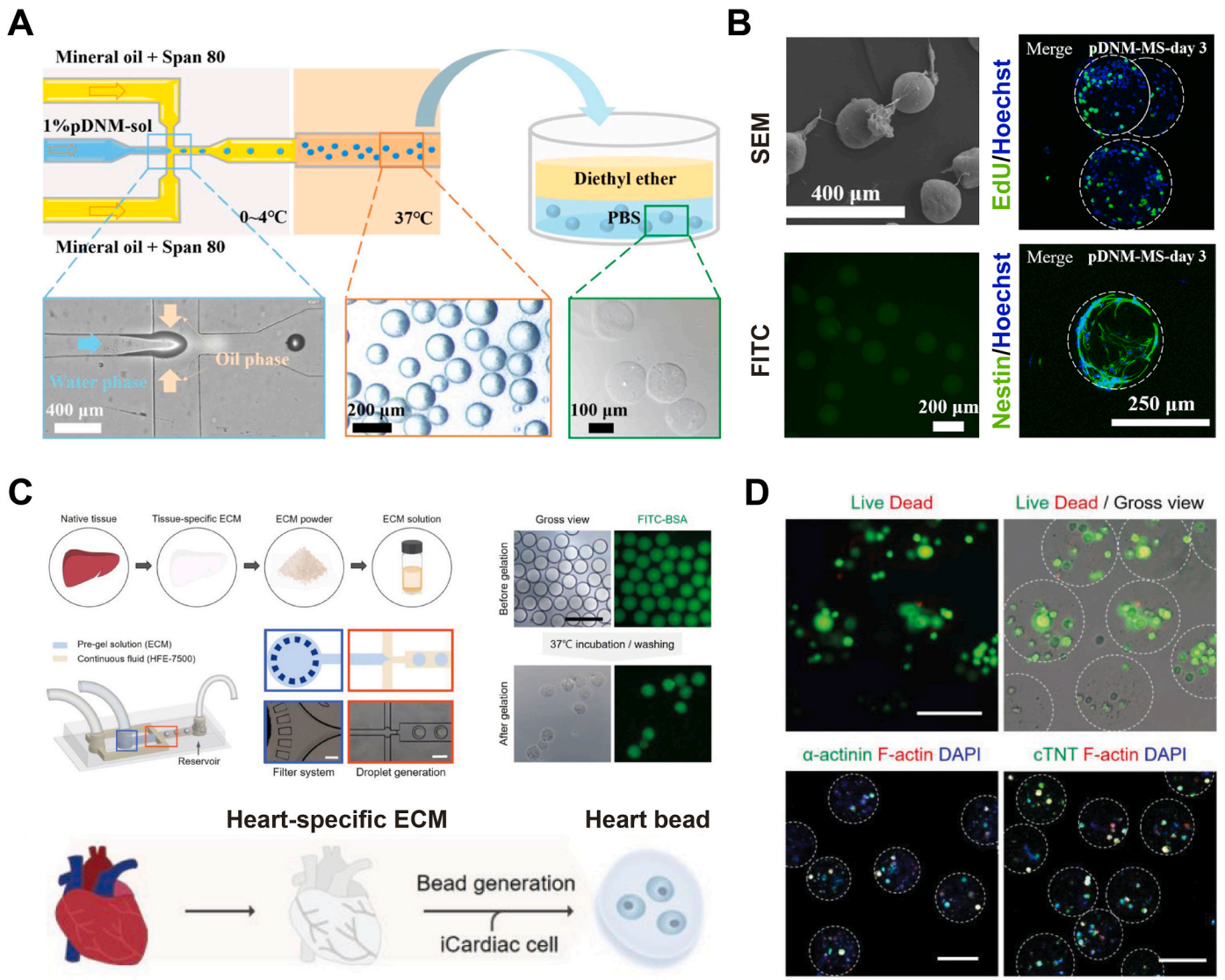

Fig. 8. Microfluidic fabrication of dECM hydrogel microspheres. (A) Schematic illustration of a two-stage temperature-controlling microfluidic system and the optical micrographs of the spherical pDNM microgels (pDNM-MSs). (B) SEM and fluorescent characterization of pDNM-MSs as well as immunofluorescence staining of cells cultured on pDNM-MSs compared with GelMA microgels. Modified and adapted with permission from Ref. [268] Copyright 2022, American Chemical Society. (C) The whole fabricating process of dECM beads from the extraction of dECM to flow-focusing microfluidic set-up and the gross view and fluorescent images of dECM microgels before and after gelation; and the scheme of building cell-encapsulating cECM microspheres. Scale bar, 200 μm. (D) Live/dead staining and immunostaining of CMs with α-actinin (green), cTNT (green), and F-actin (red) in the cECM beads. Modified and adapted with permission from Ref. [269] Copyright 2019, Wiley-VCH.

(71.05 ± 0.20 % grafting degree), which added covalent crosslinking into dECM/alginate hydrogel network. When the blending ratio of alginate to MA-dECM was 2:1, the storage modulus of the hydrogel increased from about ~10 Pa–~2100 Pa, which is suitable for cell encapsulation and 3D printing [279]. Kim et al. 3D printed cECM scaffold via fast dityrosine crosslinking as activated by dERS (Fig. 9A) [280]. This photocrosslinked cECM had a significantly higher compressive modulus of 86.4 kPa, compared to thermally crosslinked cECM hydrogel at 0.18–3.0 kPa. Moreover, dERS photocrosslinking resulted in up to 96.87 % shape recovery, compared to 22 % of the physical crosslinking group. By using this strategy, a 3D heart-shaped construct was built and increased the level of cardiac-specific proteins (Cx43 and cTNT) in iPSCs (Fig. 9A). Interestingly, Jang et al. developed a novel photosensitizer, vitamin B2, which induced cECM crosslinking when exposed to ultraviolet light (UVA) [281]. Together with temperature triggered the self-assembly of cECM, the double network of cECM resulted in an ~10^2 higher Young's modulus of 15.74 kPa compared to non-covalent network only (0.18 kPa) (Fig. 9B). The stiffer hydrogel upregulated the expressions of cardiac-differentiating factors, including myocyte-specific enhancer factor 2C (MEF2C), GATA4, and Nk2 homeobox (Nkx 2.5). However, UVA may harm cells, as vitamin B2 induced crosslinking requires 3–6 min.

Stability of dECM could also be enhanced with modification by other polymers including alginate, chitason, fibrin, HA, GAGs, GelMA, PEG and poly (ethylene glycol)-diacrylate (PEG-DA) [258,282–290]. Chu et al. crosslinked a suspension of dECM co-mixed with alginate in a calcium bath and subsequently incubated at 37 °C to enhance crosslinking to form an interpenetrating network with higher physical strength [279]. In order to improve the printability of dECM, De Santis et al. mixed alginate in the ECM solution, and the mixture rapidly solidifies in Ca^{2+} ion solution to obtain rECM, which was controllably printed into Ca bath tissue-like constructs including airway and vessel, while maintaining the viability of epithelial cells and endothelial (bEnd.3) cells and metabolic activity (Fig. 9C) [271]. rECM promoted

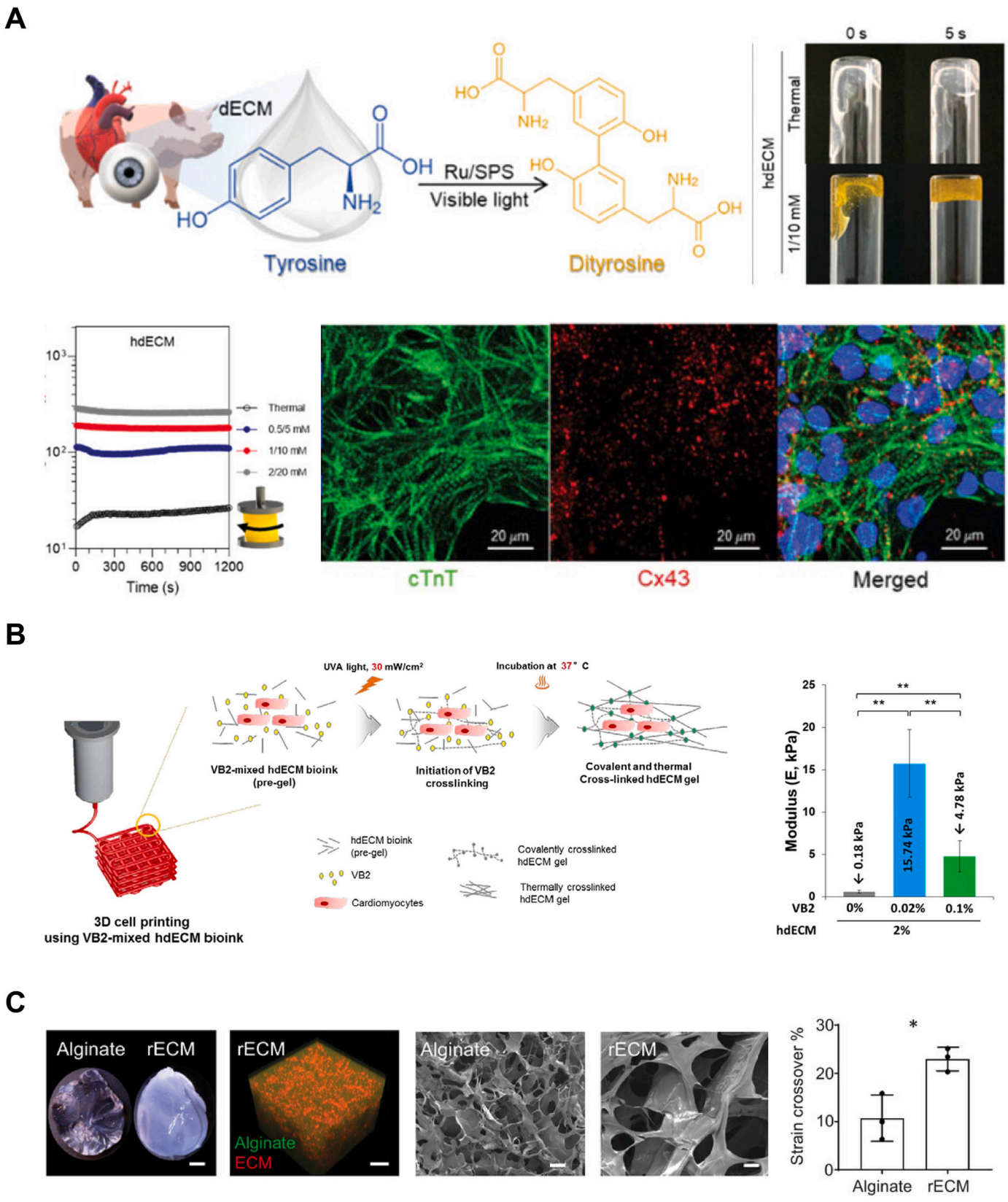

Fig. 9. (A) Tyrosine-based light-activated cross-linking reaction in dECM bioink to form yellow hydrogels with enhanced storage modulus; Immunofluorescence images of iPSCs encapsulated in dECM construct at day 14 evaluating cardiac-related markers (Cx43 and cTNT) Modified and adapted with permission from Ref. [280] Copyright 2021, Wiley-VCH. (B) 3D bioprinting the cECM bioink via concurrent crosslinking of vitamin B2-induced covalent crosslinking and thermal crosslinking; and compressive modulus of each bioink at 20 % strain depending onthe VB2 concentration. Modified and adapted with permission from Ref. [281] Copyright 2016, Elsevier. (C) Pictures of alginate and rECM hybrid hydrogels (scale bars, 1 mm) and alginate-fluorescein- and dECM-rhodamine-modified rECM hydrogel (scale bar, 200 μm) as well as their SEM images (scale bars, 50 μm) and strain stress. Modified and adapted with permission from Ref. [271] Copyright 2020, Wiley-VCH.

vascularization in constructs in a chick chorionic membrane (CAM) assay. Twenty-eight days after implantation of alginate or 3D-printed rECM composite hydrogels into T-cell-deficient FoxN1 KO mice, the rECM hydrogels integrated well with surrounding tissues without any apparent inflammation or signs of foreign body reaction, while massive infiltration of M1 macrophages was observed in alginate hydrogel. Since alginate was degraded via β-elimination mechanism, which proceeded slowly *in vivo* [291]. The addition of alginate retarded the degradation and extended the residence time of dECM. Williams et al. compounded fibrin to strengthen dECM hydrogel network, but the obtained hydrogel still presented lower Young's modulus (~2 kPa) than that of natural myocardium [292]. Thus, the authors utilized glutamine transaminase (TG) to further crosslink fibrin and enhanced the gel strength to from 2 kPa to 32 kPa depending on the amount of TG additive, showing that the Young's modulus of this composite hydrogel is highly adjustable [293]. Also, due to the added fibrin, the material exhibited a significant improvement in pro-angiogenic ability. With increased mechanical strength, the composite hydrogel containing adult human cECM promoted ~6-fold upregulation of endothelial marker vWF and 2-fold upregulation of smooth muscle marker CNN1 in c-kit + CPCs [292]. Duan et al. obtained a series of hydrogels by mixing cardiac dECM and type I collagen (Col-I, a major component of dECM) in different ratios. When the ratio of dECM versus Col-I was higher, gelation was slower. The gelation time of pure dECM was up to 60 min, making it difficult to perform designs such as cell encapsulation. As the content of Col-I increased, the gelation time of the composite reduced (at least 10 min) and its dynamic shear modulus increased from 8.6 ± 1.5 Pa to 61.5 ± 5.9 Pa [139]. While ensuring dECM gelation, the authors proved that the higher the dECM content, the better the differentiation and maturation of early CPCs and the maintenance of the contractility of CMs. Compared to 25 % dECM with exogenous growth factors, high dECM content (~75 %) enhanced the expression of cardiac troponin I (cTnI) and Cx43, reflecting the superiority of dECM in tissue regeneration.

5.1. Perspectives

dECM materials maintained the components, structure and biological cues, benefiting cell infiltration, growth and differentiation. Because of these advantages, dECM can provide a suitable microenvironment for ICM treatment. Injectable cECM (VentriGel) and SIS cardiac patches (CorMatrix) have been clinically translated into approved products and obtained desirable treatment results. Despite these achievements, dECM applications involve various risks along with opportunities.

Lowering immunogenicity and maintaining batch-to-batch stability are two major challenges associated with dECM for ICM therapy. The immunogenicity of dECM is mainly attributed to the residual pathogens and nuclei acids, contaminants from processing and surgery, and unique carbohydrate structures in non-primate dECM. These immunogenic factors may even induce severe infection and tissue necrosis, which determines the clinical applicability. Ideal decellularization methods aim to clear cells, effective sterilization is often less emphasized. Common sterilization methods for medical devices, including pressurized steam, dry heat, irradiation or ethylene oxide, compromise the mechanical properties of dECM materials and denature their proteins [294]. Peracetic acid (PAA) submersion or perfusion is the most widely-used sterilization method with a high bactericidal and fungicidal efficiency at 0.001 % and 0.003 % respectively, while preserving ECM proteins [101,295]. Maintaining the whole manufacture process in an ultra-clean and sterilized condition that has been certificated by good manufacturing practice (GMP) is important. However, sterilization usually do not address viral contamination. Donor screening and the thorough removal of residual nucleic acids in dECM are potential strategies to solve this problem [294]. Most of nuclei acids are removed during decellularization, and the residual part can be cleared through DNase and RNase enzymolysis. Yang et al. eliminated porcine endogenous retroviruses (PERVs) using CRISPR-Cas9 gene editing technique [296]. In addition to immunogenicity risks, donor variance limited the application of allogeneic cECM and pericardial dECM. The alternative dECM materials from porcine or bovine can replace the function of human-derived cECM. However, α-Gal epitope, a unique carbohydrate structure only exhibited in non-primate mammals, induces rejection to implants, upregulated immunogenicity and severe coagulation dysfunction [297,298]. SIS and urinary bladder dECM contain less α-Gals compared to pcECM and have exhibited better biocompatibility *in vivo*, yet low dose of α-Gal still causes chronic immune responses. GA crosslinking could partially mask α-Gal epitope, but cannot thoroughly remove α-Gal epitope or α-Gal induced implant rejection [297–300]. Green coffee bean α-galactosidase was an economical tool for temporarily cleaving the terminal α-Gal (since α-Gal recovers after a certain time *in vivo*) [301–304]. One ultimate solution is to generate α1,3 GT (the gene coding α-Gal epitope) knockout animals by nuclear transfer cloning [305–307]. Lu et al. knockout three genes of porcine-specific glycan epitopes and added 9 human transgenes via a combination of CRISPR-Cas9 and transposon technologies, enhancing the immune compatibility and coagulation compatibility [308]. In 2020, Revivicor received the permission of using GalSafe™ pigs (without α-Gal epitope) as food and for potential medical applications from FDA. However, gene editing and high-standard animal breeding increase the cost of dECM productions. An economical and efficient gene editing tool to obtain safe and stable dECM source from non-primate animals is desirable.

Final DNA contents in dECM products vary batch-to-batch. Although there is no industrial standard to identify DNA removal efficiency [92], some basic requirements have been proposed: 1) safe amount (≤50 ng dsDNA/mg dry ECM), 2) DNA fragments shorter than 200 dp, thus not activating inflammation, 3) no visible nuclear in hematoxylin-eosin staining or 4′,6-diamidino-2-phenylindole (DAPI) staining. For α-Gals detection, the most widely employed method is staining with Griffonia simplicifolia type I isolectin B4. Combining with monoclonal antibody M86, anti-immunoglobulin M, and anti-immunoglobulin G, one can evaluate removal of α-Gals [301].

dECMs material within myocardium may trigger arrhythmia and impair cardiac function [153]. In clinical trials, cECM has not been reported to cause arrhythmia, yet the mismatched conductivities of material and tissue still poses a risk of arrhythmia [309]. As a guiding work, Suarez et al. evaluated the influence of PEG hydrogel with different interstitial distribution on the electrophysiology of myocardium, and found that better hydrogel spread is more favorable to conduction of myocardium, establishing the site of interstitial spread properties as important factors for dECM hydrogel design [310]. Future studies should involve more electrocardiographic tests. Increasing the conductivity of dECM can promote intercellular communication and bridge electrical signals between healthy and scar tissue, which is another trend in the field. Zhang et al. employed an injectable hydrogel with a conductivity of 5.52×10^{-4} S/cm to reduce arrhythmia susceptibility and the resistivity of cardiac scar tissue [311]. Thus, improving the electrical conductivity of dECM to match that of healthy myocardium could be desirable for supporting electrical signal conduction.

Injectable dECM hydrogel can be delivered through minimally-invasive catheter implantation, showing advantages in safety. Open-heart surgery for epicardial patch implantation is more invasive and complicated than injectable dECM hydrogels, thus is not feasible for all patients, as ICM has a higher prevalence in an older population. For example, CorPatch can so far only be applied to ICM patients during CABG surgery. Wang et al. developed injectable cardiac patches by creating interconnected macropores through an ice-crystal template to obtain shape-memory compressibility, which was demonstrated in a porcine model [34]. Alternatively, dECM can be injected intrapericardially and adhere to epicardium, followed by *in situ* crosslinking.

Regenerating myocardium is the ultimate goal in ICM treatment. Although administration of dECM to the ischemic myocardium is beneficial, fibrosis inevitably occurs rather than regeneration in adult hearts [153,312]. So far, dECM materials for cardiac regeneration are

mainly used in the form of delivery vehicles for cells and growth factors to achieve better therapeutic effects. dECM materials provide the suitable microenvironment for residing exogenous cells after delivery to the myocardium, prolong cell retention, and maintain cell activity. In addition to cells delivered by the dECM materials, dECM facilitated the infiltration of progenitor cells and macrophages. By mediating the behavior of the delivered and recruited cells, dECM materials could promote vascularization, modulate the immune response, etc., which are desirable in supporting cardiac regeneration [15,70]. In the recent decade, non-mammalian zebrafish cECM was found to promote the proliferation of endogenous CMs and reactivation of epidermal growth factor receptor-2 (a key factor for the survival, growth and regeneration of CMs expression in cardiomyocytes, thereby improving histological and functional recovery, and myocardial elasticity [205]. Thus, future research can focus on two aspects. Primarily, the principles and different mechanisms of dECM promoting myocardial regeneration should be clarified from the perspective of molecular biology. Therefore, we can determine the structure-activity relationship with dECM itself and optimize dECM through material design. Secondly, combining new biotechnologies like reprogramming cell techniques with dECM materials is a multi-pronged approach to enhance regeneration effects. Sadahiro et al. discovered that overexpression of key developmental cardiac regulators (Gata4, Mef2c, and Tbx5) through retroviral directly convert resident cardiac fibroblasts to CMs. Otherwise, combining muscle-specific miR (miR-1, miR-133, miR-208, and miR-499) with cardiac fibroblasts could also *in situ* generate functional induced CMs. Thus, utilizing these novel technologies based on dECM materials is hopeful and promising to achieve better cardiac regeneration effects for ICM.

6. Conclusion

dECM material-based medical devices are attractive for ICM treatment as key therapeutic components remain in dECM after decellularization. ICM therapies by dECM patches and hydrogels have been approved for clinical use or reached clinical trial stage. dECM can not only be modified and processed through a variety of manufacturing technologies but also be composited with cells and other biologically active factors, thereby enhancing treatment effects. As the practice of dECM for ICM treatment expands and the understanding of dECM deepens, it is expected to improve therapeutic effects by reducing immunogenicity, matching cardiac electrical conductivity and inducing myocardial regeneration, leading to clinical translation of dECM technologies.

Notes

The authors declare no competing financial interest.

Ethics approval and consent to participate

The manuscript being submitting is a review article; no ethics involved.

Declaration of competing interest

The authors declare that they have no known competing financial interests or personal relationships that could have appeared to influence the work reported in this paper.

Acknowledgments

This study is financially supported by the National Key Research and Development Program of China (no. 2019YFE0117400), National Natural Science Foundation of China (no. 82202328), Fundamental Research Funds for the Central Universities (226-2023-00066).

References

[1] E.J. Benjamin, P. Muntner, A. Alonso, M.S. Bittencourt, C.W. Callaway, A. P. Carson, A.M. Chamberlain, A.R. Chang, S. Cheng, S.R. Das, F.N. Delling, L. Djousse, M.S.V. Elkind, J.F. Ferguson, M. Fornage, L.C. Jordan, S.S. Khan, B. M. Kissela, K.L. Knutson, T.W. Kwan, D.T. Lackland, T.T. Lewis, J.H. Lichtman, C. T. Longenecker, M.S. Loop, P.L. Lutsey, S.S. Martin, K. Matsushita, A.E. Moran, M.E. Mussolino, M. O'Flaherty, A. Pandey, A.M. Perak, W.D. Rosamond, G. A. Roth, U.K.A. Sampson, G.M. Satou, E.B. Schroeder, S.H. Shah, N.L. Spartano, A. Stokes, D.L. Tirschwell, C.W. Tsao, M.P. Turakhia, L.B. VanWagner, J. T. Wilkins, S.S. Wong, S.S. Virani, Heart disease and stroke statistics—2019 update: a report from the american heart association, Circulation 139 (2019) e56–e528.

[2] B. Vogel, M. Acevedo, Y. Appelman, C.N. Bairey Merz, A. Chieffo, G.A. Figtree, M. Guerrero, V. Kunadian, C.S.P. Lam, A.H.E.M. Maas, A.S. Mihailidou, A. Olszanecka, J.E. Poole, C. Saldarriaga, J. Saw, L. Zühlke, R. Mehran, The Lancet women and cardiovascular disease commission: reducing the global burden by 2030, Lancet 397 (2021) 2385–2438.

[3] S.S. Virani, A. Alonso, H.J. Aparicio, E.J. Benjamin, M.S. Bittencourt, C. W. Callaway, A.P. Carson, A.M. Chamberlain, S. Cheng, F.N. Delling, M.S. V. Elkind, K.R. Evenson, J.F. Ferguson, D.K. Gupta, S.S. Khan, B.M. Kissela, K. L. Knutson, C.D. Lee, T.T. Lewis, J. Liu, M.S. Loop, P.L. Lutsey, J. Ma, J. Mackey, S.S. Martin, D.B. Matchar, M.E. Mussolino, S.D. Navaneethan, A.M. Perak, G. A. Roth, Z. Samad, G.M. Satou, E.B. Schroeder, S.H. Shah, C.M. Shay, A. Stokes, L. B. VanWagner, N.-Y. Wang, C.W. Tsao, Heart disease and stroke statistics—2021 update, Circulation 143 (2021) e254–e743.

[4] M. Koenen, M.A. Hill, P. Cohen, J.R. Sowers, Obesity, adipose tissue and vascular dysfunction, Circ. Res. 128 (2021) 951–968.

[5] E. Muzurović, C.C. Peng, M.J. Belanger, D. Sanoudou, D.P. Mikhailidis, C. S. Mantzoros, Nonalcoholic fatty liver disease and cardiovascular disease: a review of shared cardiometabolic risk factors, Hypertension 79 (2022) 1319–1326.

[6] M. Nakamura, J. Sadoshima, Mechanisms of physiological and pathological cardiac hypertrophy, Nat. Rev. Cardiol. 15 (2018) 387–407.

[7] O. Bergmann, R.D. Bhardwaj, S. Bernard, S. Zdunek, F. Barnabé-Heide, S. Walsh, J. Zupicich, K. Alkass, B.A. Buchholz, H. Druid, S. Jovinge, J. Frisén, Evidence for cardiomyocyte renewal in humans, Science 324 (2009) 98–102, 80-.

[8] O. Bergmann, S. Zdunek, A. Felker, M. Salehpour, K. Alkass, S. Bernard, S. L. Sjostrom, M. Szewczykowska, T. Jackowska, C. Dos Remedios, T. Malm, M. Andrä, R. Jashari, J.R. Nyengaard, G. Possnert, S. Jovinge, H. Druid, J. Frisén, Dynamics of cell generation and turnover in the human heart, Cell 161 (2015) 1566–1575.

[9] X. Fang, H. Ardehali, J. Min, F. Wang, The molecular and metabolic landscape of iron and ferroptosis in cardiovascular disease, Nat. Rev. Cardiol. 20 (2023) 7–23.

[10] M. Becker, J.A. Maring, M. Schneider, A.X. Herrera Martin, M. Seifert, O. Klein, T. Braun, V. Falk, C. Stamm, Towards a novel patch material for cardiac applications: tissue-specific extracellular matrix introduces essential key features to decellularized amniotic membrane, Int. J. Mol. Sci. 19 (2018) 1032.

[11] K. Fujita, Z. Feng, D. Sato, T. Kosawada, T. Nakamura, Y. Shiraishi, M. Umezu, Modulation of the mechanical properties of ventricular extracellular matrix hydrogels with a carbodiimide crosslinker and investigation of their cellular compatibility, AIMS Mater. Sci. 5 (2018) 54–74.

[12] I.Y. Shadrin, B.W. Allen, Y. Qian, C.P. Jackman, A.L. Carlson, M.E. Juhas, N. Bursac, Cardiopatch platform enables maturation and scale-up of human pluripotent stem cell-derived engineered heart tissues, Nat. Commun. 8 (2017) 1825.

[13] L. Bacmeister, M. Schwarzl, S. Warnke, B. Stoffers, S. Blankenberg, D. Westermann, D. Lindner, Inflammation and fibrosis in murine models of heart failure, Basic Res. Cardiol. 114 (2019) 19.

[14] J.G. Travers, F.A. Kamal, J. Robbins, K.E. Yutzey, B.C. Blaxall, Cardiac fibrosis: the fibroblast awakens, Circ. Res. 118 (2016) 1021–1040.

[15] H. Hashimoto, E.N. Olson, R. Bassel-Duby, Therapeutic approaches for cardiac regeneration and repair, Nat. Rev. Cardiol. 15 (2018) 585–600.

[16] Y. Toyoda, T. Sloane Guy, A. Kashem, Present status and future perspectives of heart transplantation, Circ. J. 77 (2013) 1097–1110.

[17] M.M. Kittleson, J.A. Kobashigawa, Cardiac transplantation: current outcomes and contemporary controversies, JACC Hear, Fail 5 (2017) 857–868.

[18] B. Pitt, F. Zannad, W.J. Remme, R. Cody, A. Castaigne, A. Perez, J. Palensky, J. Wittes, The effect of spironolactone on morbidity and mortality in patients with severe heart failure, N. Engl. J. Med. 341 (1999) 709–717.

[19] M. Packer, A.J.S. Coats, M.B. Fowler, H.A. Katus, H. Krum, P. Mohacsi, J. L. Rouleau, M. Tendera, A. Castaigne, E.B. Roecker, M.K. Schultz, C. Staiger, E. L. Curtin, D.L. DeMets, Effect of carvedilol on survival in severe chronic heart failure, N. Engl. J. Med. 344 (2001) 1651–1658.

[20] J.J.V. McMurray, M. Packer, A.S. Desai, J. Gong, M.P. Lefkowitz, A.R. Rizkala, J. L. Rouleau, V.C. Shi, S.D. Solomon, K. Swedberg, M.R. Zile, Angiotensin-neprilysin inhibition versus enalapril in heart failure, N. Engl. J. Med. 371 (2014) 993–1004.

[21] K. Domae, S. Miyagawa, K. Toda, Y. Sawa, New treatment strategy for severe heart failure: combination of ventricular assist device and regenerative therapy, J. Artif. Organs 24 (2021) 1–5.

[22] J. Stehlik, J. Kobashigawa, S.A. Hunt, H. Reichenspurner, J.K. Kirklin, Honoring 50 years of clinical heart transplantation in circulation, Circulation 137 (2018) 71–87.

[23] J.R. Garcia, P.F. Campbell, G. Kumar, J.J. Langberg, L. Cesar, L. Wang, A. J. García, R.D. Levit, A minimally invasive, translational method to deliver

hydrogels to the heart through the pericardial space, JACC Basic to Transl. Sci. 2 (2017) 601–609.
[24] D. Zhu, Z. Li, K. Huang, T.G. Caranasos, J.S. Rossi, K. Cheng, Minimally invasive delivery of therapeutic agents by hydrogel injection into the pericardial cavity for cardiac repair, Nat. Commun. 12 (2021) 1412.
[25] R.Z. Zhuang, R. Lock, B. Liu, G. Vunjak-Novakovic, Opportunities and challenges in cardiac tissue engineering from an analysis of two decades of advances, Nat. Biomed. Eng. 6 (2022) 327–338.
[26] J.R. Nakkala, Z. Li, W. Ahmad, K. Wang, C. Gao, Immunomodulatory biomaterials and their application in therapies for chronic inflammation-related diseases, Acta Biomater. 123 (2021) 1–30.
[27] X. Li, J. Zhou, Z. Liu, J. Chen, S. Lü, H. Sun, J. Li, Q. Lin, B. Yang, C. Duan, M. (Mengqiu) Xing, C. Wang, A PNIPAAm-based thermosensitive hydrogel containing SWCNTs for stem cell transplantation in myocardial repair, Biomaterials 35 (2014) 5679–5688.
[28] C. Hu, W. Liu, L. Long, Z. Wang, W. Zhang, S. He, L. Lu, H. Fan, L. Yang, Y. Wang, Regeneration of infarcted hearts by myocardial infarction-responsive injectable hydrogels with combined anti-apoptosis, anti-inflammatory and pro-angiogenesis properties, Biomaterials 290 (2022), 121849.
[29] Y. Yao, A. Li, S. Wang, Y. Lu, J. Xie, H. Zhang, D. Zhang, J. Ding, Z. Wang, C. Tu, L. Shen, L. Zhuang, Y. Zhu, C. Gao, Multifunctional elastomer cardiac patches for preventing left ventricle remodeling after myocardial infarction *in vivo*, Biomaterials 282 (2022), 121382.
[30] J. Ding, Y. Yao, J. Li, Y. Duan, J.R. Nakkala, X. Feng, W. Cao, Y. Wang, L. Hong, L. Shen, Z. Mao, Y. Zhu, C. Gao, A reactive oxygen species scavenging and O-2 generating injectable hydrogel for myocardial infarction treatment *in vivo*, Small 16 (2020), 2005038.
[31] K. Reddy, Recent advances in the diagnosis and treatment of acute myocardial infarction, World J. Cardiol. 7 (2015) 243–276.
[32] R. Augustine, P. Dan, A. Hasan, I.M. Khalaf, P. Prasad, K. Ghosal, C. Gentile, L. McClements, P. Maureira, Stem cell-based approaches in cardiac tissue engineering: controlling the microenvironment for autologous cells, Biomed, Pharma 138 (2021), 111425.
[33] L. Stapleton, Y. Zhu, Y.J. Woo, E. Appel, Engineered biomaterials for heart disease, Curr. Opin. Biotechnol. 66 (2020) 246–254.
[34] L. Wang, Y. Liu, G. Ye, Y. He, B. Li, Y. Guan, B. Gong, K. Mequanint, M.M.Q. Xing, X. Qiu, Injectable and conductive cardiac patches repair infarcted myocardium in rats and minipigs, Nat. Biomed. Eng. 5 (2021) 1157–1173.
[35] T. Wu, C. Cui, Y. Huang, Y. Liu, C. Fan, X. Han, Y. Yang, Z. Xu, B. Liu, G. Fan, W. Liu, Coadministration of an adhesive conductive hydrogel patch and an injectable hydrogel to treat myocardial infarction, ACS Appl. Mater. Interfaces 12 (2020) 2039–2048.
[36] R. Bao, B. Tan, S. Liang, N. Zhang, W. Wang, W. Liu, A π-π conjugation-containing soft and conductive injectable polymer hydrogel highly efficiently rebuilds cardiac function after myocardial infarction, Biomaterials 122 (2017) 63–71.
[37] Y. Liu, R. Guo, T. Wu, Y. Lyu, M. Xiao, B. He, G. Fan, J. Yang, W. Liu, One zwitterionic injectable hydrogel with ion conductivity enables efficient restoration of cardiac function after myocardial infarction, Chem. Eng. J. 418 (2021), 129352.
[38] J. Zhou, W. Liu, X. Zhao, Y. Xian, W. Wu, X. Zhang, N. Zhao, F. Xu, C. Wang, Natural melanin/alginate hydrogels achieve cardiac repair through ROS scavenging and macrophage polarization, Adv. Sci. 8 (2021), 2100505.
[39] Y. Lu, T. Ren, H. Zhang, Q. Jin, L. Shen, M. Shan, X. Zhao, Q. Chen, H. Dai, L. Yao, J. Xie, D. Ye, T. Lin, X. Hong, K. Deng, T. Shen, J. Pan, M. Jia, J. Ling, P. Li, Y. Zhang, H. Wang, L. Zhuang, C. Gao, J. Mao, Y. Zhu, A honeybee stinger-inspired self-interlocking microneedle patch and its application in myocardial infarction treatment, Acta Biomater. 153 (2022) 386–398.
[40] M. Sepantafar, R. Maheronnaghsh, H. Mohammadi, S. Rajabi-Zeleti, N. Annabi, N. Aghdami, H. Baharvand, Stem cells and injectable hydrogels: synergistic therapeutics in myocardial repair, Biotechnol. Adv. 34 (2016) 362–379.
[41] J.W. MacArthur, A.N. Steele, A.B. Goldstone, J.E. Cohen, W. Hiesinger, Y.J. Woo, Injectable bioengineered hydrogel therapy in the treatment of ischemic cardiomyopathy, Curr. Treat. Options Cardiovasc. Med. 19 (2017) 30.
[42] Y. Zhang, W. Mu, Y. Zhang, X. He, Y. Wang, H. Ma, T. Zhu, A. Li, Q. Hou, W. Yang, Y. Ding, S. Ramakrishna, H. Li, Recent advances in cardiac patches: materials, preparations, and properties, ACS Biomater. Sci. Eng. 8 (2022) 3659–3675.
[43] D. Sharma, M. Ferguson, T.J. Kamp, F. Zhao, Constructing biomimetic cardiac tissues: a review of scaffold materials for engineering cardiac patches, Emergent Mater 2 (2019) 181–191.
[44] Y.S. Zhang, A. Khademhosseini, Advances in engineering hydrogels, Science 356 (2017), eaaf3627, 80-.
[45] A.K. Gaharwar, I. Singh, A. Khademhosseini, Engineered biomaterials for in situ tissue regeneration, Nat. Rev. Mater. 5 (2020) 686–705.
[46] S. Hinderer, S.L. Layland, K. Schenke-Layland, ECM and ECM-like materials - biomaterials for applications in regenerative medicine and cancer therapy, Adv. Drug Deliv. Rev. 97 (2016) 260–269.
[47] E. Ruvinov, S. Cohen, Alginate biomaterial for the treatment of myocardial infarction: progress, translational strategies, and clinical outlook, Adv. Drug Deliv. Rev. 96 (2016) 54–76.
[48] C.J. Curley, E.B. Dolan, M. Otten, S. Hinderer, G.P. Duffy, B.P. Murphy, An injectable alginate/extra cellular matrix (ECM) hydrogel towards acellular treatment of heart failure, Drug Deliv. Transl. Res. 9 (2019) 1–13.
[49] S. Li, H. Zhang, J. Xie, Z. Wang, K. Wang, Z. Zhai, J. Ding, S. Wang, L. Shen, J. Wen, Y.-D. Tang, H. Wang, Y. Zhu, C. Gao, In Vivo self-assembled shape-memory polyurethane for minimally invasive delivery and therapy, Mater. Horiz. (2023), https://doi.org/10.1039/d3mh00594a.
[50] M. Montgomery, S. Ahadian, L. Davenport Huyer, M. Lo Rito, R.A. Civitarese, R. D. Vanderlaan, J. Wu, L.A. Reis, A. Momen, S. Akbari, A. Pahnke, R.-K. Li, C. A. Caldarone, M. Radisic, Flexible shape-memory scaffold for minimally invasive delivery of functional tissues, Nat. Mater. 16 (2017) 1038–1046.
[51] U. Sarig, H. Sarig, E. De-Berardinis, S.-Y. Chaw, E.B.V. Nguyen, V.S. Ramanujam, V.D. Thang, M. Al-Haddawi, S. Liao, D. Seliktar, T. Kofidis, F.Y.C. Boey, S. S. Venkatraman, M. Machluf, Natural myocardial ECM patch drives cardiac progenitor based restoration even after scarring, Acta Biomater. 44 (2016) 209–220.
[52] H.E.M. Mewhort, D.A. Svystonyuk, J.D. Turnbull, G. Teng, D.D. Belke, D. G. Guzzardi, D.S. Park, S. Kang, M.D. Hollenberg, P.W.M. Fedak, Bioactive extracellular matrix scaffold promotes adaptive cardiac remodeling and repair, JACC Basic to Transl. Sci. 2 (2017) 450–464.
[53] J.H. Traverse, T.D. Henry, N. Dib, A.N. Patel, C. Pepine, G.L. Schaer, J. A. DeQuach, A.M. Kinsey, P. Chamberlin, K.L. Christman, First-in-man study of a cardiac extracellular matrix hydrogel in early and late myocardial infarction patients, JACC Basic to Transl, Science 4 (2019) 659–669.
[54] C. Prat-Vidal, L. Rodríguez-Gómez, M. Aylagas, N. Nieto-Nicolau, P. Gastelurrutia, E. Agustí, C. Gálvez-Montón, I. Jorba, A. Teis, M. Monguió-Tortajada, S. Roura, J. Vives, S. Torrents-Zapata, M.I. Coca, L. Reales, M. L. Cámara-Rosell, G. Cediel, R. Coll, R. Farré, D. Navajas, A. Vilarrodona, J. García-López, C. Muñoz-Guijosa, S. Querol, A. Bayes-Genis, First-in-human PeriCord cardiac bioimplant: scalability and GMP manufacturing of an allogeneic engineered tissue graft, EBioMedicine 54 (2020), 102729.
[55] M. Li, H. Wu, Y. Yuan, B. Hu, N. Gu, Recent fabrications and applications of cardiac patch in myocardial infarction treatment, View 3 (2022), 20200153.
[56] X. Mei, K. Cheng, Recent development in therapeutic cardiac patches, Front. Cardiovasc. Med. 7 (2020) 1–11.
[57] B. Jian, W. Wu, Y. Song, N. Tan, C. Ma, Microporous elastomeric membranes fabricated with polyglycerol sebacate improved guided bone regeneration in a rabbit model, Int. J. Nanomed. 14 (2019) 2683–2692.
[58] P. Arunkumar, J.A. Dougherty, J. Weist, N. Kumar, M.G. Angelos, H.M. Powell, M. Khan, Sustained release of basic fibroblast growth factor (bFGF) encapsulated polycaprolactone (PCL) microspheres promote angiogenesis *in vivo*, Nanomaterials 9 (2019) 1037.
[59] S. Cesur, S. Ulag, L. Ozak, A. Gumussoy, S. Arslan, B.K. Yilmaz, N. Ekren, M. Agirbasli, D.M. Kalaskar, O. Gunduz, Production and characterization of elastomeric cardiac tissue-like patches for myocardial tissue engineering, Polym. Test. 90 (2020), 106613.
[60] C. Yan, Y. Ren, X. Sun, L. Jin, X. Liu, H. Chen, K. Wang, M. Yu, Y. Zhao, Photoluminescent functionalized carbon quantum dots loaded electroactive Silk fibroin/PLA nanofibrous bioactive scaffolds for cardiac tissue engineering, J. Photochem. Photobiol. B Biol. 202 (2020), 111680.
[61] M. Khan, Y. Xu, S. Hua, J. Johnson, A. Belevych, P.M.L. Janssen, S. Gyorke, J. Guan, M.G. Angelos, Evaluation of changes in morphology and function of human induced pluripotent stem cell derived cardiomyocytes (hiPSC-CMs) cultured on an aligned-nanofiber cardiac patch, PLoS One 10 (2015) 1–19.
[62] J. Yu, A.R. Lee, W.H. Lin, C.W. Lin, Y.K. Wu, W.B. Tsai, Electrospun PLGA fibers incorporated with functionalized biomolecules for cardiac tissue engineering, Tissue Eng. 20 (2014) 1896–1907.
[63] Y. Zhu, Y. Matsumura, M. Velayutham, L.M. Foley, T.K. Hitchens, W.R. Wagner, Reactive oxygen species scavenging with a biodegradable, thermally responsive hydrogel compatible with soft tissue injection, Biomaterials 177 (2018) 98–112.
[64] K.A. Spaulding, Y. Zhu, K. Takaba, A. Ramasubramanian, A. Badathala, H. Haraldsson, A. Collins, E. Aguayo, C. Shah, A.W. Wallace, N.P. Ziats, D. H. Lovett, A.J. Baker, K.E. Healy, M.B. Ratcliffe, Myocardial injection of a thermoresponsive hydrogel with reactive oxygen species scavenger properties improves border zone contractility, J. Biomed. Mater. Res., Part A 108 (2020) 1736–1746.
[65] C. Zhang, M.-H. Hsieh, S.-Y. Wu, S.-H. Li, J. Wu, S.-M. Liu, H.-J. Wei, R.D. Weisel, H.-W. Sung, R.-K. Li, A self-doping conductive polymer hydrogel that can restore electrical impulse propagation at myocardial infarct to prevent cardiac arrhythmia and preserve ventricular function, Biomaterials 231 (2020), 119672.
[66] Q.A. Majid, A.T.R. Fricker, D.A. Gregory, N. Davidenko, O. Hernandez Cruz, R. J. Jabbour, T.J. Owen, P. Basnett, B. Lukasiewicz, M. Stevens, S. Best, R. Cameron, S. Sinha, S.E. Harding, I. Roy, Natural biomaterials for cardiac tissue engineering: a highly biocompatible solution, Front. Cardiovasc. Med. 7 (2020) 1–32.
[67] P. Chandika, S.Y. Heo, T.H. Kim, G.W. Oh, G.H. Kim, M.S. Kim, W.K. Jung, Recent advances in biological macromolecule based tissue-engineered composite scaffolds for cardiac tissue regeneration applications, Int. J. Biol. Macromol. 164 (2020) 2329–2357.
[68] L. Huleihel, G.S. Hussey, J.D. Naranjo, L. Zhang, J.L. Dziki, N.J. Turner, D. B. Stolz, S.F. Badylak, Matrix-bound nanovesicles within ECM bioscaffolds, Sci. Adv. 2 (2016), e1600502.
[69] X. Zhang, X. Chen, H. Hong, R. Hu, J. Liu, C. Liu, Decellularized extracellular matrix scaffolds: recent trends and emerging strategies in tissue engineering, Bioact. Mater. 10 (2022) 15–31.
[70] M.T. Spang, K.L. Christman, Extracellular matrix hydrogel therapies: *In vivo* applications and development, Acta Biomater. 68 (2018) 1–14.
[71] D.A. Taylor, L.C. Sampaio, Z. Ferdous, A.S. Gobin, L.J. Taite, Decellularized matrices in regenerative medicine, Acta Biomater. 74 (2018) 74–89.
[72] G.S. Hussey, J.L. Dziki, S.F. Badylak, Extracellular matrix-based materials for regenerative medicine, Nat. Rev. Mater. 3 (2018) 159–173.

[73] S. Cho, D.E. Discher, K.W. Leong, G. Vunjak-Novakovic, J.C. Wu, Challenges and opportunities for the next generation of cardiovascular tissue engineering, Nat. Methods 19 (2022) 1064–1071.
[74] D. Bejleri, M.E. Davis, Decellularized extracellular matrix materials for cardiac repair and regeneration, Adv. Healthcare Mater. 8 (2019) 1–29.
[75] M. Brown, J. Li, C. Moraes, M. Tabrizian, N.Y.K. Li-Jessen, Decellularized extracellular matrix: new promising and challenging biomaterials for regenerative medicine, Biomaterials 289 (2022), 121786.
[76] M. Santschi, A. Vernengo, D. Eglin, M. D'Este, K. Wuertz-Kozak, Decellularized matrix as a building block in bioprinting and electrospinning, Curr. Opin. Biomed. Eng. 10 (2019) 116–122.
[77] K. Dzobo, K.S.C.M. Motaung, A. Adesida, Recent trends in decellularized extracellular matrix bioinks for 3D printing: an updated review, Int. J. Mol. Sci. 20 (2019) 1–28.
[78] A.R. Pinto, A. Ilinykh, M.J. Ivey, J.T. Kuwabara, M.L. D'antoni, R. Debuque, A. Chandran, L. Wang, K. Arora, N.A. Rosenthal, M.D. Tallquist, Revisiting cardiac cellular composition, Circ. Res. 118 (2016) 400–409.
[79] D.L. Brutsaert, L.J. Andries, The endocardial endothelium, Am. J. Physiol. Circ. Physiol. 263 (1992) H985–H1002.
[80] T. Ishihara, V.J. Ferrans, M. Jones, S.W. Boyce, O. Kawanami, W.C. Roberts, Histologic and ultrastructural features of normal human parietal pericardium, Am. J. Cardiol. 46 (1980) 744–753.
[81] H. Li, M. Bao, Y. Nie, Extracellular matrix–based biomaterials for cardiac regeneration and repair, Heart Fail, Rev 26 (2021) 1231–1248.
[82] R.I. Bashey, A. Martinez-Hernandez, S.A. Jimenez, Isolation, characterization, and localization of cardiac collagen type VI: associations with other extracellular matrix components, Circ. Res. 70 (1992) 1006–1017.
[83] S.F. Badylak, D. Taylor, K. Uygun, Whole-organ tissue engineering: decellularization and recellularization of three-dimensional matrix scaffolds, Annu. Rev. Biomed. Eng. 13 (2011) 27–53.
[84] M.A. Karsdal, S.H. Nielsen, D.J. Leeming, L.L. Langholm, M.J. Nielsen, T. Manon-Jensen, A. Siebuhr, N.S. Gudmann, S. Rønnow, J.M. Sand, S.J. Daniels, J. H. Mortensen, D. Schuppan, The good and the bad collagens of fibrosis – their role in signaling and organ function, Adv. Drug Deliv. Rev. 121 (2017) 43–56.
[85] S. Zhang, J.A. Crow, X. Yang, J. Chen, A. Borazjani, K.B. Mullins, W. Chen, R. C. Cooper, R.M. McLaughlin, J. Liao, The correlation of 3D DT-MRI fiber disruption with structural and mechanical degeneration in porcine myocardium, Ann. Biomed. Eng. 38 (2010) 3084–3095.
[86] N.U.B. Hansen, F. Genovese, D.J. Leeming, M.A. Karsdal, The importance of extracellular matrix for cell function and *in vivo* likeness, Exp. Mol. Pathol. 98 (2015) 286–294.
[87] J.P. Guyette, J.M. Charest, R.W. Mills, B.J. Jank, P.T. Moser, S.E. Gilpin, J. R. Gershlak, T. Okamoto, G. Gonzalez, D.J. Milan, G.R. Gaudette, H.C. Ott, Bioengineering human myocardium on native extracellular matrix, Circ. Res. 118 (2016) 56–72.
[88] W.E. Poel, Preparation of acellular homogenates from muscle samples, Science 108 (1948) 390–391, 80-.
[89] H. Capella-Monsonís, D.I. Zeugolis, Decellularized xenografts in regenerative medicine: from processing to clinical application, Xenotransplantation 28 (2021), e12683.
[90] B.S. Kim, H. Kim, G. Gao, J. Jang, D.-W. Cho, Decellularized extracellular matrix: a step towards the next generation source for bioink manufacturing, Biofabrication 9 (2017), 034104.
[91] P. Kc, Y. Hong, G. Zhang, Cardiac tissue-derived extracellular matrix scaffolds for myocardial repair: advantages and challenges, Regen. Biomater. 6 (2019) 185–199.
[92] L. Zhu, J. Yuhan, H. Yu, B. Zhang, K. Huang, L. Zhu, Decellularized extracellular matrix for remodeling bioengineering organoid's microenvironment, Small 19 (2023), 2207752.
[93] E. Garreta, R. Oria, C. Tarantino, M. Pla-Roca, P. Prado, F. Fernández-Avilés, J. M. Campistol, J. Samitier, N. Montserrat, Tissue engineering by decellularization and 3D bioprinting, Mater. Today 20 (2017) 166–178.
[94] S. Badylak, D. Freytes, T. Gilbert, Extracellular matrix as a biological scaffold material: structure and function, Acta Biomater. 5 (2009) 1–13.
[95] H.C. Ott, T.S. Matthiesen, S.K. Goh, L.D. Black, S.M. Kren, T.I. Netoff, D.A. Taylor, Perfusion-decellularized matrix: using nature's platform to engineer a bioartificial heart, Nat. Med. 14 (2008) 213–221.
[96] A.F.G. Godier-Furnémont, T.P. Martens, M.S. Koeckert, L. Wan, J. Parks, K. Arai, G. Zhang, B. Hudson, S. Homma, G. Vunjak-Novakovic, Composite scaffold provides a cell delivery platform for cardiovascular repair, Proc. Natl. Acad. Sci. U.S.A. 108 (2011) 7974–7979.
[97] T.-Y. Lu, B. Lin, J. Kim, M. Sullivan, K. Tobita, G. Salama, L. Yang, Repopulation of decellularized mouse heart with human induced pluripotent stem cell-derived cardiovascular progenitor cells, Nat. Commun. 4 (2013) 2307.
[98] H. Kitahara, H. Yagi, K. Tajima, K. Okamoto, A. Yoshitake, R. Aeba, M. Kudo, I. Kashima, S. Kawaguchi, A. Hirano, M. Kasai, Y. Akamatsu, H. Oka, Y. Kitagawa, H. Shimizu, Heterotopic transplantation of a decellularized and recellularized whole porcine heart, Interact. Cardiovasc. Thorac. Surg. 22 (2016) 571–579.
[99] D.A. Taylor, L.C. Sampaio, Z. Ferdous, A.S. Gobin, L.J. Taite, Decellularized matrices in regenerative medicine, Acta Biomater. 74 (2018) 74–89.
[100] J.E. Arenas-Herrera, I.K. Ko, A. Atala, J.J. Yoo, Decellularization for whole organ bioengineering, Biomed. Mater. 8 (2013), 014106.
[101] F. Pati, J. Jang, D.-H.H. Ha, S. Won Kim, J.-W.W. Rhie, J.-H.H. Shim, D.-H.H. Kim, D.-W.W. Cho, Printing three-dimensional tissue analogues with decellularized extracellular matrix bioink, Nat. Commun. 5 (2014) 3935.
[102] N. Momtahan, N. Poornejad, J.A. Struk, A.A. Castleton, B.J. Herrod, B.R. Vance, J. P. Eatough, B.L. Roeder, P.R. Reynolds, A.D. Cook, Automation of pressure control improves whole porcine heart decellularization, Tissue Eng. C Methods 21 (2015) 1148–1161.
[103] W. Han, N.K. Singh, J.J. Kim, H. Kim, B.S. Kim, J.Y. Park, J. Jang, D.-W. Cho, Directed differential behaviors of multipotent adult stem cells from decellularized tissue/organ extracellular matrix bioinks, Biomaterials 224 (2019), 119496.
[104] S. Jalili-Firoozinezhad, S. Rajabi-Zeleti, A. Marsano, N. Aghdami, H. Baharvand, Influence of decellularized pericardium matrix on the behavior of cardiac progenitors, J. Appl. Polym. Sci. 133 (2016), 43255.
[105] I. Perea-Gil, C. Gálvez-Montón, C. Prat-Vidal, I. Jorba, C. Segú-Vergés, S. Roura, C. Soler-Botija, O. Iborra-Egea, E. Revuelta-López, M.A. Fernández, R. Farré, D. Navajas, A. Bayes-Genis, Head-to-head comparison of two engineered cardiac grafts for myocardial repair: from scaffold characterization to pre-clinical testing, Sci. Rep. 8 (2018) 6708.
[106] Y. Wang, J. Bao, Q. Wu, Y. Zhou, Y. Li, X. Wu, Y. Shi, L. Li, H. Bu, Method for perfusion decellularization of porcine whole liver and kidney for use as a scaffold for clinical-scale bioengineering engrafts, Xenotransplantation 22 (2015) 48–61.
[107] C. Zhao, Y. Li, G. Peng, X. Lei, G. Zhang, Y. Gao, Decellularized liver matrix-modified chitosan fibrous scaffold as a substrate for C3A hepatocyte culture, J. Biomater. Sci. Polym. Ed. 31 (2020) 1041–1056.
[108] M. Lorvellec, A.F. Pellegata, A. Maestri, C. Turchetta, E. Alvarez Mediavilla, S. Shibuya, B. Jones, F. Scottoni, D.P. Perocheau, A.C. Cozmescu, J.M. Delhove, D. Kysh, A. Gjinovci, J.R. Counsell, W.E. Heywood, K. Mills, T.R. McKay, P. De Coppi, P. Gissen, An *in vitro* whole-organ liver engineering for testing of genetic therapies, iScience 23 (2020), 101808.
[109] L.C. Caires-Júnior, E. Goulart, K.A. Telles-Silva, B.H.S. Araujo, C.M. Musso, G. Kobayashi, D. Oliveira, A. Assoni, V.M. Carvalho, A.F. Ribeiro-Jr, R. Ishiba, K. A.O. Braga, N. Nepomuceno, E. Caldini, T. Rangel, S. Raia, P.I. Lelkes, M. Zatz, Pre-coating decellularized liver with HepG2-conditioned medium improves hepatic recellularization, Mater. Sci. Eng. C 121 (2021), 111862.
[110] E.A. Ross, D.R. Abrahamson, P. St John, W.L. Clapp, M.J. Williams, N. Terada, T. Hamazaki, G.W. Ellison, C.D. Batich, Mouse stem cells seeded into decellularized rat kidney scaffolds endothelialize and remodel basement membranes, Organogenesis 8 (2012) 49–55.
[111] J.J. Song, J.P. Guyette, S.E. Gilpin, G. Gonzalez, J.P. Vacanti, H.C. Ott, Regeneration and experimental orthotopic transplantation of a bioengineered kidney, Nat. Med. 19 (2013) 646–651.
[112] A.P. Price, L.M. Godin, A. Domek, T. Cotter, J. D'Cunha, D.A. Taylor, A. Panoskaltsis-Mortari, Automated decellularization of intact, human-sized lungs for tissue engineering, Tissue Eng. C Methods 21 (2015) 94–103.
[113] S.R. Franzdóttir, I.T. Axelsson, A.J. Arason, Ó. Baldursson, T. Gudjonsson, M. K. Magnusson, Airway branching morphogenesis in three dimensional culture, Respir. Res. 11 (2010) 162.
[114] D. Huh, B.D. Matthews, A. Mammoto, M. Montoya-Zavala, H.Y. Hsin, D.E. Ingber, Reconstituting organ-level lung functions on a chip, Science 328 (2010) 1662–1668, 80-.
[115] P. Aguiari, L. Iop, F. Favaretto, C.M.L. Fidalgo, F. Naso, G. Milan, V. Vindigni, M. Spina, F. Bassetto, A. Bagno, R. Vettor, G. Gerosa, *In vitro* comparative assessment of decellularized bovine pericardial patches and commercial bioprosthetic heart valves, Biomed. Mater. 12 (2017), 015021.
[116] S. Zouhair, E. Dal Sasso, S.R. Tuladhar, C. Fidalgo, L. Vedovelli, A. Filippi, G. Borile, A. Bagno, M. Marchesan, G. De Rossi, D. Gregori, W.F. Wolkers, F. Romanato, S. Korossis, G. Gerosa, L. Iop, A comprehensive comparison of bovine and porcine decellularized pericardia: new insights for surgical applications, Biomolecules 10 (2020) 371.
[117] M. Spina, F. Ortolani, A. El Messlemani, A. Gandaglia, J. Bujan, N. Garcia-Honduvilla, I. Vesely, G. Gerosa, D. Casarotto, L. Petrelli, M. Marchini, Isolation of intact aortic valve scaffolds for heart-valve bioprostheses: extracellular matrix structure, prevention from calcification, and cell repopulation features, J. Biomed. Mater. Res., Part A 67A (2003) 1338–1350.
[118] M. Gallo, F. Naso, H. Poser, A. Rossi, P. Franci, R. Bianco, M. Micciolo, F. Zanella, U. Cucchini, L. Aresu, E. Buratto, R. Busetto, M. Spina, A. Gandaglia, G. Gerosa, Physiological performance of a detergent decellularized heart valve implanted for 15 months in Vietnamese pigs: surgical procedure, follow-up, and explant inspection, Artif. Organs 36 (2012) E138–E150.
[119] T. Bottio, V. Tarzia, G. Rizzoli, G. Gerosa, The changing spectrum of bioprostheses hydrodynamic performance: considerations on in-vitro tests, Interact. Cardiovasc. Thorac. Surg. 7 (2008) 750–754.
[120] F. Naso, A. Gandaglia, M. Formato, A. Cigliano, A.J. Lepedda, G. Gerosa, M. Spina, Differential distribution of structural components and hydration in aortic and pulmonary heart valve conduits: impact of detergent-based cell removal, Acta Biomater. 6 (2010) 4675–4688.
[121] L. Iop, A. Paolin, P. Aguiari, D. Trojan, E. Cogliati, G. Gerosa, Decellularized cryopreserved allografts as off-the-shelf allogeneic alternative for heart valve replacement: *In vitro* assessment before clinical translation, J. Cardiovasc. Transl. Res. 10 (2017) 93–103.
[122] P.M. Crapo, T.W. Gilbert, S.F. Badylak, An overview of tissue and whole organ decellularization processes, Biomaterials 32 (2011) 3233–3243.
[123] T. Palmosi, A.M. Tolomeo, C. Cirillo, D. Sandrin, M. Sciro, S. Negrisolo, M. Todesco, F. Caicci, M. Santoro, E. Dal Lago, M. Marchesan, M. Modesti, A. Bagno, F. Romanato, P. Grumati, A. Fabozzo, G. Gerosa, Small intestinal submucosa-derived extracellular matrix as a heterotopic scaffold for cardiovascular applications, Front. Bioeng. Biotechnol. 10 (2022) 1–23.

[124] G. Agmon, K.L. Christman, Controlling stem cell behavior with decellularized extracellular matrix scaffolds, Curr. Opin. Solid State Mater. Sci. 20 (2016) 193–201.
[125] E. Rieder, M.-T. Kasimir, G. Silberhumer, G. Seebacher, E. Wolner, P. Simon, G. Weigel, Decellularization protocols of porcine heart valves differ importantly in efficiency of cell removal and susceptibility of the matrix to recellularization with human vascular cells, J. Thorac. Cardiovasc. Surg. 127 (2004) 399–405.
[126] N. Merna, C. Robertson, A. La, S.C. George, Optical imaging predicts mechanical properties during decellularization of cardiac tissue, Tissue Eng. C Methods 19 (2013) 802–809.
[127] L. Formigli, S. Zecchi-Orlandini, E. Meacci, D. Bani, Skeletal myoblasts for heart regeneration and repair: state of the art and perspectives on the mechanisms for functional cardiac benefits, Curr. Pharmaceut. Des. 16 (2010) 915–928.
[128] M.A. Laflamme, C.E. Murry, Regenerating the heart, Nat. Biotechnol. 23 (2005) 845–856.
[129] P. Menasché, A. Hagège, M. Scorsin, B. Pouzet, M. Desnos, D. Duboc, K. Schwartz, J.T. Vilquin, J.P. Marolleau, Autologous skeletal myoblast transplantation for cardiac insufficiency. First clinical case, Arch. Mal. Coeur. Vaiss. 94 (2001) 180–182.
[130] F. Carton, D. Di Francesco, L. Fusaro, E. Zanella, C. Apostolo, F. Oltolina, D. Cotella, M. Prat, F. Boccafoschi, Myogenic potential of extracellular matrix derived from decellularized bovine pericardium, Int. J. Mol. Sci. 22 (2021) 9406.
[131] H. Reinecke, G.H. MacDonald, S.D. Hauschka, C.E. Murry, Electromechanical coupling between skeletal and cardiac muscle: implications for infarct repair, J. Cell Biol. 149 (2000) 731–740.
[132] P. Menasché, O. Alfieri, S. Janssens, W. McKenna, H. Reichenspurner, L. Trinquart, J.T. Vilquin, J.P. Marolleau, B. Seymour, J. Larghero, S. Lake, G. Chatellier, S. Solomon, M. Desnos, A.A. Hagège, The myoblast autologous grafting in ischemic cardiomyopathy (MAGIC) trial: first randomized placebo-controlled study of myoblast transplantation, Circulation 117 (2008) 1189–1200.
[133] M.N. Banerjee, R. Bolli, J.M. Hare, Clinical studies of cell therapy in cardiovascular medicine recent developments and future directions, Circ. Res. 123 (2018) 266–287.
[134] X. Lin, M. Robinson, T. Petrie, V. Spandler, W.D. Boyd, C.S. Sondergaard, Small intestinal submucosa-derived extracellular matrix bioscaffold significantly enhances angiogenic factor secretion from human mesenchymal stromal cells, Stem Cell Res. Ther. 6 (2015) 1–12.
[135] C. Hodonsky, L. Mundada, S. Wang, R. Witt, G. Raff, S. Kaushal, M.S. Si, Effects of scaffold material used in cardiovascular surgery on mesenchymal stem cells and cardiac progenitor cells, Ann. Thorac. Surg. 99 (2015) 605–611.
[136] C.W. Chang, T. Petrie, A. Clark, X. Lin, C.S. Sondergaard, L.G. Griffiths, Mesenchymal stem cell seeding of porcine small intestinal submucosal extracellular matrix for cardiovascular applications, PLoS One 11 (2016) 1–19.
[137] M.Y. Tan, W. Zhi, R.Q. Wei, Y.C. Huang, K.P. Zhou, B. Tan, L. Deng, J.C. Luo, X. Q. Li, H.Q. Xie, Z.M. Yang, Repair of infarcted myocardium using mesenchymal stem cell seeded small intestinal submucosa in rabbits, Biomaterials 30 (2009) 3234–3240.
[138] E. Garreta, L. de Oñate, M.E. Fernández-Santos, R. Oria, C. Tarantino, A. M. Climent, A. Marco, M. Samitier, E. Martínez, M. Valls-Margarit, R. Matesanz, D.A. Taylor, F. Fernández-Avilés, J.C. Izpisua Belmonte, N. Montserrat, Myocardial commitment from human pluripotent stem cells: rapid production of human heart grafts, Biomaterials 98 (2016) 64–78.
[139] Y. Duan, Z. Liu, J. O'Neill, L.Q. Wan, D.O. Freytes, G. Vunjak-Novakovic, Hybrid gel composed of native heart matrix and collagen induces cardiac differentiation of human embryonic stem cells without supplemental growth factors, J. Cardiovasc. Transl. Res. 4 (2011) 605–615.
[140] C. Hochman-Mendez, D.B. Pereira de Campos, R.S. Pinto, B.J. da S. Mendes, G. M. Rocha, G. Monnerat, G. Weissmuller, L.C. Sampaio, A.B. Carvalho, D. A. Taylor, A.C.C. de Carvalho, Tissue-engineered human embryonic stem cell-containing cardiac patches: evaluating recellularization of decellularized matrix, J. Tissue Eng. 11 (2020), 204173142092148.
[141] C.L. Mummery, J. Zhang, E.S. Ng, D.A. Elliott, A.G. Elefanty, T.J. Kamp, Differentiation of human embryonic stem cells and induced pluripotent stem cells to cardiomyocytes, Circ. Res. 111 (2012) 344–358.
[142] B. Oberwallner, A. Brodarac, P. Anić, T. Šarić, K. Wassilew, K. Neef, Y.H. Choi, C. Stamm, Human cardiac extracellular matrix supports myocardial lineage commitment of pluripotent stem cells, Eur. J. Cardio. Thorac. Surg. 47 (2015) 416–425.
[143] J. Schwan, A.T. Kwaczala, T.J. Ryan, O. Bartulos, Y. Ren, L.R. Sewanan, A. H. Morris, D.L. Jacoby, Y. Qyang, S.G. Campbell, Anisotropic engineered heart tissue made from laser-cut decellularized myocardium, Sci. Rep. 6 (2016), 32068.
[144] A. Di Baldassarre, E. Cimetta, S. Bollini, G. Gaggi, B. Ghinassi, Human-induced pluripotent stem cell technology and cardiomyocyte generation: progress and clinical applications, Cells 7 (2018) 48.
[145] Z. Wang, D.W. Long, Y. Huang, W.C.W. Chen, K. Kim, Y. Wang, Decellularized neonatal cardiac extracellular matrix prevents widespread ventricular remodeling in adult mammals after myocardial infarction, Acta Biomater. 87 (2019) 140–151.
[146] T.D. Johnson, J.A. DeQuach, R. Gaetani, J. Ungerleider, D. Elhag, V. Nigam, A. Behfar, K.L. Christman, Human versus porcine tissue sourcing for an injectable myocardial matrix hydrogel, Biomater. Sci. 2 (2014) 735–744.
[147] T. Meyer, S. Cebotari, G. Brandes, D. Hartung, F. Wacker, M. Theis, T. Kaufeld, I. Tudorache, I. Nolte, A. Haverich, T. Schilling, Decellularized porcine pericardium enhances autologous vascularized matrix as a prosthesis for left ventricular full-wall myocardial reconstruction, Prosthesis 5 (2023) 113–129.
[148] A.-M. Kajbafzadeh, S.H.A. Tafti, R. Khorramirouz, S. Sabetkish, S.M. Kameli, S. Orangian, S. Rabbani, N. Oveisi, M. Golmohammadi, Z. Kashani, Evaluating the role of autologous mesenchymal stem cell seeded on decellularized pericardium in the treatment of myocardial infarction: an animal study, Cell Tissue Bank. 18 (2017) 527–538.
[149] C. Gálvez-Montón, R. Bragós, C. Soler-Botija, I. Díaz-Güemes, C. Prat-Vidal, V. Crisóstomo, F.M. Sánchez-Margallo, A. Llucià-Valldeperas, P. Bogónez-Franco, I. Perea-Gil, S. Roura, A. Bayes-Genis, Noninvasive assessment of an engineered bioactive graft in myocardial infarction: impact on cardiac function and scar healing, Stem Cells Transl. Med. 6 (2017) 647–655.
[150] C. Prat-Vidal, C. Gálvez-Montón, V. Puig-Sanvicens, B. Sanchez, I. Díaz-Güemes, P. Bogónez-Franco, I. Perea-Gil, A. Casas-Solà, S. Roura, A. Llucià-Valldeperas, C. Soler-Botija, F.M. Sánchez-Margallo, C.E. Semino, R. Bragos, A. Bayes-Genis, Online monitoring of myocardial bioprosthesis for cardiac repair, Int. J. Cardiol. 174 (2014) 654–661.
[151] M. Shah, P. Kc, G. Zhang, *In vivo* assessment of decellularized porcine myocardial slice as an acellular cardiac patch, ACS Appl. Mater. Interfaces 11 (2019) 23893–23900.
[152] T.D. Johnson, S.Y. Lin, K.L. Christman, Tailoring material properties of a nanofibrous extracellular matrix derived hydrogel, Nanotechnology 22 (2011).
[153] S.B. Seif-Naraghi, J.M. Singelyn, M.A. Salvatore, K.G. Osborn, J.J. Wang, U. Sampat, O.L. Kwan, G.M. Strachan, J. Wong, P.J. Schup-Magoffin, R.L. Braden, K. Bartels, J.A. DeQuach, M. Preul, A.M. Kinsey, A.N. DeMaria, N. Dib, K. L. Christman, Safety and efficacy of an injectable extracellular matrix hydrogel for treating myocardial infarction, Sci. Transl. Med. 5 (2013) 173ra25.
[154] H.L.B. Tran, T.T.H. Dinh, M.T.N. Nguyen, Q.M. To, A.T.T. Pham, Preparation and characterization of acellular porcinepericardium for cardiovascular surgery, Turkish J. Biol. 40 (2016) 1243–1250.
[155] Y. Wang, J. Zhang, Z. Qin, Z. Fan, C. Lu, B. Chen, J. Zhao, X. Li, F. Xiao, X. Lin, Z. Wu, Preparation of high bioactivity multilayered bone-marrow mesenchymal stem cell sheets for myocardial infarction using a 3D-dynamic system, Acta Biomater. 72 (2018) 182–195.
[156] B. Yanagawa, V. Rao, T.M. Yau, R.J. Cusimano, Initial experience with intraventricular repair using cormatrix extracellular matrix, Innovat. Tech. Tech. CardioThorac. Vasc Surg. 8 (2013) 348–352.
[157] V. Vasanthan, M. Biglioli, A.F. Hassanabad, J. Dundas, R.G. Matheny, P.W.W. M. Fedak, The CorMatrix Cor^{TM} PATCH for epicardial infarct repair, Future Cardiol. 17 (2021) 1297–1305.
[158] R.A. McCready, C.S. Kiell, A.R. Chugh, B.M. Rapp, T.H. Webb, A. Barksdale, M. Parikshak, M.W. Gerdisch, Long-term results with corMatrix extracellular matrix patches after carotid endarterectomy, J. Surg. Res. 262 (2021) 21–26.
[159] Z. Mosala Nezhad, A. Poncelet, L. De Kerchove, P. Gianello, C. Fervaille, G. El Khoury, Small intestinal submucosa extracellular matrix (CorMatrix®) in cardiovascular surgery: a systematic review, Interact. Cardiovasc. Thorac. Surg. 22 (2016) 839–850.
[160] W.D. Boyd, R.G. Matheny, J.N. Young, A.M. Fallon, Injectable matrix bioscaffolds improve LV function and stimulate cardiomyocyte regeneration in infarcted hearts, J. Heart Lung Transplant. 32 (2013) S46.
[161] S. Higuchi, Q. Lin, J. Wang, T.K. Lim, S.B. Joshi, G.S. Anand, M.C.M. Chung, M. P. Sheetz, H. Fujita, Heart extracellular matrix supports cardiomyocyte differentiation of mouse embryonic stem cells, J. Biosci. Bioeng. 115 (2013) 320–325.
[162] M. Tabuchi, J. Negishi, A. Yamashita, T. Higami, A. Kishida, S. Funamoto, Effect of decellularized tissue powders on a rat model of acute myocardial infarction, Mater. Sci. Eng. C 56 (2015) 494–500.
[163] S. Mirsadraee, H.E. Wilcox, K.G. Watterson, J.N. Kearney, J. Hunt, J. Fisher, E. Ingham, Biocompatibility of acellular human pericardium, J. Surg. Res. 143 (2007) 407–414.
[164] M.T. Lam, J.C. Wu, Biomaterial applications in cardiovascular tissue repair and regeneration, Expert Rev. Cardiovasc Ther. 10 (2012) 1039–1049.
[165] S.G. Ozcebe, G. Bahcecioglu, X.S. Yue, P. Zorlutuna, Effect of cellular and ECM aging on human iPSC-derived cardiomyocyte performance, maturity and senescence, Biomaterials 268 (2021), 120554.
[166] J.T. Kuwabara, A. Hara, J.R. Heckl, B. Peña, S. Bhutada, R. DeMaris, M.J. Ivey, L. P. DeAngelo, X. Liu, J. Park, J.R. Jahansooz, L. Mestroni, T.A. McKinsey, S. S. Apte, M.D. Tallquist, Regulation of extracellular matrix composition by fibroblasts during perinatal cardiac maturation, J. Mol. Cell. Cardiol. 169 (2022) 84–95.
[167] S.B. Seif-Naraghi, D. Horn, P.J. Schup-Magoffin, K.L. Christman, Injectable extracellular matrix derived hydrogel provides a platform for enhanced retention and delivery of a heparin-binding growth factor, Acta Biomater. 8 (2012) 3695–3703.
[168] S.B. Sonnenberg, A.A. Rane, C.J. Liu, N. Rao, G. Agmon, S. Suarez, R. Wang, A. Munoz, V. Bajaj, S. Zhang, R. Braden, P.J. Schup-Magoffin, O.L. Kwan, A. N. DeMaria, J.R. Cochran, K.L. Christman, Delivery of an engineered HGF fragment in an extracellular matrix-derived hydrogel prevents negative LV remodeling post-myocardial infarction, Biomaterials 45 (2015) 56–63.
[169] F. Peysselon, S. Ricard-Blum, Heparin-protein interactions: from affinity and kinetics to biological roles. Application to an interaction network regulating angiogenesis, Matrix Biol. 35 (2014) 73–81.
[170] L. Pellegrini, Role of heparan sulfate in fibroblast growth factor signalling: a structural view, Curr. Opin. Struct. Biol. 11 (2001) 629–634.
[171] G. D'Uva, A. Aharonov, M. Lauriola, D. Kain, Y. Yahalom-Ronen, S. Carvalho, K. Weisinger, E. Bassat, D. Rajchman, O. Yifa, M. Lysenko, T. Konfino, J. Hegesh, O. Brenner, M. Neeman, Y. Yarden, J. Leor, R. Sarig, R.P. Harvey, E. Tzahor,

ERBB2 triggers mammalian heart regeneration by promoting cardiomyocyte dedifferentiation and proliferation, Nat. Cell Biol. 17 (2015) 627–638.
[172] B.D. Polizzotti, B. Ganapathy, S. Walsh, S. Choudhury, N. Ammanamanchi, D. G. Bennett, C.G. dos Remedios, B.J. Haubner, J.M. Penninger, B. Kühn, Neuregulin stimulation of cardiomyocyte regeneration in mice and human myocardium reveals a therapeutic window, Sci. Transl. Med. 7 (2015).
[173] C. Gálvez-Montón, M.T. Fernandez-Figueras, M. Martí, C. Soler-Botija, S. Roura, I. Perea-Gil, C. Prat-Vidal, A. Llucià-Valldeperas, Á. Raya, A. Bayes-Genis, Neoinnervation and neovascularization of acellular pericardial-derived scaffolds in myocardial infarcts, Stem Cell Res. Ther. 6 (2015) 108.
[174] C. Williams, K.P. Quinn, I. Georgakoudi, L.D. Black, Young developmental age cardiac extracellular matrix promotes the expansion of neonatal cardiomyocytes *in vitro*, Acta Biomater. 10 (2014) 194–204.
[175] A.C. Silva, S.C. Rodrigues, J. Caldeira, A.M. Nunes, V. Sampaio-Pinto, T. P. Resende, M.J. Oliveira, M.A. Barbosa, S. Thorsteinsdóttir, D.S. Nascimento, P. Pinto-do-Ó, Three-dimensional scaffolds of fetal decellularized hearts exhibit enhanced potential to support cardiac cells in comparison to the adult, Biomaterials 104 (2016) 52–64.
[176] Y. Jin, H. Kim, S. Min, Y.S. Choi, S.J. Seo, E. Jeong, S.K. Kim, H.-A. Lee, S.-H. Jo, J.-H. Park, B.-W. Park, W.-S. Sim, J.-J. Kim, K. Ban, Y.-G. Kim, H.-J. Park, S.-W. Cho, Three-dimensional heart extracellular matrix enhances chemically induced direct cardiac reprogramming, Sci. Adv. 8 (2022), eabn5768.
[177] J.M. Singelyn, P. Sundaramurthy, T.D. Johnson, P.J. Schup-Magoffin, D.P. Hu, D. M. Faulk, J. Wang, K.M. Mayle, K. Bartels, M. Salvatore, A.M. Kinsey, A. N. DeMaria, N. Dib, K.L. Christman, Catheter-deliverable hydrogel derived from decellularized ventricular extracellular matrix increases endogenous cardiomyocytes and preserves cardiac function post-myocardial infarction, J. Am. Coll. Cardiol. 59 (2012) 751–763.
[178] M.T. Spang, K.L. Christman, Extracellular matrix hydrogel therapies: *In vivo* applications and development, Acta Biomater. 68 (2018) 1–14.
[179] J.M. Singelyn, J.A. DeQuach, S.B. Seif-Naraghi, R.B. Littlefield, P.J. Schup-Magoffin, K.L. Christman, Naturally derived myocardial matrix as an injectable scaffold for cardiac tissue engineering, Biomaterials 30 (2009) 5409–5416.
[180] M.D. Diaz, E. Tran, M. Spang, R. Wang, R. Gaetani, C.G. Luo, R. Braden, R.C. Hill, K.C. Hansen, A.N. DeMaria, K.L. Christman, Injectable myocardial matrix hydrogel mitigates negative left ventricular remodeling in a chronic myocardial infarction model, JACC Basic to Transl. Sci. 6 (2021) 350–361.
[181] A.W. Pearl, P. Woo, R. Ostrowski, J. Mojica, D.L. Mandell, P. Costantino, A preliminary report on micronized AlloDerm injection laryngoplasty, Laryngoscope 112 (2002) 990–996.
[182] M. Shevach, R. Zax, A. Abrahamov, S. Fleischer, A. Shapira, T. Dvir, Omentum ECM-based hydrogel as a platform for cardiac cell delivery, Biomed. Mater. 10 (2015), 034106.
[183] R.M. Wang, K.L. Christman, Decellularized myocardial matrix hydrogels: in basic research and preclinical studies, Adv. Drug Deliv. Rev. 96 (2016) 77–82.
[184] S.F. Badylak, R. Tullius, K. Kokini, K.D. Shelbourne, T. Klootwyk, S.L. Voytik, M. R. Kraine, C. Simmons, The use of xenogeneic small intestinal submucosa as a biomaterial for Achille's tendon repair in a dog model, J. Biomed. Mater. Res. 29 (1995) 977–985.
[185] G. Cao, Y. Huang, K. Li, Y. Fan, H. Xie, X. Li, Small intestinal submucosa: superiority, limitations and solutions, and its potential to address bottlenecks in tissue repair, J. Mater. Chem. B 7 (2019) 5038–5055.
[186] B.B. Scully, C. Fan, B. Grigoryan, J.G. Jacot, G.W. Vick, J.J. Kim, C.D. Fraser, K. J. Grande-Allen, D.L.S. Morales, Remodeling of ECM patch into functional myocardium in an ovine model: a pilot study, J. Biomed. Mater. Res. Part B Appl. Biomater. 104 (2016) 1713–1720.
[187] M. Okada, T.R. Payne, H. Oshima, N. Momoi, K. Tobita, J. Huard, Differential efficacy of gels derived from small intestinal submucosa as an injectable biomaterial for myocardial infarct repair, Biomaterials 31 (2010) 7678–7683.
[188] S. Ma, J. Wu, H. Hu, Y. Mu, L. Zhang, Y. Zhao, X. Bian, W. Jing, P. Wei, B. Zhao, J. Deng, Z. Liu, Novel fusion peptides deliver exosomes to modify injectable thermo-sensitive hydrogels for bone regeneration, Mater. Today Bio. 13 (2022), 100195.
[189] X. Yang, S. Chen, J. Chen, Y. Liu, Y. Bai, S. Yin, D. Quan, The different effect of decellularized myocardial matrix hydrogel and decellularized small intestinal submucosa matrix hydrogel on cardiomyocytes and ischemic heart, Appl. Sci. 11 (2021) 7768.
[190] P. Wu, X. Yuan, F. Li, J. Zhang, W. Zhu, M. Wei, J. Li, X. Wang, Myocardial upregulation of cathepsin D by ischemic heart disease promotes autophagic flux and protects against cardiac remodeling and heart failure, Circ. Hear. Fail. 10 (2017), e004044.
[191] E. Bassat, Y.E. Mutlak, A. Genzelinakh, I.Y. Shadrin, K. Baruch Umansky, O. Yifa, D. Kain, D. Rajchman, J. Leach, D. Riabov Bassat, Y. Udi, R. Sarig, I. Sagi, J. F. Martin, N. Bursac, S. Cohen, E. Tzahor, The extracellular matrix protein agrin promotes heart regeneration in mice, Nature 547 (2017) 179–184.
[192] J.A. DeQuach, V. Mezzano, A. Miglani, S. Lange, G.M. Keller, F. Sheikh, K. L. Christman, Simple and high yielding method for preparing tissue specific extracellular matrix coatings for cell culture, PLoS One 5 (2010), e13039.
[193] E. Bassat, Y.E. Mutlak, A. Genzelinakh, I.Y. Shadrin, K. Baruch Umansky, O. Yifa, D. Kain, D. Rajchman, J. Leach, D. Riabov Bassat, Y. Udi, R. Sarig, I. Sagi, J. F. Martin, N. Bursac, S. Cohen, E. Tzahor, The extracellular matrix protein agrin promotes heart regeneration in mice, Nature 547 (2017) 179–184.
[194] K. Huang, E.W. Ozpinar, T. Su, J. Tang, D. Shen, L. Qiao, S. Hu, Z. Li, H. Liang, K. Mathews, V. Scharf, D.O. Freytes, K. Cheng, An off-the-shelf artificial cardiac patch improves cardiac repair after myocardial infarction in rats and pigs, Sci. Transl. Med. 12 (2020), eaat9683.
[195] D. Bejleri, B.W. Streeter, A.L.Y. Nachlas, M.E. Brown, R. Gaetani, K.L. Christman, M.E. Davis, A bioprinted cardiac patch composed of cardiac-specific extracellular matrix and progenitor cells for heart repair, Adv. Healthcare Mater. 7 (2018) 1–13.
[196] J. Jang, H.-J. Park, S.-W.S.W. Kim, H.J.H. Kim, J.Y. Park, S.J. Na, H.J.H. Kim, M. N. Park, S.H. Choi, S.H. Park, S.-W.S.W. Kim, S.-M. Kwon, P.-J. Kim, D.-W. Cho, 3D printed complex tissue construct using stem cell-laden decellularized extracellular matrix bioinks for cardiac repair, Biomaterials 112 (2017) 264–274.
[197] D.A. Svystonyuk, H.E.M. Mewhort, A.F. Hassanabad, B. Heydari, Y. Mikami, J. D. Turnbull, G. Teng, D.D. Belke, K.T. Wagner, S.A. Tarraf, E.S. DiMartino, J. A. White, J.A. Flewitt, M. Cheung, D.G. Guzzardi, S. Kang, P.W.M. Fedak, Acellular bioscaffolds redirect cardiac fibroblasts and promote functional tissue repair in rodents and humans with myocardial injury, Sci. Rep. 10 (2020) 9459.
[198] Y. Jiang, L. Zhang, F. Zhang, W. Bi, P. Zhang, X.-J. Yu, S.-L. Rao, S. Wang, Q. Li, C. Ding, Y. Jin, Z. Liu, H. Yang, Dual human iPSC-derived cardiac lineage cell-seeding extracellular matrix patches promote regeneration and long-term repair of infarcted hearts, Bioact. Mater. 28 (2023) 206–226.
[199] I.G. Kim, M.P. Hwang, J.S. Park, S.H. Kim, J.H. Kim, H.J. Kang, R. Subbiah, U. H. Ko, J.H. Shin, C.H. Kim, D. Choi, K. Park, Stretchable ECM patch enhances stem cell delivery for post-MI cardiovascular repair, Adv. Healthcare Mater. 8 (2019), e1900593.
[200] P. Kong, J. Dong, W. Li, Z. Li, R. Gao, X. Liu, J. Wang, Q. Su, B. Wen, W. Ouyang, S. Wang, F. Zhang, S. Feng, D. Zhuang, Y. Xie, G. Zhao, H. Yi, Z. Feng, W. Wang, X. Pan, Extracellular matrix/glycopeptide hybrid hydrogel as an immunomodulatory niche for endogenous cardiac repair after myocardial infarction, Adv. Sci. (2023), e2301244.
[201] X. Wang, A. Ansari, V. Pierre, K. Young, C.R. Kothapalli, H.A. von Recum, S. E. Senyo, Injectable extracellular matrix microparticles promote heart regeneration in mice with post-ischemic heart injury, Adv. Healthcare Mater. 11 (2022), 2102265.
[202] K. Wu, Y. Wang, H. Yang, Y. Chen, K. Lu, Y. Wu, C. Liu, H. Zhang, H. Meng, Q. Yu, Y. Zhang, Z. Shen, Injectable decellularized extracellular matrix hydrogel containing stromal cell-derived factor 1 promotes transplanted cardiomyocyte engraftment and functional regeneration after myocardial infarction, ACS Appl. Mater. Interfaces 15 (2023) 2578–2589.
[203] G.R. Liguori, T.T.A. Liguori, S.R. de Moraes, V. Sinkunas, V. Terlizzi, J.A. van Dongen, P.K. Sharma, L.F.P. Moreira, M.C. Harmsen, Molecular and biomechanical clues from cardiac tissue decellularized extracellular matrix drive stromal cell plasticity, Front. Bioeng. Biotechnol. 8 (2020) 520.
[204] G. Guan, D. Huo, Y. Li, X. Zhao, Y. Li, Z. Qin, D. Sun, G. Yang, M. Yang, J. Tan, W. Zeng, C. Zhu, Engineering hiPSC-CM and hiPSC-EC laden 3D nanofibrous splenic hydrogel for improving cardiac function through revascularization and remuscularization in infarcted heart, Bioact. Mater. 6 (2021) 4415–4429.
[205] W.C.W. Chen, Z. Wang, M.A. Missinato, D.W. Park, D.W. Long, H.-J. Liu, X. Zeng, N.A. Yates, K. Kim, Y. Wang, Decellularized zebrafish cardiac extracellular matrix induces mammalian heart regeneration, Sci. Adv. 2 (2016), e1600844.
[206] P.L. Sánchez, M.E. Fernández-Santos, S. Costanza, A.M. Climent, I. Moscoso, M. A. Gonzalez-Nicolas, R. Sanz-Ruiz, H. Rodríguez, S.M. Kren, G. Garrido, J. L. Escalante, J. Bermejo, J. Elizaga, J. Menarguez, R. Yotti, C. Pérez del Villar, M. A. Espinosa, M.S. Guillem, J.T. Willerson, A. Bernad, R. Matesanz, D.A. Taylor, F. Fernández-Avilés, Acellular human heart matrix: a critical step toward whole heart grafts, Biomaterials 61 (2015) 279–289.
[207] T. Holubec, E. Caliskan, S.H. Sündermann, C.T. Starck, A. Plass, D. Bettex, V. Falk, F. Maisano, The use of extracellular matrix patches in cardiac surgery, J. Card. Surg. 30 (2015) 145–148.
[208] E.P. Mihalko, K. Huang, E.P. Sproul, K. Cheng, A.C. Brown, Targeted treatment of ischemic and fibrotic complications of myocardial infarction using a dual-delivery microgel therapeutic, Trans. Annu. Meet. Soc. Biomater. Annu. Int. Biomater. Symp. 40 (2019) 440.
[209] H.E.M. Mewhort, J.D. Turnbull, A. Satriano, K. Chow, J.A. Flewitt, A.-C. Andrei, D.G. Guzzardi, D.A. Svystonyuk, J.A. White, P.W.M. Fedak, Epicardial infarct repair with bioinductive extracellular matrix promotes vasculogenesis and myocardial recovery, J. Heart Lung Transplant. 35 (2016) 661–670.
[210] U. Sarig, G.C.T. Au-Yeung, Y. Wang, T. Bronshtein, N. Dahan, F.Y.C. Boey, S. S. Venkatraman, M. Machluf, Thick acellular heart extracellular matrix with inherent vasculature: a potential platform for myocardial tissue regeneration, Tissue Eng. 18 (2012) 2125–2137.
[211] S. Pok, I.V. Stupin, C. Tsao, R.G. Pautler, Y. Gao, R.M. Nieto, Z.W. Tao, C. D. Fraser, A.V. Annapragada, J.G. Jacot, Full-thickness heart repair with an engineered multilayered myocardial patch in rat model, Adv. Healthcare Mater. 6 (2017) 1–6.
[212] L. Da, M. Gong, A. Chen, Y. Zhang, Y. Huang, Z. Guo, S. Li, J. Li-Ling, L. Zhang, H. Xie, Composite elastomeric polyurethane scaffolds incorporating small intestinal submucosa for soft tissue engineering, Acta Biomater. 59 (2017) 45–57.
[213] L.-M. Zhao, L. Wang, W.-Q. Zhang, R. Wang, X.-Z. Zhang, X.-X. Lei, Y. Liang, Y.-T. Song, Q.-Y. Zhang, K. Lin, H.-Q. Xie, Promotion of right ventricular outflow tract reconstruction using a novel cardiac patch incorporated with hypoxia-pretreated urine-derived stem cells, Bioact. Mater. 14 (2022) 206–218.
[214] N. Kashiyama, R.L. Kormos, Y. Matsumura, A. D'Amore, S. Miyagawa, Y. Sawa, W.R. Wagner, Adipose-derived stem cell sheet under an elastic patch improves cardiac function in rats after myocardial infarction, J. Thorac. Cardiovasc. Surg. 163 (2022) e261–e272.
[215] U. Sarig, M. Machluf, Engineering cell platforms for myocardial regeneration, Expet Opin. Biol. Ther. 11 (2011) 1055–1077.
[216] U. Sarig, E.B.-V. Nguyen, Y. Wang, S. Ting, T. Bronshtein, H. Sarig, N. Dahan, M. Gvirtz, S. Reuveny, S.K.W. Oh, T. Scheper, Y.C.F. Boey, S.S. Venkatraman,

M. Machluf, Pushing the envelope in tissue engineering: *Ex vivo* production of thick vascularized cardiac extracellular matrix constructs, Tissue Eng. 21 (2015) 1507–1519.
[217] L.A. Reis, L.L.Y. Chiu, N. Feric, L. Fu, M. Radisic, Biomaterials in myocardial tissue engineering, J. Tissue Eng. Regen. Med. 10 (2016) 11–28.
[218] G. Zhao, X. Zhang, T.J. Lu, F. Xu, Recent advances in electrospun nanofibrous scaffolds for cardiac tissue engineering, Adv. Funct. Mater. 25 (2015) 5726–5738.
[219] R. Deng, Z. Luo, Z. Rao, Z. Lin, S. Chen, J. Zhou, Q. Zhu, X. Liu, Y. Bai, D. Quan, Decellularized extracellular matrix containing electrospun fibers for nerve regeneration: a comparison between core–shell structured and preblended composites, Adv. Fiber Mater. 4 (2022) 503–519.
[220] S. Krishtul, L. Baruch, M. Machluf, Processed tissue-derived extracellular matrices: tailored platforms empowering diverse therapeutic applications, Adv. Funct. Mater. 30 (2020), 1900386.
[221] A. Ghofrani, L. Taghavi, B. Khalilivavdareh, A. Rohani Shirvan, A. Nouri, Additive manufacturing and advanced functionalities of cardiac patches: a review, Eur. Polym. J. 174 (2022), 111332.
[222] E.C. Beck, D.K. Jarrell, A.C. Lyons, E.J. Vanderslice, M.C. VeDepo, J.G. Jacot, Assessment of electrospun cardiac patches made with sacrificial particles and polyurethane-polycaprolactone blends, J. Biomed. Mater. Res., Part A 109 (2021) 2154–2163.
[223] H.M. Mousa, K.H. Hussein, M.M. Sayed, M.R. El-Aassar, I.M.A. Mohamed, H.-H. Kwak, H.-M. Woo, A. Abdal-hay, Development of biocompatible tri-layered nanofibers patches with endothelial cells for cardiac tissue engineering, Eur. Polym. J. 129 (2020), 109630.
[224] L. Vogt, L.R. Rivera, L. Liverani, A. Piegat, M. El Fray, A.R. Boccaccini, Poly (ε-caprolactone)/poly(glycerol sebacate) electrospun scaffolds for cardiac tissue engineering using benign solvents, Mater. Sci. Eng. C 103 (2019), 109712.
[225] M.K. Krishnamoorthi, U. Sarig, L. Baruch, S. Ting, S. Reuveny, S. Oh, I. Goldfracht, L. Gepstein, S.S. Venkatraman, L.P. Tan, M. Machluf, Robust fabrication of composite 3D scaffolds with tissue-specific bioactivity: a proof-of-concept Study, ACS Appl. Bio Mater. 3 (2020) 4974–4986.
[226] S. Heydarkhan-Hagvall, K. Schenke-Layland, A.P. Dhanasopon, F. Rofail, H. Smith, B.M. Wu, R. Shemin, R.E. Beygui, W.R. MacLellan, Three-dimensional electrospun ECM-based hybrid scaffolds for cardiovascular tissue engineering, Biomaterials 29 (2008) 2907–2914.
[227] B. Schoen, R. Avrahami, L. Baruch, Y. Efraim, I. Goldfracht, O. Elul, T. Davidov, L. Gepstein, E. Zussman, M. Machluf, Electrospun extracellular matrix: paving the way to tailor-made natural scaffolds for cardiac tissue regeneration, Adv. Funct. Mater. 27 (2017), 1700427.
[228] S. Liu, L. Yao, Y. Wang, Y. Li, Y. Jia, Y. Yang, N. Li, Y. Hu, D. Kong, X. Dong, K. Wang, M. Zhu, Immunomodulatory hybrid micro-nanofiber scaffolds enhance vascular regeneration, Bioact. Mater. 21 (2023) 464–482.
[229] V. Leszczak, L.W. Place, N. Franz, K.C. Popat, M.J. Kipper, Nanostructured biomaterials from electrospun demineralized bone matrix: a survey of processing and crosslinking strategies, ACS Appl. Mater. Interfaces 6 (2014) 9328–9337.
[230] S. Gao, M. Chen, P. Wang, Y. Li, Z. Yuan, W. Guo, Z. Zhang, X. Zhang, X. Jing, X. Li, S. Liu, X. Sui, T. Xi, Q. Guo, An electrospun fiber reinforced scaffold promotes total meniscus regeneration in rabbit meniscectomy model, Acta Biomater. 73 (2018) 127–140.
[231] N.W. Garrigues, D. Little, J. Sanchez-Adams, D.S. Ruch, F. Guilak, Electrospun cartilage-derived matrix scaffolds for cartilage tissue engineering, J. Biomed. Mater. Res., Part A 102 (2014) 3998–4008.
[232] H. Hasmad, M.R. Yusof, Z.R. Mohd Razi, R.B. Hj Idrus, S.R. Chowdhury, Human amniotic membrane with aligned electrospun fiber as scaffold for aligned tissue regeneration, Tissue Eng. C Methods 24 (2018) 368–378.
[233] X. Wen, Y. Wang, Z. Guo, H. Meng, J. Huang, L. Zhang, B. Zhao, Q. Zhao, Y. Zheng, J. Peng, Cauda equina-derived extracellular matrix for fabrication of nanostructured hybrid scaffolds applied to neural tissue engineering, Tissue Eng. 21 (2015) 1095–1105.
[234] Q. Yan, H. Dong, J. Su, J. Han, B. Song, Q. Wei, Y. Shi, A review of 3D printing technology for medical applications, Engineering 4 (2018) 729–742.
[235] Y.S. Zhang, K. Yue, J. Aleman, K. Mollazadeh-Moghaddam, S.M. Bakht, J. Yang, W. Jia, V. Dell'Erba, P. Assawes, S.R. Shin, M.R. Dokmeci, R. Oklu, A. Khademhosseini, 3D bioprinting for tissue and organ fabrication, Ann. Biomed. Eng. 45 (2017) 148–163.
[236] S. V Murphy, A. Atala, 3D bioprinting of tissues and organs, Nat. Biotechnol. 32 (2014) 773–785.
[237] A.C. Daly, L. Riley, T. Segura, J.A. Burdick, Hydrogel microparticles for biomedical applications, Nat. Rev. Mater. 5 (2019) 20–43.
[238] H. Lee, W. Han, H. Kim, D.-H. Ha, J. Jang, B.S. Kim, D.-W. Cho, Development of liver decellularized extracellular matrix bioink for three-dimensional cell printing-based liver tissue engineering, Biomacromolecules 18 (2017) 1229–1237.
[239] F. Pati, D.-H. Ha, J. Jang, H.H. Han, J.-W. Rhie, D.-W. Cho, Biomimetic 3D tissue printing for soft tissue regeneration, Biomaterials 62 (2015) 164–175.
[240] D.L. Helseth, A. Veis, Collagen self-assembly *in vitro*. Differentiating specific telopeptide-dependent interactions using selective enzyme modification and the addition of free amino telopeptide, J. Biol. Chem. 256 (1981) 7118–7128.
[241] G. Ahn, K.-H. Min, C. Kim, J.-S. Lee, D. Kang, J.-Y. Won, D.-W. Cho, J.-Y. Kim, S. Jin, W.-S. Yun, J.-H. Shim, Precise stacking of decellularized extracellular matrix based 3D cell-laden constructs by a 3D cell printing system equipped with heating modules, Sci. Rep. 7 (2017) 8624.
[242] A. Blaeser, D.F. Duarte Campos, U. Puster, W. Richtering, M.M. Stevens, H. Fischer, Controlling shear stress in 3D bioprinting is a key factor to balance printing resolution and stem cell integrity, Adv. Healthcare Mater. 5 (2016) 326–333.
[243] C.K. Kuo, P.X. Ma, Ionically crosslinked alginate hydrogels as scaffolds for tissue engineering: Part 1. Structure, gelation rate and mechanical properties, Biomaterials 22 (2001) 511–521.
[244] Y.-J. Choi, T.G. Kim, J. Jeong, H.-G. Yi, J.W. Park, W. Hwang, D.-W. Cho, 3D cell printing of functional skeletal muscle constructs using skeletal muscle-derived bioink, Adv. Healthcare Mater. 5 (2016) 2636–2645.
[245] P.L. Lewis, M. Yan, J. Su, R.N. Shah, Directing the growth and alignment of biliary epithelium within extracellular matrix hydrogels, Acta Biomater. 85 (2019) 84–93.
[246] B. Ren, K. Song, A.R. Sanikommu, Y. Chai, M.A. Longmire, W. Chai, W.L. Murfee, Y. Huang, Study of sacrificial ink-assisted embedded printing for 3D perfusable channel creation for biomedical applications, Appl. Phys. Rev. 9 (2022), 011408.
[247] S.R. Moxon, M.E. Cooke, S.C. Cox, M. Snow, L. Jeys, S.W. Jones, A.M. Smith, L. M. Grover, Suspended manufacture of biological structures, Adv. Mater. 29 (2017), 1605594.
[248] S. Chae, Y.-J. Choi, D.-W. Cho, Mechanically and biologically promoted cell-laden constructs generated using tissue-specific bioinks for tendon/ligament tissue engineering applications, Biofabrication 14 (2022), 025013.
[249] X. Zeng, Z. Meng, J. He, M. Mao, X. Li, P. Chen, J. Fan, D. Li, Embedded bioprinting for designer 3D tissue constructs with complex structural organization, Acta Biomater. 140 (2022) 1–22.
[250] T.J. Hinton, Q. Jallerat, R.N. Palchesko, J.H. Park, M.S. Grodzicki, H.-J. Shue, M. H. Ramadan, A.R. Hudson, A.W. Feinberg, Three-dimensional printing of complex biological structures by freeform reversible embedding of suspended hydrogels, Sci. Adv. 1 (2015), e1500758.
[251] Y.-J. Choi, Y.-J. Jun, D.Y. Kim, H.-G. Yi, S.-H. Chae, J. Kang, J. Lee, G. Gao, J.-S. Kong, J. Jang, W.K. Chung, J.-W. Rhie, D.-W. Cho, A 3D cell printed muscle construct with tissue-derived bioink for the treatment of volumetric muscle loss, Biomaterials 206 (2019) 160–169.
[252] S. Das, S.-W. Kim, Y.-J. Choi, S. Lee, S.-H. Lee, J.-S. Kong, H.-J. Park, D.-W. Cho, J. Jang, Decellularized extracellular matrix bioinks and the external stimuli to enhance cardiac tissue development *in vitro*, Acta Biomater. 95 (2019) 188–200.
[253] H. Zhang, Y. Wang, Z. Zheng, X. Wei, L. Chen, Y. Wu, W. Huang, L. Yang, Strategies for improving the 3D printability of decellularized extracellular matrix bioink, Theranostics 13 (2023) 2562–2587.
[254] H. Lee, S. Chae, J.Y. Kim, W. Han, J. Kim, Y. Choi, D.-W. Cho, Cell-printed 3D liver-on-a-chip possessing a liver microenvironment and biliary system, Biofabrication 11 (2019), 025001.
[255] J.U. Lind, T.A. Busbee, A.D. Valentine, F.S. Pasqualini, H. Yuan, M. Yadid, S.-J. Park, A. Kotikian, A.P. Nesmith, P.H. Campbell, J.J. Vlassak, J.A. Lewis, K. K. Parker, Instrumented cardiac microphysiological devices via multimaterial three-dimensional printing, Nat. Mater. 16 (2017) 303–308.
[256] U. Yong, D. Kim, H. Kim, D.G. Hwang, S. Cho, H. Nam, S. Kim, T. Kim, U. Jeong, K. Kim, W.K. Chung, W. Yeo, J. Jang, Biohybrid 3D printing of a tissue-sensor platform for wireless, real-time, and continuous monitoring of drug-induced cardiotoxicity, Adv. Mater. 35 (2023), 2208983.
[257] B. Peterson, P.G. Whang, R. Iglesias, J.C. Wang, J.R. Lieberman, Osteoinductivity of commercially available demineralized bone matrix, J. Bone Jt. Surg. 86 (2004) 2243–2250.
[258] V. Beachley, G. Ma, C. Papadimitriou, M. Gibson, M. Corvelli, J. Elisseeff, Extracellular matrix particle-glycosaminoglycan composite hydrogels for regenerative medicine applications, J. Biomed. Mater. Res., Part A 106 (2018) 147–159.
[259] D.O. Freytes, J. Martin, S.S. Velankar, A.S. Lee, S.F. Badylak, Preparation and rheological characterization of a gel form of the porcine urinary bladder matrix, Biomaterials 29 (2008) 1630–1637.
[260] J.W. Wassenaar, R. Gaetani, J.J. Garcia, R.L. Braden, C.G. Luo, D. Huang, A. N. Demaria, J.H. Omens, K.L. Christman, Evidence for mechanisms underlying the functional benefits of a myocardial matrix hydrogel for post-MI treatment, J. Am. Coll. Cardiol. 67 (2016) 1074–1086.
[261] R.J. Playford, T. Marchbank, D.P. Calnan, J. Calam, P. Royston, J.J. Batten, H. F. Hansen, Epidermal growth factor is digested to smaller, less active forms in acidic gastric juice, Gastroenterology 108 (1995) 92–101.
[262] T. Marchbank, Human transforming growth factor α(TGF-α)is digested to a smaller (1-43), less biologically active, form in acidic gastric juice, Gut 51 (2002) 787–792.
[263] G.D. Kusuma, M.C. Yang, S.P. Brennecke, A.J. O'Connor, B. Kalionis, D.E. Heath, Transferable matrixes produced from decellularized extracellular matrix promote proliferation and osteogenic differentiation of mesenchymal stem cells and facilitate scale-up, ACS Biomater. Sci. Eng. 5 (2018) 1760–1769.
[264] C.J. Poon, M.V. Maria, S. Sinha, J.A. Palmer, A.A. Woods, W.A. Morrison, K. M. Abberton, Preparation of an adipogenic hydrogel from subcutaneous adipose tissue, Acta Biomater. 9 (2013) 5609–5620.
[265] S. Uriel, J.J. Huang, M.L. Moya, M.E. Francis, R. Wang, S. ying Chang, M. H. Cheng, E.M. Brey, The role of adipose protein derived hydrogels in adipogenesis, Biomaterials 29 (2008) 3712–3719.
[266] G.S. Hussey, D.G. Nascari, L.T. Saldin, B. Kolich, Y.C. Lee, R.J. Crum, S.O. El-Mossier, W. D'Angelo, J.L. Dziki, S.F. Badylak, Ultrasonic cavitation to prepare ECM hydrogels, Acta Biomater. 108 (2020) 77–86.
[267] P. Du, A.D.S. Da Costa, C. Savitri, S.S. Ha, P.Y. Wang, K. Park, An injectable, self-assembled multicellular microsphere with the incorporation of fibroblast-derived extracellular matrix for therapeutic angiogenesis, Mater. Sci. Eng. C 113 (2020), 110961.

[268] Z. Lin, Z. Rao, J. Chen, H. Chu, J. Zhou, L. Yang, D. Quan, Y. Bai, Bioactive decellularized extracellular matrix hydrogel microspheres fabricated using a temperature-controlling microfluidic system, ACS Biomater. Sci. Eng. 8 (2022) 1644–1655.
[269] J.S. Lee, Y.H. Roh, Y.S. Choi, Y. Jin, E.J. Jeon, K.W. Bong, S. Cho, Tissue beads: tissue-specific extracellular matrix microbeads to potentiate reprogrammed cell-based therapy, Adv. Funct. Mater. 29 (2019), 1807803.
[270] R.A. Pouliot, P.A. Link, N.S. Mikhaiel, M.B. Schneck, M.S. Valentine, F.J. Kamga Gninzeko, J.A. Herbert, M. Sakagami, R.L. Heise, Development and characterization of a naturally derived lung extracellular matrix hydrogel, J. Biomed. Mater. Res., Part A 104 (2016) 1922–1935.
[271] M.M. De Santis, H.N. Alsafadi, S. Tas, D.A. Bölükbas, S. Prithiviraj, I.A.N. Da Silva, M. Mittendorfer, C. Ota, J. Stegmayr, F. Daoud, M. Königshoff, K. Swärd, J. A. Wood, M. Tassieri, P.E. Bourgine, S. Lindstedt, S. Mohlin, D.E. Wagner, Extracellular-matrix-reinforced bioinks for 3D bioprinting human tissue, Adv. Mater. 33 (2021), 2005476.
[272] K.E. Kadler, A. Hill, E.G. Canty-Laird, Collagen fibrillogenesis: fibronectin, integrins, and minor collagens as organizers and nucleators, Curr. Opin. Cell Biol. 20 (2008) 495–501.
[273] M. Raspanti, M. Viola, M. Sonaggere, M.E. Tira, R. Tenni, Collagen fibril structure is affected by collagen concentration and decorin, Biomacromolecules 8 (2007) 2087–2091.
[274] D.M. Simmons, J.N. Kearney, Evaluation of collagen cross-linking techniques for the stabilization of tissue matrices, Biotechnol. Appl. Biochem. 17 (1993) 23–29.
[275] I. Migneault, C. Dartiguenave, M.J. Bertrand, K.C. Waldron, Glutaraldehyde: behavior in aqueous solution, reaction with proteins, and application to enzyme crosslinking, Biotechniques 37 (2004) 790–802.
[276] L.H.H. Olde Damink, P.J. Dijkstra, M.J.A. Van Luyn, P.B. Van Wachem, P. Nieuwenhuis, J. Feijen, Glutaraldehyde as a crosslinking agent for collagen-based biomaterials, J. Mater. Sci. Mater. Med. 6 (1995) 460–472.
[277] S.P. Pilipchuk, M.K. Vaicik, J.C. Larson, E. Gazyakan, M.H. Cheng, E.M. Brey, Influence of crosslinking on the stiffness and degradation of dermis-derived hydrogels, J. Biomed. Mater. Res., Part A 101 (2013) 2883–2895.
[278] J.E. Barthold, K.P. McCreery, J. Martinez, C. Bellerjeau, Y. Ding, S.J. Bryant, G. L. Whiting, C.P. Neu, Particulate ECM biomaterial ink is 3D printed and naturally crosslinked to form structurally-layered and lubricated cartilage tissue mimics, Biofabrication 14 (2022), 025021.
[279] T.L. Chu, G. Tripathi, M. Park, S.H. Bae, B.T. Lee, In-vitro and in-vivo biocompatibility of dECM-alginate as a promising candidate in cell delivery for kidney regeneration, Int. J. Biol. Macromol. 211 (2022) 616–625.
[280] H. Kim, B. Kang, X. Cui, S. Lee, K. Lee, D. Cho, W. Hwang, T.B.F. Woodfield, K. S. Lim, J. Jang, Light-activated decellularized extracellular matrix-based bioinks for volumetric tissue analogs at the centimeter scale, Adv. Funct. Mater. 31 (2021), 2011252.
[281] J. Jang, T.G. Kim, B.S. Kim, S.-W. Kim, S.-M. Kwon, D.-W. Cho, Tailoring mechanical properties of decellularized extracellular matrix bioink by vitamin B2-induced photo-crosslinking, Acta Biomater. 33 (2016) 88–95.
[282] E.L. Smith, J.M. Kanczler, D. Gothard, C.A. Roberts, J.A. Wells, L.J. White, O. Qutachi, M.J. Sawkins, H. Peto, H. Rashidi, L. Rojo, M.M. Stevens, A.J. El Haj, F.R.A.J. Rose, K.M. Shakesheff, R.O.C. Oreffo, Evaluation of skeletal tissue repair, Part 2: enhancement of skeletal tissue repair through dual-growth-factor-releasing hydrogels within an *ex vivo* chick femur defect model, Acta Biomater. 10 (2014) 4197–4205.
[283] D. Gothard, E.L. Smith, J.M. Kanczler, C.R. Black, J.A. Wells, C.A. Roberts, L. J. White, O. Qutachi, H. Peto, H. Rashidi, L. Rojo, M.M. Stevens, A.J. El Haj, F.A. R.J. Rose, K.M. Shakesheff, R.O.C. Oreffo, *In vivo* assessment of bone regeneration in alginate/bone ECM hydrogels with incorporated skeletal stem cells and single growth factors, PLoS One 10 (2015) 1–23.
[284] Y. Hong, A. Huber, K. Takanari, N.J. Amoroso, R. Hashizume, S.F. Badylak, W. R. Wagner, Mechanical properties and *in vivo* behavior of a biodegradable synthetic polymer microfiber–extracellular matrix hydrogel biohybrid scaffold, Biomaterials 32 (2011) 3387–3394.
[285] J. Dai, W. Qiao, J. Shi, C. Liu, X. Hu, N. Dong, Modifying decellularized aortic valve scaffolds with stromal cell-derived factor-1α loaded proteolytically degradable hydrogel for recellularization and remodeling, Acta Biomater. 88 (2019) 280–292.
[286] W. He, X. Zhang, X. Li, D. Ju, T. Mao, Y. Lu, Y. Gu, L. Qi, Q. Wang, Q. Wu, C. Dong, A decellularized spinal cord extracellular matrix-gel/GelMA hydrogel three-dimensional composite scaffold promotes recovery from spinal cord injury via synergism with human menstrual blood-derived stem cells, J. Mater. Chem. B 10 (2022) 5753–5764.
[287] M.K. Ravari, S. Mashayekhan, F. Zarei, F.A. Sayyahpour, L. Taghiyar, M. Baghban Eslaminejad, M.B. Eslaminejad, Fabrication and characterization of an injectable reinforced composite scaffold for cartilage tissue engineering: an *in vitro* study, Biomed. Mater. 16 (2021), 045007.
[288] F. Navaee, P. Renaud, A. Kleger, T. Braschler, Highly efficient cardiac differentiation and maintenance by thrombin-coagulated fibrin hydrogels enriched with decellularized porcine heart extracellular matrix, Int. J. Mol. Sci. 24 (2023) 2842.
[289] Y. Xu, Z. Wang, Y. Hua, X. Zhu, Y. Wang, L. Duan, L. Zhu, G. Jiang, H. Xia, Y. She, G. Zhou, Photocrosslinked natural hydrogel composed of hyaluronic acid and gelatin enhances cartilage regeneration of decellularized trachea matrix, Mater. Sci. Eng. C 120 (2021), 111628.
[290] Y.J. Shin, R.T. Shafranek, J.H. Tsui, J. Walcott, A. Nelson, D.-H. Kim, 3D bioprinting of mechanically tuned bioinks derived from cardiac decellularized extracellular matrix, Acta Biomater. 119 (2021) 75–88.
[291] H.-M. Qin, T. Miyakawa, A. Inoue, R. Nishiyama, A. Nakamura, A. Asano, T. Ojima, M. Tanokura, Structural basis for controlling the enzymatic properties of polymannuronate preferred alginate lyase FlAlyA from the PL-7 family, Chem. Commun. 54 (2018) 555–558.
[292] C. Williams, E. Budina, W.L. Stoppel, K.E. Sullivan, S. Emani, S.M. Emani, L. D. Black, Cardiac extracellular matrix-fibrin hybrid scaffolds with tunable properties for cardiovascular tissue engineering, Acta Biomater. 14 (2015) 84–95.
[293] C.S. Greenberg, P.J. Birckbichler, R.H. Rice, Transglutaminases: multifunctional cross-linking enzymes that stabilize tissues, Faseb. J. 5 (1991) 3071–3077.
[294] J.J. Song, H.C. Ott, Organ engineering based on decellularized matrix scaffolds, Trends Mol. Med. 17 (2011) 424–432.
[295] B. Brown, K. Lindberg, J. Reing, D.B. Stolz, S.F. Badylak, The basement membrane component of biologic scaffolds derived from extracellular matrix, Tissue Eng. 12 (2006) 519–526.
[296] L. Yang, M. Guell, D. Niu, H. George, E. Lesha, D. Grishin, J. Aach, E. Shrock, W. Xu, J. Poci, R. Cortazio, R.A. Wilkinson, J.A. Fishman, G. Church, Genome-wide inactivation of porcine endogenous retroviruses (PERVs), Science 350 (2015) 1101–1104.
[297] K.Z. Konakci, B. Bohle, R. Blumer, W. Hoetzenecker, G. Roth, B. Moser, G. Boltz-Nitulescu, M. Gorlitzer, W. Klepetko, E. Wolner, H.J. Ankersmit, Alpha-Gal on bioprostheses: xenograft immune response in cardiac surgery, Eur. J. Clin. Invest. 35 (2005) 17–23.
[298] U. Galili, The α-gal epitope and the anti-Gal antibody in xenotransplantation and in cancer immunotherapy, Immunol, Cell Biol. 83 (2005) 674–686.
[299] A. Vincentelli, C. Latrémouille, R. Zegdi, M. Shen, P.S. Lajos, J.C. Chachques, J.-N. Fabiani, Does glutaraldehyde induce calcification of bioprosthetic tissues? Ann. Thorac. Surg. 66 (1998) S255–S258.
[300] O. Bloch, P. Golde, P.M. Dohmen, S. Posner, W. Konertz, W. Erdbrügger, Immune response in patients receiving a bioprosthetic heart valve: lack of response with decellularized valves, Tissue Eng. 17 (2011) 2399–2405.
[301] S. Park, W.-H. Kim, S.-Y. Choi, Y.-J. Kim, Removal of alpha-Gal epitopes from porcine aortic valve and pericardium using recombinant human alpha galactosidase A, J. Kor. Med. Sci. 24 (2009) 1126.
[302] R. Oriol, Y. Ye, E. Koren, D.K.C. Cooper, Carbohydrate antigens of pig tissues reacting with human natural antibodies as potential targets for hyperacute vascular rejection in pig-to-man organ xenotransplantation, Transplantation 56 (1993) 1433–1442.
[303] H. Watier, J.-M. Guillaumin, F. Piller, M. Lacord, G. Thibault, Y. Lebranchu, M. Monsigny, P. Bardos, Removal of terminal alpha-galactosyl residues from xenogeneic porcine endothelial cells, Transplantation 62 (1996) 105–113.
[304] Y. Luo, J. Wen, C. Luo, R.D. Cummings, D.K.C. Cooper, Pig xenogeneic antigen modification with green coffee bean α-galactosidase, Xenotransplantation 6 (1999) 238–248.
[305] C.J. Phelps, C. Koike, T.D. Vaught, J. Boone, K.D. Wells, S.-H. Chen, S. Ball, S. M. Specht, I.A. Polejaeva, J.A. Monahan, P.M. Jobst, S.B. Sharma, A.E. Lamborn, A.S. Garst, M. Moore, A.J. Demetris, W.A. Rudert, R. Bottino, S. Bertera, M. Trucco, T.E. Starzl, Y. Dai, D.L. Ayares, Production of α1,3-galactosyltransferase-deficient pigs, Science 299 (2003) 411–414, 80-.
[306] L. Lai, D. Kolber-Simonds, K.-W. Park, H.-T. Cheong, J.L. Greenstein, G.-S. Im, M. Samuel, A. Bonk, A. Rieke, B.N. Day, C.N. Murphy, D.B. Carter, R.J. Hawley, R. S. Prather, Production of α-1,3-galactosyltransferase knockout pigs by nuclear transfer cloning, Science 295 (2002) 1089–1092, 80-.
[307] Y. Dai, T.D. Vaught, J. Boone, S.-H. Chen, C.J. Phelps, S. Ball, J.A. Monahan, P. M. Jobst, K.J. McCreath, A.E. Lamborn, J.L. Cowell-Lucero, K.D. Wells, A. Colman, I.A. Polejaeva, D.L. Ayares, Targeted disruption of the α1,3-galactosyltransferase gene in cloned pigs, Nat. Biotechnol. 20 (2002) 251–255.
[308] Y. Yue, W. Xu, Y. Kan, H.-Y. Zhao, Y. Zhou, X. Song, J. Wu, J. Xiong, D. Goswami, M. Yang, L. Lamriben, M. Xu, Q. Zhang, Y. Luo, J. Guo, S. Mao, D. Jiao, T. D. Nguyen, Z. Li, J.V. Layer, M. Li, V. Paragas, M.E. Youd, Z. Sun, Y. Ding, W. Wang, H. Dou, L. Song, X. Wang, L. Le, X. Fang, H. George, R. Anand, S. Y. Wang, W.F. Westlin, M. Güell, J. Markmann, W. Qin, Y. Gao, H.-J. Wei, G. M. Church, L. Yang, Extensive germline genome engineering in pigs, Nat. Biomed. Eng. 5 (2020) 134–143.
[309] W. Liang, J. Chen, L. Li, M. Li, X. Wei, B. Tan, Y. Shang, G. Fan, W. Wang, W. Liu, Conductive hydrogen sulfide-releasing hydrogel encapsulating ADSCs for myocardial infarction treatment, ACS Appl. Mater. Interfaces 11 (2019) 14619–14629.
[310] S.L. Suarez, A.A. Rane, A. Muñoz, A.T. Wright, S.X. Zhang, R.L. Braden, A. Almutairi, A.D. McCulloch, K.L. Christman, Intramyocardial injection of hydrogel with high interstitial spread does not impact action potential propagation, Acta Biomater. 26 (2015) 13–22.
[311] L. Zhang, T. Li, Y. Yu, K. Shi, Z. Bei, Y. Qian, Z. Qian, An injectable conductive hydrogel restores electrical transmission at myocardial infarct site to preserve cardiac function and enhance repair, Bioact. Mater. 20 (2023) 339–354.
[312] K. Kikuchi, K.D. Poss, Cardiac regenerative capacity and mechanisms, Annu. Rev. Cell Dev. Biol. 28 (2012) 719–741.